CEREBRAL HAEMODYNAMICS AND THE ROLE OF NITRIC OXIDE PRODUCTION FOLLOWING TRANSIENT CEREBRAL ISCHAEMIA IN THE DEVELOPING BRAIN

Kyla-Anna Marks

Thesis submitted for the degree of Doctor of Medicine to the University of London

January 1996

Department of Paediatrics and Neonatal Medicine
Royal Postgraduate Medical School
Hammersmith Hospital
Du Cane Road
London W12 0NN

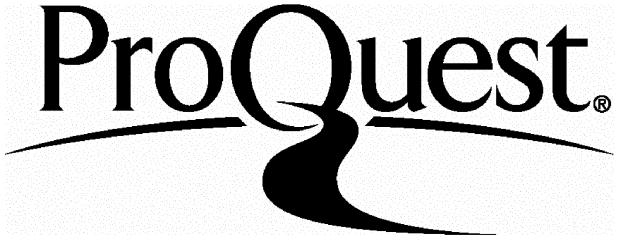

This work is dedicated to my mother and father

ABSTRACT

Birth asphyxia is associated with mortality and long-term neurodevelopmental sequelae in the survivors. The clinical features of hypoxic-ischaemic encephalopathy are well recognised in the days following resuscitation and reflect the pathophysiological processes that are occurring.

There is substantial evidence from asphyxiated infants and animal models of perinatal hypoxia-ischaemia that cerebral injury during and following ischaemia is biphasic: early and delayed. Many neurons recover from the early ischaemic insult, but succumb later by a cascade of processes that culminate in delayed derangements in cerebral energetics. An understanding of the mechanisms that precede and accompany delayed cerebral injury is critical to the management of perinatal hypoxia ischaemia. In this thesis, some of the mechanisms implicated were investigated.

The changes in cerebral perfusion and oxygenation were investigated in the fetal sheep preparation of severe transient cerebral ischaemia, in which a biphasic increase in cortical impedance (CI) reflects the presence of cytotoxic oedema. Near infrared spectroscopy (NIRS) was employed to measure continuously changes in oxyhaemoglobin (HbO_2), deoxyhaemoglobin (Hb), and their sum total cerebral haemoglobin (tHb), and oxidised cytochrome oxidase ($CytO_2$). There was an early and delayed increase in [tHb], and a progressive fall in [$CytO_2$]. The delayed increase in [tHb] preceded and accompanied the delayed increase in CI. The extent of these changes related to histological outcome.

Nitric oxide (NO), an ubiquitous gas generated from L-arginine by several isoforms of the enzyme NO synthase (NOS) produces neuronal death in cell culture through the production of highly potent oxidants, in particular peroxynitrite; but as a potent vasodilator has also been shown to improve cerebral perfusion following cerebral ischaemia. The role of NO was examined by first demonstrating the presence of NOS isoforms in the ischaemic fetal sheep brain using immunohistochemical techniques. Next, the effect of NOS inhibition on the delayed

increase in cerebral perfusion following transient cerebral ischaemia was investigated using L^G-nitro-L-arginine.

NOS inhibition attenuated the delayed increase in cerebral perfusion and was associated with an increase in the extent of cerebral injury.

In summary, by combining the technique of NIRS with those measuring CI in an animal model of perinatal cerebral ischaemia, the changes in cerebral perfusion and oxygenation were temporally related to the development of delayed cerebral injury. Further study of the role of NO revealed important information on the pathogenesis of hypoxic-ischaemic brain injury.

CONTENTS

CHAPTER FOUR - Delayed vasodilation and altered oxygenation following cerebral ischaemia

CHAPTER FIVE - Role of NO following cerebral ischaemia in the perinatal brain

CHAPTER SIX - Discussion

LIST OF FIGURES

LIST OF TABLES

ACKNOWLEDGMENTS

I am greatly indebted to both my supervisors and mentors, Professors David Edwards and Peter Gluckman for their encouragement, support and patience during the course of this project.

A special mention is due to Dr Christopher Williams whose advice at all stages of these studies was greatly appreciated. I am grateful for the patience and willingness shown by Dr Carina Mallard who taught me every detail I needed to know about the fetal sheep preparation. Her sense of humour and reassurance kept me going during the many long hours spent in the basement animal laboratories of Auckland Medical School.

I would further like to thank Idris Roberts for making the fibreoptic cables and for maintaining the near infrared spectroscope soft and hardware; and to Heiko Weix and Mark Gunning whose ingenuity ensured the successful outcome of these studies. The contribution of Professor David Delpy and Dr Mark Cope at the Department of Medical Physics, University College London for measuring the pathlength through the fetal sheep brain was greatly appreciated. Also I wish to thank Lee Buttery at the Department of Histochemistry, Royal Postgraduate Medical School, for preparing and staining the fetal sheep brain tissue for immunohistochemistry. I am grateful Vernon Jansen, Sarah Maasland and all the staff of the basement laboratories at The University of Auckland.

I would like to acknowledge here the generous financial assistance of The Wellcome Trust which made this research possible.

Finally, I would like to thank Dr Sailesh Kotecha whose continuous encouragement and willingness to help throughout the writing of this manuscript has been invaluable.

ABBREVIATIONS

Ach	Acetylcholine
ADP	Adenosine diphosphate
AMP	Adenosine monophosphate
ANOVA	Analysis of variance
AOCC	Agonist operated calcium channel
AP	Amniotic pressure
ATP	Adenosine triphosphate
CA1/2/3	Cornu amnosis regions of the hippocampus
Ca^{2+}	Calcium ions
CBF	Cerebral blood flow
CBFV	Cerebral blood flow velocity
CBV	Cerebral blood volume
cGMP	cyclic guanosine monophosphate
CI	Cortical impedance
Cl^-	Chloride ions
CNS	Central nervous system
dB	Decibels
DPF	Differential pathlength factor
EAA's	Excitatory amino acids
ECoG	Electrocortical activity
EDRF	Endothelium derived relaxing factor
EEG	Electroencephalogram
EMG	Electromyographic activity
e-NOS	Endothelial nitric oxide synthase
GA	Gestational age
GABA	Gamma-amino-butyric-acid
Glut	Glutamine
H^+	Hydrogen ions
Hb	Deoxyhaemoglobin
HbO_2	Oxyhaemoglobin
H_2O_2	Hydrogen peroxide
Hz	Hertz
IGF-1	Insulin like growth factor-1

i-NOS	Inducible nitric oxide synthase
K^+	Potassium ions
L-NNA	L^G-Nitro-N-arginine
MAP	Mean arterial blood pressure
$\mu mol.L^{-1}$	micromoles.litre^{-1}
MRI	Magnetic resonance imaging
MRS	Magnetic resonance spectroscopy
Na^+	Sodium ions
NIRS	Near infrared spectroscopy
NMDA	N-methyl-D-aspartate glutamate receptor
n-NOS	Neuronal nitric oxide synthase
NO^+	Nitrosium ions
NO_2	Nitrigen dioxide
NOS	Nitric oxide synthase
OD	Optical densities
OH^-	Hydroxyl ions
$OHOO^-$	Peroxynitrite ions
Δp	Proton motive force
$PaCO_2$	Arterial carbon dioxide tension
PaO_2	Arterial oxygen tension
PCr	Phosphocreatinine
Pi	Inorganic phosphorus
^{31}P MRS	Phosphorus spectra magnetic resonance spectroscopy
ROS	Reactive oxygen species
SaO_2	Arterial oxygen saturation
SEM	Standard Error of the mean
SO^-_2	Superoxide radicals
VSCC	Voltage sensitive calcium channels
^{133} Xe	Radiolabelled xenon ions

Chapter 1

Perinatal Birth Asphyxia

1.1 Introduction

Historically, perinatal "brain damage" was a major cause for neonatal mortality, and cerebral palsy or mental retardation in the survivors. During the time of the classic nineteenth century reports of Little, and well before the availability of caesarean sections and modern obstetrics monitoring, labors were often very prolonged and involved traumatic instrumental deliveries. In modern obstetrics, intrapartum physical trauma as a cause of brain damage has been largely eliminated. However re-evaluation of the antecedents and causes of cerebral palsy by the American Academy of Pediatrics and American College of Obstetrics and Gynecology, and studies based in United Kingdom, have determined that currently 10% of the cases of cerebral palsy and mental retardation, are associated with evidence of perinatal asphyxia in term infants (American Academy of Pedatrics 1992; Naeye RL et al 1989; Yudkin PL et al 1995).

Perinatal birth asphyxia therefore remains a significant cause of concern for obstetricians, neonatologists and paediatricians alike. In the Western industrialised world the rate of cerebral palsy in term infants has remained 1 to 2 per 1000 births for the last 30 years despite the universal availability of electronic fetal monitoring during the perinatal period (Nelson KB 1988) Between 3-5/1000 full term infants are thought to suffer asphyxiation before or during birth, and depending on the gestational age, between 10-60% of those with evidence of neonatal neurological depression or seizures, expire during the neonatal period (Mulligan JC et al 1980; Ellenberg JH and Nelson KB1988). Survivors have at least a 25% chance of later developing cerebral palsy, mental retardation, learning disability or epilepsy as a clinical consequence of the permanent brain damage incurred during the perinatal period (Freeman JM and Nelson KB 1988; Becerra JE et al 1991; Finer NN et al 1981; Erganger U et al 1983; Nelson KB 1988).

1.2 Definition

Asphyxia can be defined as a disruption of intrapartum organ gas exchange associated with a depletion of cerebral high energy phosphates (Phibbs RH 1981). Its biochemical hallmark is a profound acidemia characterised as being both metabolic associated with hypoxemia and a base deficit, and respiratory (hypercarbia). *In utero*, total cessation of gas exchange is rare, but varying degrees of hypoxaemia and transient interference with maternal-fetal respiratory exchange are common.

1.3 Clinical Features

The diagnosis of birth asphyxia, which is clinically relevant to long term neurodevelopmental prognosis, depends on the association between perinatal factors and long term neurodevelopmental outcome (Paneth N and Stark RI et al 1983; Carter BS et al 1993). The intrapartum markers commonly used to identify birth asphyxia include meconium in the amniotic fluid, abnormal fetal heart rate, low five minute Apgar score and low pH (Phelan JP and Ahn MO 1994). However the neurological sequelae and multiple organ dysfunction observed in asphyxiated infants during the first days of life offer more accurate prognostic information (Erganger U et al 1983).

1.3.1 Intrapartum Features

Meconium staining is common, and its major predictor is advanced gestational age (Katz VL and Bower WA 1992). The presence of meconium in the amniotic fluid of the term infant does not incur any significant increase in the risk of cerebral palsy except in the small minority of infants in whom the 5 minute Apgar score is also low (Miller FC et al 1975; Meis PJ et al 1982). Marked fetal bradycardia (below 60 beats per minute) however has been shown to be associated with some increase in the risk of cerebral palsy (Nelson KB and Ellenberg JH 1986). However in randomised clinical trials, the instigation of electronic fetal monitoring of fetal heart rate patterns in labor has not been shown to improve long-term neurological outcome (Grant A et al 1989; Langendoerfer S et al 1980; Shy KK et al 1990). The addition of

ST waveform monitoring to cardiotocography has been shown to improve the predictive value of intrapartum monitoring and substantially reduce the proportion of deliveries for fetal distress (Westgate J et al 1992).

Low blood pH has been considered the best, and most widely available, measure for identification of asphyxia during labor and delivery (D'Souza SW et al 1983; Gilstrap LC et al 1989; Ruth VJ and Raivio KO 1988). However, the relationship of low pH to neurological symptomology, even in the perinatal period, has not been impressive. Most acidotic babies do not become neurologically symptomatic and some neurologically symptomatic infants are not markedly acidotic. In a large series of consecutively studied infants the acid-base status and occurrence of neonatal seizures in term singleton infants whose umbilical artery pH was below 7.20, among more than 693 term singleton births whose pH was measured (Winkler CL et al 1991). A relationship between low pH and neonatal seizures was only observed with extremely low pH: infants whose pH was <7.05 had a higher rate of neonatal seizures but an absolute rate of only 1%, while infants whose pH was <7.00 had an appreciable absolute rate of otherwise unexplained neonatal seizures, 9.2%. However, infants whose pH was < 7.00 were less than 0.03% of the total sample. The vast majority of children so severely acidotic did not die and did not have seizures. Therefore for pH, as for Apgar scores, it is only the extreme and rare values that predicted even short term neurological outcome (Perlman JM and Rissler R 1993).

1.3.2 Postpartum Features

Low Apgar scores, usually defined as less than 5, describe the degree of clinical depression in the first minutes of life (Sykes G et al 1982). Elements of low Apgar score can occur as a consequence of brain stem dysfunction, and pre-existing neurological impairment and is not specific to any particular illness but rather reflects many disorders producing neonatal neurological depression.. Moderate and briefly low Apgar scores haven not been shown to be related to neurological outcome (Gilstrap LC et al 1989). In contrast very low and very late Apgar scores are quite good predictors of cerebral palsy infants who have Apgar scores of less than 5 after 15 minutes active efforts at resuscitation have a 50-50 chance of manifesting cerebral palsy if they survive (Holst K et al 1989).

1.3.3 Multiple Organ Dysfunction

Important systemic abnormalities, presumably related to ischaemia, often accompany the neonatal neurological syndrome. In a prospective study performed by Perlman et al of 35 term infants where asphyxia was defined as 5-minute Apgar score ≤ 5 and/or umbilical cord arterial pH ≤ 7.20, one third of infants with apparent fetal asphyxia have no evidence for organ injury; of those with evidence for organ injury, renal manifestations were the most common (77%); neurological manifestations alone occurred only 14% of the symptomatic infants and overall in 58% of the symptomatic infants (Perlman JM et al 1989).

In a more recent report with umbilical cord pH ≤ 7.00, 43% had no organ injury; whereas 31% had central nervous system (CNS) injury, manifested as seizures in 76%; 26% had renal injury; 31% had cardiac injury; and 38% had pulmonary injury (Goodwin TM et al 1992). It has been observed that CNS involvement is the only organ system that has residual sequelae at long-term follow up and all other organ systems affected in the neonatal period resolve including pulmonary, renal, and cardiac (Perlman JM 1989).

It is unlikely that any single variable or observation during the perinatal period, such as abnormal fetal heart rate trace, low Apgar score, the presence of meconium stained liquors or fetal acidemia can be used to define birth asphyxia as a cause of subsequent neurodevelopmental sequelae.

1.3.4 Neurological Features

The occurrence of a recognisable neonatal neurological syndrome is the single most useful indicator that a significant hypoxic-ischaemic insult to the brain has occurred. Neonatal hypoxic-ischemic encephalopathy was characterised by Sarnat and Sarnat in 1976 as a neurological syndrome with recognisable clinical and electroencephalographic features (Sarnat HB and Sarnat MS 1976). The Sarnat classification of encephalopathy remains the most appropriate clinical method of defining an asphyxial insult. The scoring includes three stages: mild, moderate and severe encephalopathy or stages I, II, and III (table 1.1).

Table 1.1 **Classification of hypoxic-ischaemic encephalopathy in the newborn infant**

Clinical features	Staging of encephalopathy		
	I	II	III
	Mild	Moderate	Severe
Level of consciousness	Hyperalert	Lethargic	Stuporous, comatose
Muscle tone	Normal	Mild hypotonia	Flaccid
Seizures	None	Common	Intractable
Intracranial pressure		Normal	Elevated
Primitive reflexes			
Suck	Weak	Weak / absent	Absent
Moro	Strong	Weak	Absent
Autonomic function	Generalised sympathetic activity	Generalised parasympathetic activity	Both systems depressed
EEG findings	Normal (awake)	Early: low voltage delta and theta	Early: periodic pattern and suppression
		Later: periodic pattern, seizures	Later: generalized suppression

The severity of the hypoxic-ischaemic encephalopathy in the newborn infant has been classified according to the neurological findings and electroencephalographic changes. The classification has proved a better predictor of outcome than Apgar scores or measures of fetal blood gases.

Sarnat H, Sarnat M: Neonatal Encephalopathy following fetal distress (Sarnat HB, Sarnat MS, 1976)

Following birth asphyxia, a constellation of neurological signs evolves over the first few days of life and comprises the syndrome of hypoxic-ischaemic encephalopathy (table 1.2). It is important to note that the clinical features determining the degree of hypoxic-ischaemic encephalopathy may not become obvious until some 12-36 hours after birth. In the term infant, the primary signs of CNS injury following asphyxia include seizures; abnormal respiratory patterns to include apnea and respiratory arrest; an apparent state of hyperalertness; jitteriness; posturing and movement disorders; impaired suck, swallow, gag, and feeding; abnormal oculomotor and pupillary responses; pervasive hypotonia; and bulging anterior fontanelle

Table 1.2. **Clinical features of hypoxic-ischaemic encephalopathy**

Neurological features	**Birth to 12 hours**	**12 to 24 hours**	**24 to 72 hours**	**Beyond 72 hours**
Level of Consciousness	Deep stupor or coma	Apparent increase in level of alertness	Stupor or coma ± deterioration /death	Persistent yet diminished stupor
Respiratory pattern	Periodic breathing	Apnoeic spells	Respiratory arrest	± Apnoeic spells
Other brain stem function	Intact pupillary responses and extraocular movements	Impaired visual fixation	Oculomotor / pupil disturbances	Disturbed gag, sucking, and tongue movements
Motor examination	Hypotonia, minimal movement	Proximal weakness, greater in upper than lower limbs and hemiparesis	Minimal movement	Hypotonia greater than hypertonia; weakness
Seizures	Subtle and other seizures	Jitteriness, more seizures	Seizures often refractory to therapy	± Seizures

The clinical features of hypoxic-ischaemic encephalopathy progress over several hours and reflect the pathophysiological processes. Apparent improvement within the first hours of life often precedes a further deterioration in the level of consciousness and the onset of seizures

Modified from: Volpe JJ: Hypoxic-ischemic encephalopathy: Clinical aspects. (Volpe JJ 1995).

Early neonatal seizures, although not specific for asphyxia, are thought to be related to hypoxic-ischaemic encephalopathy in approximately 60% of cases (Andre M et al 1988; Minchom P et al 1987). The presence of neonatal seizures as part of the neonatal neurological syndrome has a substantial bearing on survival (Legido A et al 1991). Neonatal seizures in children with low Apgar scores and other neonatal signs are associated with a very high rate of cerebral palsy (see tables 1. 3 and 1.4) (Holden KR et al 1982; Mellits ED et al 1982). Furthermore seizures occurring within the first 12 hours of life, and refractory to conventional anticonvulsive treatments, are particularly likely to be associated with the later neurodevelopmental sequelae (Wical BS 1994).

Table 1.3

Presence of obstetric complications and signs of neonatal encephalopthy as predictors of cerebral palsy in infants >2500 gram

	Cerebral Palsy Rate Per Thousand	
Obstetric complications	**No NE* signs**	**3 + NE signs**
No	**2.4**	**70**
Yes	**2.3**	**122**
Yes and low Apgar †	**3.5**	**269**

*NE = neonatal encephalopathy
†Low Apgar score = 5-minute Apgar score ≤ 5

Obstetric complications were not associated with a higher rate of cerebral palsy unless one or more of six signs of neonatal encephalopathy were also present; those with three of more signs had a higher rate of cerebral palsy. NE signs were: reduced activity after day 1; incubator care for>3 days; feeding problems; poor suck; respiratory difficulties; and seizures. Modified from: (Nelson KB and Ellenberg JH 1987)

Table 1.4

Cluster of neonatal characteristics as predictors of cerebral palsy in infants >2500 gram

Low Apgar score *	Neonatal signs	Neonatal seizures	Cerebral palsy rate per thousand
0	**0**	**0**	**13**
0	**0**	**+**	**13**
+	**+**	**+**	**550**

* 5-minute Apgar score of ≤ 5

A very high rate of cerebral palsy was noted in children who had low Apgar scores, and neonatal signs and neonatal seizures. Neonatal seizures without the other indicators were not associated with increased risk. Once neonatal characteristics were taken into account, the occurrence of obstetric complications added no further predictive information, suggesting that essentially all children in whom obstetric disaster was part of the causal path to long term disability were identified through manifestations of neurological abnormality in the neonatal period. Neonatal signs were those described in table 1.3

Modified from: Ellenberg JH, Nelson KB: Cluster of perinatal events identifying infants at high risk for death or disability (Ellenberg JH and Nelson KB 1988).

1.4 Neurodiagnostic Studies

Current evidence suggests that the intrapartum features of birth asphyxia reflect the consequences of impaired gas exchange to the fetus. The clinical features observed over the subsequent hours reflect the pathophysiological mechanisms that are occurring and that culminate in the development of perinatal brain injury. Understanding these mechanisms is critically important if the management and prognosis of infants subjected to birth asphyxia is to be improved.

Neuroimaging, and techniques capable of assessing cerebral electrical activity, metabolism, blood flow and oxygenation have become increasingly available over the last decade. The early changes observed during the first few hours of life are particularly pertinent to understanding the pathogenesis of hypoxic-ischaemic brain injury in the perinatal brain.

1.4.1 Electroencephalography

Electroencephalographic (EEG) recordings commenced shortly after birth have demonstrated early changes in background continuity and seizure activity that appear to reflect the severity of the injury. Wertheim et al recorded continuous EEG activity in 37 infants with hypoxic-ischaemic encephalopathy as soon as possible after birth (Wertheim D et al 1994). Maximal depression and status epilepticus are particularly important in the development of severe neurodevelopmental impairment. Hellstrom-Westas et al has further indicated that a continuous, but extremely low voltage, EEG pattern within the first 6 hours and prior to the development of seizures is associated with the development of severe neurodevelopmental handicap (Hellstrom Westas L et al 1995). EEG has proved to be a useful tool in the management of asphyxiated infants and may shed further light on the pathogenesis.

1.4.2 Magnetic Resonance Imaging

Magnetic resonance imaging (MRI) has been used in a growing number of infants with hypoxic-ischaemic encephalopathy in the neonatal period and during the first year of life. The superlative anatomical detail offered by MRI has proved the technique to be the most informative of all imaging modalities. In hypoxic-ischaemic encephalopathy, the important findings include brain swelling, cortical highlighting, diffuse loss of grey/white differentiation and loss of signal in the posterior limb of the internal capsule (Goplerud JM and Delivoria Papadopoulos M 1993; Barkovich AJ 1992; Pasternak JF et al 1991). Brain swelling has been observed in the first week of life in all grades of hypoxic-ischaemic encephalopathy. The exact pattern of injury is best identified after the first week of life once the brain swelling has resolved.

In a prospective study performed by Kuenzle et al, the prognostic significance of MRI in 43 term infants with perinatal asphyxia was assessed (Kuenzle C et al 1994). MRI was performed between 1 and 14 days after birth and neurodevelopmental outcome was assessed during the second year of life. Severe diffuse brain injury and lesions of thalamus and basal ganglia were strongly associated with poor outcome and greatly reduced head growth; mild diffuse brain injury, parasagittal lesions, periventricular hyperintensity, focal brain necrosis and hemorrhage and periventricular hypointense stripes led in one third of the infants to minor neurological disturbances and mild developmental delay; infants with normal MRI findings developed normally with the exception of one infant who was mildly delayed at 18 months.

Diagnostic information has been obtained using diffusion-weighted MRI in the very early neonatal period (Cowan FM et al. 1994). Using this technique, in which image contrast depends on differences in the molecular motion of water, abnormalities are observed well before those seen by conventional imaging. The changes might represent a reduction in intracellular transport, influx of water into the intracellular space, decrease brain pulsatility and other mechanisms. In term infants, MRI examination shortly after birth, and during the first two weeks of life is important in the management of the infant suffering from perinatal asphyxia.

1.4.3 Magnetic Resonance Spectroscopy

Magnetic resonance spectroscopy (MRS) is a diagnostic modality of enormous importance in the evaluation of the infant with perinatal hypoxic-ischaemic brain injury. Most studies of infants with perinatal asphyxia have focused on the ^{31}P spectra, but the results of some studies using ^{1}H MRS have been published recently.

^{31}P MRS captures the phosphorous metabolites as levels rise and fall and shift in relation to each other to maintain cellular energy homeostasis in the face of oxygen depletion (Azzopardi D and Edwards AD 1995). The sequence of findings has been initially normal spectra (concentrations of phosphocreatinine [PCr], inorganic phosphate [Pi], and adenosine triphosphate [ATP]) in the first hours after birth, followed by a decline in concentration of PCr and a rise in Pi (and thus a decline in PCr/Pi ratio) over approximately 24-72 hours (Wyatt JS et al 1989). In the most severely affected infants, ATP concentrations also declined at this time, and this was universally associated with death (Azzopardi D et al 1989). Subsequently spectra returned to normal over the ensuing weeks, although the total ^{31}P signal may be reduced when marked loss of brain tissue has occurred .

The findings of these studies suggest that impairment in cerebral energy metabolism in the developing brain after hypoxia-ischaemia is biphasic: a transient fall in cerebral energy phosphates during the insult is followed by a later decline. Furthermore the severity of the delayed energy failure can be correlated with subsequent neurodevelopmental abnormality and reduced cranial growth within the first year of life (Roth SC et al 1992). The greater the extent of delayed derangements in cerebral energy metabolism measured by PCr/Pi ratios 2-4 days after resuscitation, the greater the likelihood of death, or serious neurodevelopmental impairments and microcephaly in the survivors (figure 1.1a and b). The biphasic nature of hypoxic-ischaemic cerebral energy has recently been demonstrated in piglets and rat pups (Lorek A et al 1994; Blumberg RM et al 1994).

Figure 1.1 **(a) Mean values for PCr/Pi according to neurodevelopmental outcome group**
(b) Values of PCr/Pi standard deviation scores according to neurodevelopmental outcome

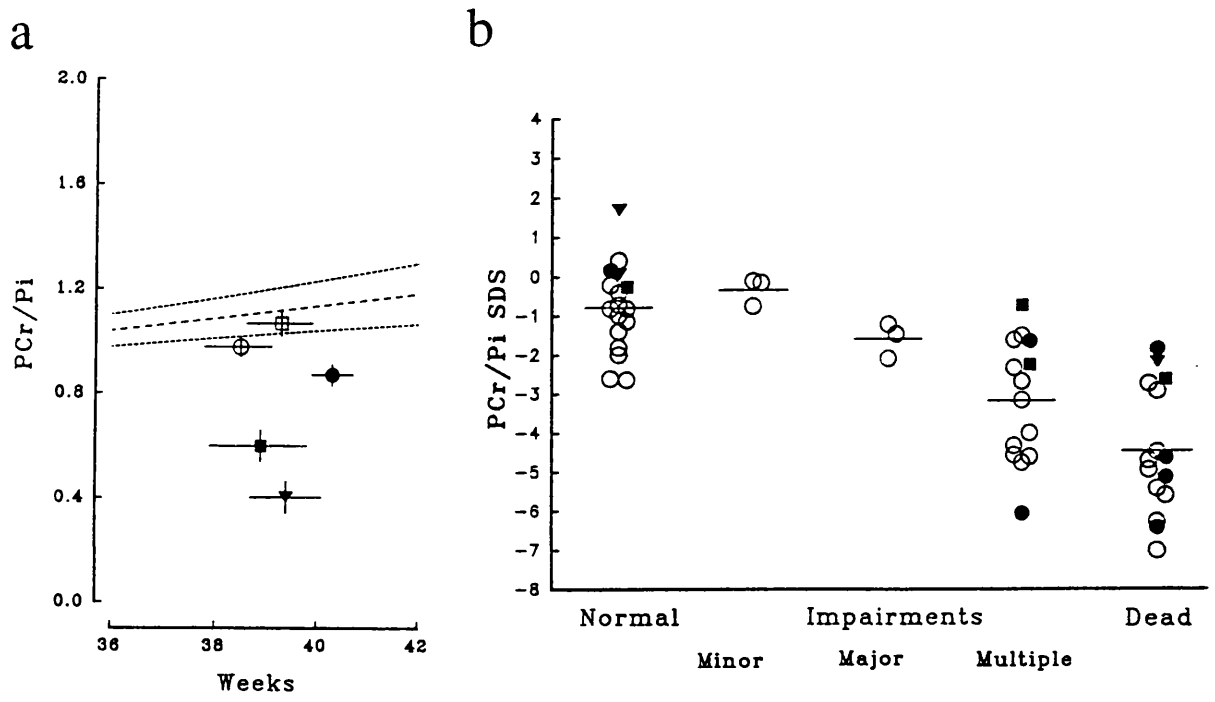

Figure 1.1a shows the mean values (±SEM) for PCr/Pi according to neurodevelopmental outcome group: regression with its 95% confidence intervals for normal control infants vs gestation plus postnatal age also shown. O normal; □ minor impairment; • major impairments; ♦ died. One-way analysis of variance (SPSS) showed highly significant differences between groups ($p<0.001$).

Figure 1.1b shows values for PCr/Pi SDS according to neurodevelopmental outcome group: O term AGA; • term SGA infants; ♦preterm AGA infants; □preterm SGA infants.

From: Roth SC et al 1992

There have been few ^{1}H MRS studies in neonates within the first hours of life after hypoxia-ischaemia. Several days after the ischaemic insult, N-acetyl aspartate/choline ratios were shown to be of important prognostic value (Groenendaal F et al 1994). However a more recent study, in which ^{1}H MRS spectra were obtained within 18 hours of life from 16 asphyxiated infants, increased cerebral lactate concentrations were significantly related to the severity of the delayed cerebral energy failure (Azzopardi D and Edwards AD 1995). Furthermore, increased cerebral lactate concentrations have persisted for many weeks in the most severely affected infants (Azzopardi D. Personal communication).

1.4.4 *Measurement of cerebral haemodynamics*

Although abnormalities in cerebral perfusion and altered cerebrovascular responses have been observed in the hours following resuscitation from perinatal asphyxia, the exact relation between these changes and the development of delayed cerebral injury is not known. It has been suggested from experimental studies that ongoing cerebral ischaemia may further contribute to the development of hypoxic-ischaemic brain injury in the hours following resuscitation, however this finding has not been confirmed in asphyxiated infants during the first days of life (Hossmann KA 1993; Kagstrom E et al 1983; Mujsce DJ et al 1990).

The technique of near infrared spectroscopy (NIRS), which is described in more detail in chapter 2, is capable of providing crucial information concerning cerebral haemoglobin oxygen saturation, cerebral blood volume (CBV), cerebral blood flow (CBF), cerebral oxygen delivery, cerebral venous oxygen saturation, cerebral oxygen availability and utilisation (Reynolds EOR et al 1988). NIRS studies, performed in infants with acute encephalopathy secondary to asphyxia, have found evidence of increased CBV, reduced responsitivity of CBV to changes in carbon dioxide tension and a degree of haemodynamic disturbance that appears to correlate with the clinical severity of the encephalopathy (Wyatt JS et al 1989).

The delayed cerebrovascular consequences of perinatal cerebral ischaemia have been studied extensively in asphyxiated infants. Studies performed by Wyatt et al in asphyxiated infants have demonstrated an increase in CBV within the first 48 hours following resuscitation (Wyatt JS et

al 1993). The highest values were observed in infants who had sustained severe birth asphyxia. In addition, the cerebrovascular responsitivity to changes in $paCO_2$ is diminished.

Furthermore, preliminary studies combining the technique of NIRS with ^{31}P MRS showed that the haemodynamic abnormalities, with elevation of CBV and attenuation of cerebrovascular response to changes in $paCO_2$, preceded the delayed failure of energy metabolism detected as a decline in the PCr:Pi ratio. Follow-up studies have found an association between increased CBV at one to two days of age and worse neurodevelopmental outcome, suggesting that the early haemodynamic changes might reflect the extent of cerebral injury (Wyatt JS et al 1989).

Cerebral haemodynamics following asphyxia have also been investigated using the ^{133}Xenon-clearance technique. Pryds et al used the ^{133}Xe-clearance method to determine the relationship of CBF to acute changes in arterial CO_2 and arterial blood pressure during the first day of life in 19 severely asphyxiated term infants supported by mechanical ventilation (Pryds O et al 1990). 5 of the asphyxiated infants, who had isoelectric electroencephalograms and died later of severe brain injury, had high CBF, and abolished CO_2 and arterial blood pressure reactivity. Lower CBF and abolished arterial blood pressure reactivity were found in another 5 asphyxiated infants who developed brain lesions, although CO_2 reactivity was preserved in these infants. In the remaining 9 asphyxiated infants without signs of central nervous system abnormality, CO_2 and arterial blood pressure reactivity were preserved. In this study, cerebral hyperperfusion and loss of CO_2 reactivity appeared to be an early indicator of very severe brain damage.

Studies using Doppler ultrasonography have measured cerebral blood flow velocities (CBFV) in the major intracerebral arteries of term infants with severe hypoxic-ischaemic encephalopathy. Levene et al studied CBFV in thirty-four asphyxiated infants during the first and second days of life (Levene MI et al 1989). None of the infants with CBFV greater than 3 standard deviations of the control survived without severe impairment.

The results of studies performed on asphyxiated infants suggest that birth asphyxia has a profound effect on the cerebral vasoreactivity and blood flow in the first few days following resuscitation. Cerebral vasodilation and a reduced responsiveness to changes in $paCO_2$ and arterial blood pressure are the predominant findings.

Furthermore, some of these changes may precede the onset of delayed changes in cerebral energetics. Whether the vascular alterations represent a response to tissue necrosis through the release of vasoactive substances, or are in themselves injurious to the ischaemic brain has yet to be elucidated.

The neurodiagnostic studies in asphyxiated infants have improved our understanding of the early changes in cerebral energetics and metabolism that follow birth asphyxia. However, the information that has been obtained is limited to periodic measurements using different techniques. A clearer understanding of the pathophysiological mechanism that culminate in brain injury may be obtained by combining the aforementioned techniques in a preparation known to demonstrate delayed derangements in cerebral energetics.

1.5 Pathophysiology of Perinatal Asphyxia

The progressive signs and symptoms observed in asphyxiated infants over the first few days of life are likely to be closely related to the underlying pathophysiological and biochemical alterations involved in the development of hypoxic-ischaemic brain injury.

The studies described in the previous sections indicate that, in term infants, cerebral injury following birth asphyxia is biphasic and the extent of the delayed disruptions in cerebral energetics is closely related to the severity of the neurodevelopmental outcome. The hypothesis that secondary energy failure is a significant feature has been confirmed in perinatal animal models of hypoxia-ischaemia. In rat pups and piglets, ^{31}P MRS has demonstrated a fall in PCr:Pi during hypoxia-ischaemia followed by a recovery and a further fall commencing several hours later. Furthermore, the severity of the delayed energy failure is directly related to

the extent of acute energy depletion in piglets and the degree of histological damage in rat pups.

Delayed derangements in cellular metabolism have also been demonstrated in fetal sheep by measuring changes in cortical impedance (CI) (Williams CE et al 1991; Williams CE et al 1992). Tissue impedance is increased when there is a reduction in extracellular space as a consequence of intracellular swelling and therefore an increase in CI reflects the presence of cytotoxic oedema. In fetal sheep, a severe cerebral ischaemic insult of 30 minutes duration is accompanied by an acute increase in CI that quickly resolves following reperfusion. 10-15 hours after resuscitation, a 'second' or delayed increase in CI commences and persists for many hours (figure 1.2). The acute and delayed increases in CI is thought to reflect failure of ionic pump mechanism and an influx of Na^+ and Cl^- together with osmotically obligated water (de Boer J et al 1989).

Figure 1.2 **The early and delayed changes in cortical impedance and electrocortical activity during and following transient cerebral ischaemia in fetal sheep**

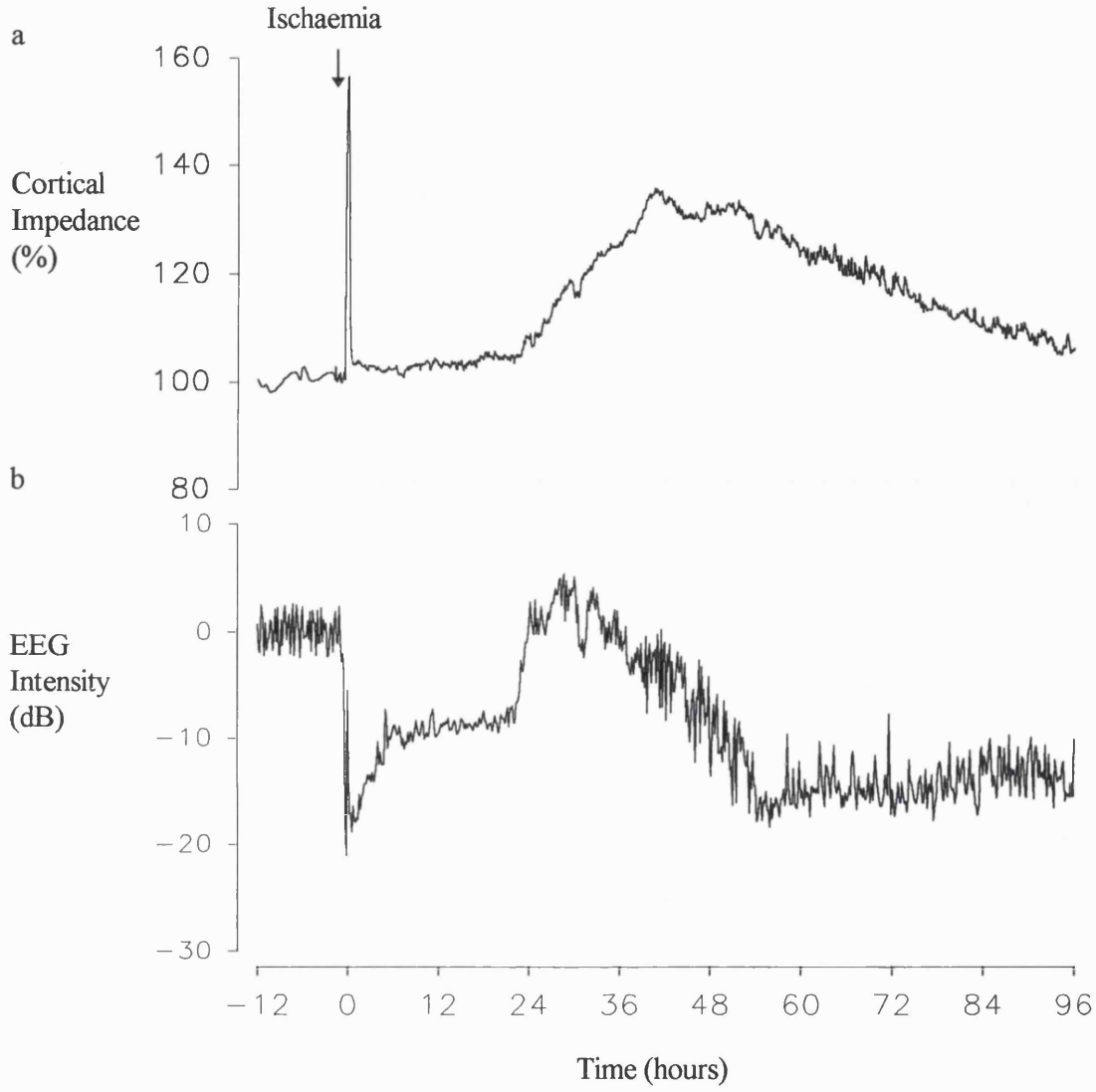

The pathophysiological phases of hypoxic-ischaemic cerebral injury are shown. Following 30 minutes of cerebral ischaemia (ending at time 0) in the late gestation fetal sheep, the upper panel shows the time course of changes in cortical impedance. An increase occurs concomitantly with cytotoxic swelling of cells. Cell size recovers rapidly after the acute injury but then there is a secondary loss of membrane function some hours later during the period of hyperexcitability. The lower panel shows the changes in cortical electroencephalopgraphic activity (EEG). EEG activity is depressed for several hours followed by a period of hyperexcitability and finally a loss of activity is due to neuronal loss.

Adapted from: CE Williams et al 1994

The clinical significance of 'delayed cerebral injury' is substantial, as it may offer a therapeutic window during which time the instigation of 'rescue' therapy to the asphyxiated infant will reduce the extent of cerebral damage and improve long-term outcome (Palmer C and Vannucci RC 1993). In the experimental piglet preparation of hypoxia-ischaemia neuroprotective intervention with mild hypothermia greatly reduced the secondary energy failure and improved histological outcome (Thoresen M et al 1995). It is clear that a considerable proportion of neurons previously thought to be irreversibly lost during the insult can be rescued by treatment instigated after the insult.

The precise mechanisms that leads to secondary deterioration are unclear, although multiple processes have been implicated. A clear temporal picture of the cascade of processes has not yet been obtained because of the diversity of experimental protocols ranging from the study of physiological responses to ischaemia in the brain *in vivo*, to the effect of neurotoxins on cell lines *in vitro*. The gross cerebral responses to ischaemic injury have been studied in the adult and perinatal brain *in vivo* and the results implicate changes in cerebral perfusion and seizure activity. From histological examination of brain tissue, mitochondrial dysfunction appears to be an important early finding that may result in energy disruptions. The mechanisms contributing to the appearance of apoptosis or "programmed cell death" also appear to play an integral role. The effect of a treatment protocols on histological outcome in hypoxic-ischaemic preparations, and the action of neurotoxins on cell lines within the laboratory have expanded our knowledge of the biochemical mechanisms of brain injury. For clarity the sections have been divided into systemic, cellular and biochemical mechanisms that contribute to delayed cerebral injury although the mechanisms undoubtedly overlap. Figure 1.3 shows the interrelation between these events leading to hypoxic-ischaemic brain damage.

Although all these experiments have contributed to our understanding they do not describe the sequence of the pathophysiological mechanisms that precede the secondary deterioration. For this a combination of techniques in a carefully chosen model of perinatal cerebral ischaemia, in which delayed derangements are known to occur. In the subsequent section, the early changes that may be relevant to the development of delayed cerebral injury are described.

Figure 1.3 **A schematic representation of some of the proposed vascular and biochemical mechanisms leading to hypoxic-ischaemic brain damage**

Hypoxia-ischaemia sets into motion a cascade of vascular and biochemical cellular events that result in the development of hypoxic-ischaemic brain injury. Commencing with a shift from oxidative to anaerobic metabolism, there is a failure of transcellular membrane pump mechanisms leading to the intracellular accumulation of Na^+, Cl^- and obligatory H_2O, and the development of cytotoxic oedema. Hypoxia-ischaemia also stimulates the release of excitatory amino acids (glutamate) resulting in a further influx of Ca^{2+} and Na^+ ions. Increased intracellular Ca^{2+} activates a number of mechanisms. The activation of xanthine oxidase (XO) contributes to the accumulation of free radicals which cause cerebral endothelial injury and lipid peroxidation. Activation of nitric oxide synthase (NOS) generates nitric oxide (NO), which is thought to improve cerebral perfusion, but also causes cell death through a reaction with superoxide radicals (SO^-_2) to generate peroxynitrite ($OHOO^-$), nitrogen dioxide (NO^-_2) and hydroxyl radicals (OH^-). Energy is expended in an attempt to maintain Ca^{2+} homeostasis resulting in a further uncoupling of oxidative phosphorylation

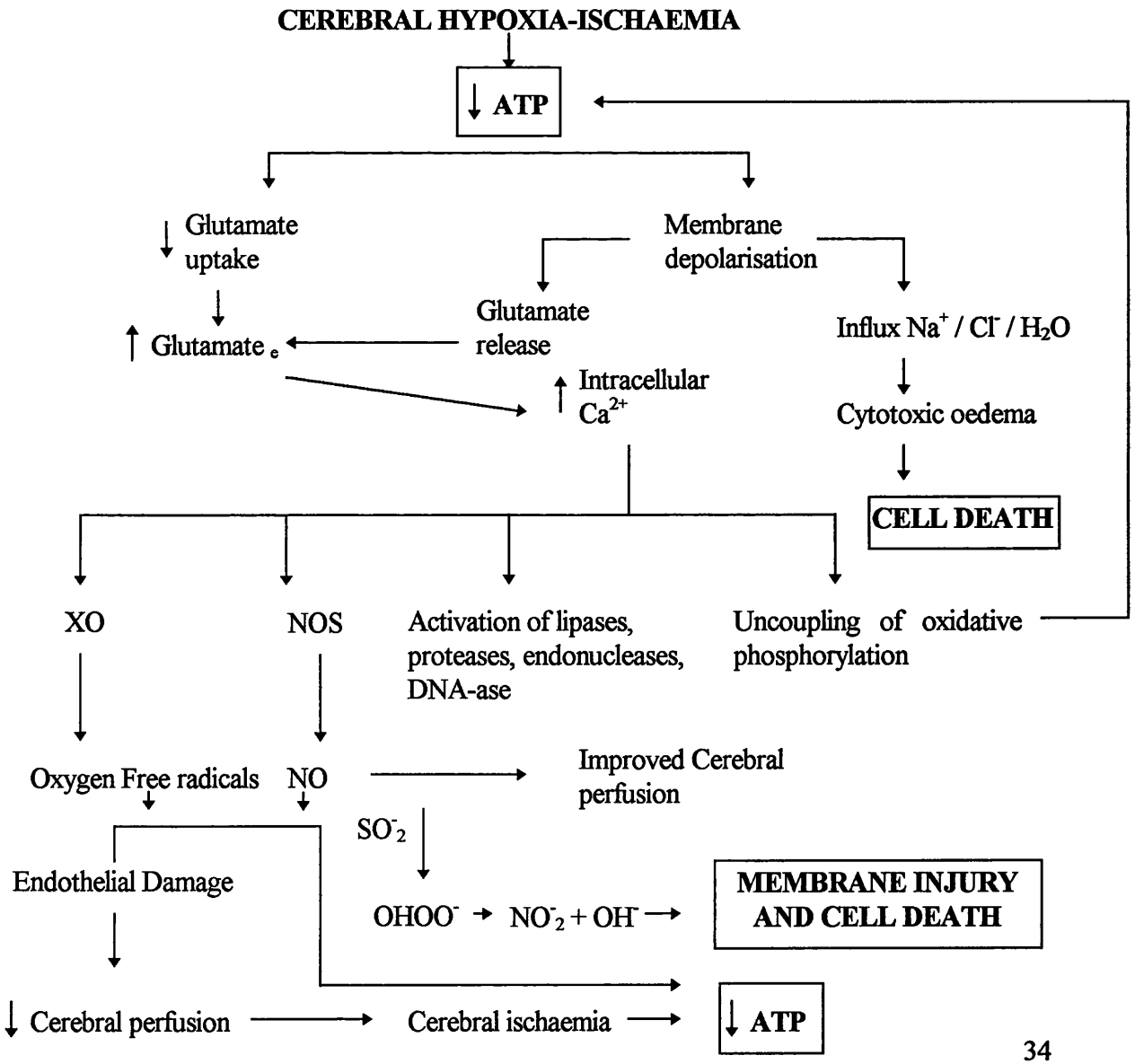

1.5.1 Systemic Changes measured *in vivo*

1.5.1.1 Possible role of cerebral haemodynamic abnormalities

The changes in cerebral haemodynamics that have been observed following cerebral ischaemia have been implicated in the development of delayed cerebral injury. The increases in CBV, loss of cerebral autoregulation and CO_2 responsiveness observed in asphyxiated infants during the first days following resuscitation have already been discussed in the previous sections.

However, few animal studies have investigated the long term cerebrovascular consequences of hypoxia-ischaemia in the hours or days following resuscitation. Mujsce et al measured the changes in CBF and the development of cerebral oedema in seven day old rat pups (Mujsce et al 1990). Changes in CBF were measured using an indicator fraction technique, during, and for up to six days following cerebral hypoxia-ischaemia. The results suggested that a period of increased CBF immediately after resuscitation was followed by a recovery of CBF to pre-ischaemic values for the subsequent 24 hours. However, a period of cerebral hypoperfusion commenced at three days and was still prominent six days after resuscitation. The conclusion was that although there was no early hypoperfusion, delayed hypoperfusion may occur as a consequence of tissue necrosis. Furthermore, as the decrease in CBF coincided with a period of marked cerebral oedema, it was postulated that cerebral oedema may impede flow through the cerebral microcirculation.

In the neonatal lambs, Rosenberg et al investigated the consequence of asphyxia induced by increasing CO_2 and reducing O_2 in the inspired gases under general anaesthesia (Rosenberg A 1988). During a four hour study period, CBF was measured using radiolabelled microspheres. At five minutes following resuscitation, a period of increased CBF was followed at two hours by a marked fall in CBF that persisted throughout the study period. It was therefore suggested that cerebral hypoperfusion may cause further ischaemic damage in the early recovery period. Mayhan et al proposed that the impaired vasodilation after ischaemia, in the face of maintained cerebral vasoconstriction, contributed to the delayed hypoperfusion or 'no-reflow

phenomenon', as it is sometimes referred to (Mayhan WG et al 1988). They described a decreased vasodilatory response in the cerebral vessels of cats to direct application of acetylcholine and serotonin, both endothelial dependent vasodilators, following brief episodes of cerebral ischaemia. As the vasodilatory response induced by these agents is dependent on intact endothelial function, it was suggested that endothelial dysfunction may result from the injury induced during ischaemia-reperfusion.

'Reperfusion injury' following ischaemia is thought to be related to endothelial damage induced by free radicals generated during ischaemia/reperfusion. The generation of free radicals has been demonstrated in piglets, cats and fetal sheep during early reperfusion (Armstead WM et al. 1988; Nelson CW et al 1992; Bagenholm R et al 1994). Following hypoxia-ischaemia, an increase in CBF is associated with the generation of highly reactive oxygen species (ROS), in particular superoxide radicals (SO^{-}_{2}) and hydrogen peroxide (H_2O_2), capable of destroying the chemical nature of target molecules. Free radicals donate or take electrons from other biomolecules and in this way destroy the chemical structure of their target molecules, which include DNA, protein, and most common membrane lipids. Production of ROS is enhanced both by free iron (by the Fenton Reaction) and by NO capable of transforming relatively mild reactive oxygen species into more damaging free radicals especially hydroxyl ions (Beckman JS et al 1990; Traystman RJ et al 1991). During reperfusion, the endogenous scavenger systems may well be inundated. The brain being rich in polyunsaturated phospholipids is particularly susceptible to free radical attack that results in lipid peroxidation. Furthermore, the relative deficiency of endogenous antioxidant enzymes combined with a reduced ability to sequester iron, makes the newborn brain particularly susceptible (Takashima S et al 1990).

Furthermore, vascular dysfunction can be reduced with agents that destroy free radicals. In newborn piglets the impaired cerebral reactivity in response to hypercapnia can all be improved by free radical scavengers (Kirsch JR et al 1993). Prevention of secondary hypoperfusion and depressed oxygen consumption observed in newborn lambs following asphyxia can be induced by pretreatment with superoxide dismutase (SOD) and catalase, and this further indicates that

the antioxidant enzymes protect the endothelium against oxidant damage (Rosenberg A et al 1989).

Endothelial damage induced by free radicals may play a critical role in diminishing cerebral perfusion by (i) producing leukotrienes that induce cerebral vasoconstriction; (ii) promoting the influx and clumping of leukocytes due to an increased production of chemoattractants, (iii) upregulating adhesion factors and increasing platelet adhesion and aggregation. All these factors may compromise cerebral perfusion and further aggravate cerebral injury in the ischaemic brain (Palmer C 1995).

In summary, vascular injury induced by free radicals may compromise cerebral perfusion in the ischaemic brain following reperfusion. It remains to be seen whether the alterations within the cerebral vasculature contribute to the development of hypoxic-ischaemic brain injury. Indeed, there is a great absence of literature relating changes in cerebral perfusion and oxygenation to the development of the secondary disruption of cerebral energetics. Changes in cerebral perfusion need to be measured in an animal preparation of perinatal hypoxia-ischaemia in which there is evidence of delayed cerebral injury in order to determine if the haemodynamic disruptions precede the onset of delayed disruption of cerebral energetics.

1.5.1.2 Contribution of Altered Electrocortical activity

Following severe asphyxia, newborn infants remain neurologically depressed and hypotonic for several hours following resuscitation. EEG activity is concomitantly suppressed to a degree that is likely to be predictive of neurodevelopmental outcome during the first year of life (Hellstrom Westas L et al 1995; Wertheim D et al 1994). The duration of EEG depression following resuscitation is also strongly predictive of histological outcome in fetal sheep following transient cerebral ischaemia and poor outcome is associated with suppression lasting for more than 5 hours (Williams CE et al 1992).

Suppressed cortical activity may result from the accumulation of inhibitory neuromodulators such as adenosine, opiates and GABA (Tan WK et al 1995; Hagberg H et al. 1987). During this depressed period, the perinatal brain has a heightened susceptibility to cerebral injury that may occur as a consequence of repeated asphyxial insults (Mallard CE et al 1993).

The presence of post-asphyxial seizures is well recognised in the asphyxiated infants. Seizures often develop several hours after resuscitation and when they persist for more that 30 minutes these are often associated with poor neurological outcome and cerebral infarction (Legido A et al 1991; Holden KR et al 1982; Wasterlain CG et al 1993). Seizures greatly increase metabolic demands both centrally and peripherally and the increase demands may trigger energy failure in the already compromised ischaemic brain (Williams CE et al 1990).

After hypoxic-ischaemic injuries in fetal sheep, cortical cytotoxic oedema develops synchronously with the development of cortical seizures, and suggests that seizures may compromise cellular metabolism (Williams CE et al 1991). Furthermore seizures worsen outcome after global cerebral ischaemia and suppression of epileptiform activity with MK-801, an NMDA Glut-receptor antagonist, can reduce neuronal loss in the hippocampus and lateral cortex without preventing the development of delayed increase in cortical impedance (Tan WK et al 1992).

Many anticonvulsants that act through the inhibitory GABA-ergic pathways are relatively ineffective in suppressing post-asphyxial seizures in the newborn infant. Studies in asphyxiated sheep suggest that there is a loss of the inhibitory GABA-ergic pathways and a vast increase in the release of the EAA's, aspartate and Glut, over a similar duration (Mallard CE et al 1995; Tan WK et al 1995). Excitotoxic activity is thought to be an important mechanism of secondary damage after hypoxic-ischaemic injury in the developing brain.

1.5.2 Cellular Mechanisms

1.5.2.1 Mitochondrial Dysfunction

Delayed perturbations in cerebral energy metabolism might result from mitochondrial dysfunction such that oxidative phosphorylation is disrupted (Sims NR and Pulsinelli WA 1987; Sun D and Gilboe DD 1994). Mitochondrial damage results in 'uncoupling' of oxidative phosphorylation such that the mitochondria are unable to regenerate chemical energy in the form of ATP and any energy that is produced via electron transport and oxygen consumption is dissipated as heat.

Morphologically, mitochondria appear to be the first neuronal organelle damaged showing dilation and separation of the christae shortly after an ischaemic injury (McGee Russell SM et al 1970; Brown AW and Brierley JB 1973). Functionally, many studies have determined the activity of the mitochondrial enzymes, in particular that of cytochrome oxidase - the terminal complex of the mitochondrial respiratory chain that receives electrons from the cytochrome *c* enzyme and reduces oxygen to water. Acute disruption of cytochrome oxidase activity in the brain has been observed in a perinatal rat stroke model as early as one hour following resuscitation (Nelson C and Silverstein FS 1994). Ischaemia induced suppression of cytochrome oxidase activity corresponds with the distribution of irreversible injury (Dimlich R et al 1990) and the onset of neurological deficits (Wagner KR et al 1990).

The histological techniques for measuring cytochrome oxidase activity in the brain all require that the animal be sacrificed at different time points following the injury and brain tissue be obtained. The technique of NIRS can monitor the changes in concentration of oxidised cytochrome oxidase *in vivo* and changes in the redox state of this respiratory enzyme may yield important information about the mechanism and timing of changes in mitochondrial oxygenation.

1.5.2.2 Apoptosis and the role of trophic factors

The presence of cytotoxic oedema implies that some cells undoubtedly die by necrosis, but evidence suggests that neurons may also die individually over the days and weeks following cerebral ischaemia by processes that appear analogous to the cell death present during normal CNS development, namely apoptosis or programmed cell death (Raff MC et al 1993). Apoptotic cell death is identified morphologically by the presence of chromatin condensation with nuclear shrinkage (pyknosis) and fragmentation (karyorrhexis), and the formation of apoptotic bodies (Wyllie AH et al 1984; Wyllie AH 1981). The processes that culminate in cell death by apoptosis may be initiated early in the cascade and therefore the mechanism inducing apoptosis may be occurring prior to the delayed disruptions in cerebral energetics.

A direct relationship has recently been demonstrated between the number of apoptotic cells in the cingulate gyrus of newborn piglets, 2 days after hypoxia-ischaemia, and the degree of high energy phosphate depletion during the insult, as measured by ^{31}P-MRS (Mehmet H et al 1994). The mechanism involved is unclear but the finding implies that depletion of high energy phosphates may alter the intracellular phosphorylation balance and activate apoptotic signalling pathways. Alternatively, acute loss of cells by necrosis may result in a reduction of intracellular survival signals to neighbouring cells and so lead to delayed cell death by apoptosis. Furthermore, the number of cells dying by apoptosis in cell culture is reduced in the presence of hypothermia, a potentially neuroprotective therapeutic manoeuvre in the immature brain (Kozma M et al 1995).

Apoptosis may be triggered by loss of growth factors or intercellular survival signals from neighbouring cells and has been offered as one of the explanations for the neuroprotective effects of insulin-like growth factor (IGF-1) following hypoxia-ischaemia in fetal sheep (Johnston BM et al 1995). A parallel activation of macrophages in selective injury raises the possibility that the signal for apoptotic cell death might involve macrophages (Beilharz EJ et al 1995). The role of neurotrophic factors in these processes and the early induction of neurotrophic factors in the neonatal rat brain following hypoxia-ischaemia, has focused interest

on the potential use of growth factors to inhibit apoptotic-like mechanisms and macrophage activation. It is likely that the induction of insulin-like growth factor-1 (IGF-1) expression within astrocytes at 24 hours, and transforming growth factor beta (TGF-β) expression in macrophage-like cells within 5 hours, are both endogenous mechanisms to limit injury and promote repair. Exogenous administration of both IGF-1 and TGF-β in adult rats 2 hours after injury is remarkably neuroprotective (Guan J et al 1993; McNeill H et al 1994). Similarly, IGF-1 administration 2 hours after a severe hypoxic-ischaemic insult is neuroprotective in all regions of the brain in fetal sheep (Johnston BM et al 1995).

1.5.3 Biochemical mechanisms

1.5.3.1 Primary Derangements in energy metabolism

'Primary' neuronal death occurs as a consequence of failure of energy dependent pump mechanisms across cellular membranes and subsequent cellular necrosis. During hypoxia-ischaemia, oxidative phosphorylation is inhibited and there is a drastic fall in the mitochondrial production of the high energy phosphates ATP and PCr, and an accumulation of adenosine diphosphate (ADP), adenosine monophosphate (AMP), inorganic phosphate (Pi), adenine nucleotides and bases, including hypoxanthine. The decrease in ATP concentration affects a multitude of energy dependent reactions and the most important are those governing ionic homeostasis. The ion gradients across cell membranes are maintained at the expense of energy in the form of ATP, and energy failure leads to the dissipation of the ionic gradients, with an efflux of K^+ ions from the cells and an influx of Na^+, Cl^- and Ca^{2+}. The time course of these changes suggest that an initial slow rise in extracellular K^+ and fall in extracellular pH, is followed by a sudden increase in extracellular K^+ and decrease in extracellular Na^+, Cl^- and Ca^{2+}. The rise in extracellular K^+ depolarises cells and, by an event termed anoxic depolarisation, leads to electrical silence in that part of the brain.

1.5.3.2 Excitatory Neurotransmitters

The excitotoxic hypothesis is supported by the impressive neuroprotective efficacy of antagonists to the NMDA and AMPA Glut receptors (McDonald JW et al 1990). The ability of NMDA antagonists ketamine, phenylcyclidine and MK-801 to prevent seizure-related damage in several brain regions of the neonatal rat, without suppressing seizure activity, suggested that in these brain regions persistent seizure activity could be maintained by other transmitter systems, with or without NMDA receptor participation (Clifford DB et al 1990). Pharmacological manipulation to increase the concentration of kynurenic acid, the only known endogenous EAA receptor antagonist in the CNS, has also been shown to be moderately neuroprotective when initiated prior to hypoxia-ischaemia in 7 day old rats (Nozaki K and Beal MF 1992). Efficacy of NMDA receptor antagonists may depend on variations in the density and distribution of Glut receptors and the effects may be less marked in brain regions, such as the cortex, where there are fewer NMDA receptors (Ford LM et al 1989).

Glut can continue to induce neuronal injury during recovery from ischaemia and NMDA receptor antagonists can prevent neuronal damage when implemented even after the ischaemic event has terminated. It has been suggested that after ischaemia, NMDA-receptor currents are potentiated, which may imply that more Glut is released from presynaptic terminals or there is a larger postsynaptic response to the Glut released (Szatkowski M and Attwell D 1994). In this case continued NMDA/AMPA receptor activation promotes neuronal death. There is also a massive delayed increase in Glut concentrations in the brains of fetal sheep several hours following severe cerebral ischaemia, which coincides with the development of cortical seizures and can promote further cerebral injury (Tan WK et al 1995; Hagberg H et al 1987).

The excitatory events that lead to neuronal death include release of Glut, and Glut activation of receptors which causes Na^+ influx and depolarisation, followed by Ca^{2+} influx via multiple channels, and forms part of a physiological signalling system that utilises Ca^{2+} as a second messenger (Benveniste H et al 1988). The massive influx of Ca^{2+} ion influxes promotes the production of NO which is a vital element of Glut-induced neurotoxicity (Dawson VL et al

1991; Lafon Cazal M et al 1993). Inhibitors of NOS can reduce the injury induced by Glut both *in vitro* and *in vivo* (Vige X et al 1993). The increased intracellular Ca^{2+} binds to calmodulin and activates NOS to generate NO. Once NO is formed it freely diffuses to adjacent cells, and under certain conditions, is highly cytotoxic through the generation of powerful oxidants.

1.5.3.3 Disruption of calcium homeostasis

As a cofactor in numerous cellular reactions, disruption of intracellular Ca^{2+} homeostasis has wide ranging effects on neuronal metabolism and function. Almost all intracellular Ca^{2+} is bound within subcellular organelles and there is therefore an enormous gradient driving free Ca^{2+} ions into the cell across the plasma membrane. Specific ion channels exist in all cells, and Ca^{2+} influx from the extracellular space to the cytosol occurs via voltage sensitive Ca^{2+} channels (VSCC) in response to depolarisation, and via agonist operated calcium channels (AOCC) in response to Glut stimulation of the NMDA receptor (Siesjo BK 1988; Siesjo BK and Bengtsson A 1989).

An increase in free cytosolic Ca^{2+} concentrations occurs both during, and in the hours following hypoxia-ischaemia, and arises from an increased release of intracellular stores, and an increased influx across the plasma membrane (Uematsu D et al 1988; Stein DT and Vannucci RC 1988; Kirino T et al 1992). The presence of acidosis favours the unbinding of intracellular bound Ca^{2+} from the microsomes of the endoplasmic reticulum and, by changing the electrochemical gradient across the matrix membrane, causes an increased extrusion and decreased entry of Ca^{2+} from and into the mitochondria (Siesjo BK 1988). Increased Ca^{2+} flux across the plasma membrane occurs in response to depolarisation, opening VSCC, as well as stimulation of NMDA receptor AOCC by Glut. Ca^{2+} efflux through the plasma membranes is disrupted by energy failure accompanying hypoxia-ischaemia, upon which Ca^{2+}-ATPase is dependent, and by curtailment or even reversal of the Na^{+}/ Ca^{2+} exchange system (Katsura K et al 1993; Siesjo BK 1988; Siesjo BK et al 1989). Neurons in the CA3 region of the hippocampus seem to survive because of a well preserved metabolic function to cope with

excessive Ca^{2+} ions (Hashimoto K et al 1992).

The mechanisms by which increased intracellular Ca^{2+} threatens the cell relates to disturbances in the intracellular reactions subserved by Ca^{2+} (Nakamura K et al 1993). Ca^{2+} activates several lipases, proteases and endonucleases which attack the structural integrity of the cell. Endonucleases may lead to strand breaks and DNA fragmentation sufficient to lethally damage the genetic machinery. The continued activation of phospholipase C, in particularly, promotes the progressive breakdown of the phospholipid component of plasma membranes (Katsura K et al 1993; Umemura A et al 1992). Persisting alteration on protein phosphorylation may inhibit protein synthesis to the extent that the cell stores of proteins essential for cell survival, including vital growth factors, are depleted. Ca^{2+} also contributes to the generation of oxygen free radicals, via the formation of xanthine and prostaglandins (Kontos HA and Wei EP 1986). High intracellular free Ca^{2+} concentrations can lead to uncoupling of oxidative phosphorylation within mitochondria as energy is futily expended in an attempt to maintain Ca^{2+} homeostasis (Vlessis AA et al 1990). By these mechanisms, early increases in intracellular Ca^{2+} concentration during ischaemic insult will cause persistent cellular dysfunction many hours later.

The lipophilic Ca^{2+} channel blockers, flunarizine and nipodipine, are neuroprotective in several models of cerebral ischaemia. A few authors have reported efficacy when Ca^{2+} antagonists are administered to adult animals following hypoxia-ischaemia, although this has not been observed in immature animals where only pre-treatment is beneficial (Silverstein FS et al 1986; Gunn AJ 1991). Most Ca^{2+} channel blockers are poorly efficacious in reducing damage and this may relate to the marked hypotensive side-effects associated with most of these agents. Indeed, in four asphyxiated infants, a study looking at the protective effect of nicardipine, a Ca^{2+} antagonist, had to be abandoned when two subjects sustained a sudden and dramatic episode of hypotension 3 hours after the infusion was commenced (Levene MI et al 1990). This is perhaps a salutary reminder of the extreme caution that must be exercised when extrapolating from experimental findings to clinical practice. The interrelation between Ca^{2+} and Glut are illustrated in figure 4.

Figure 1.4 **Schematic diagram illustrating calcium homeostasis under physiological and pathological conditions**

Pre- and post-synaptic voltage-dependent calcium channels (VDCC) and post-synaptic agonist-operated calcium channels allow calcium (Ca^{2+}) to enter the cell. The post-synaptic agonist-operated Ca^{2+} channels are gated by 2 types of glutamate receptors. Receptors selectively activated by kainate (K) and quisqualate (Q) are linked to a channel permeable to K^+ and Na^+. By allowing Na^+ to enter, the opening of this channel leads to depolarisation. The other subtype of glutamate receptor, selectively activated by N-methyl-D-aspartate (NMDA), gate a channel permeable to monovalent cations and Ca^{2+}.

Adapted from Siesjo et al 1989

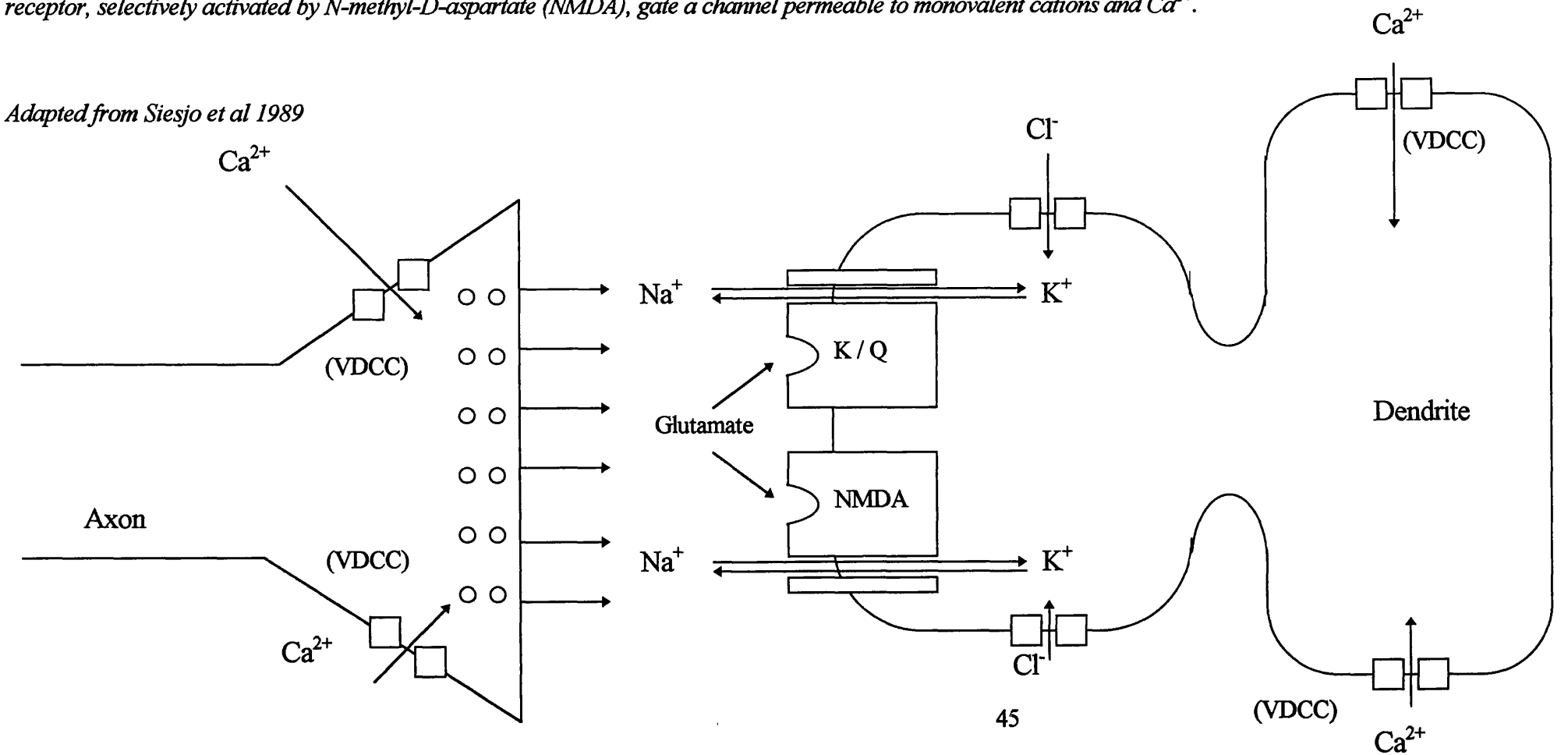

1.5.3.4 Nitric oxide and cerebral injury

The role of NO as the final mediator of neuronal death for both Glut and intracellular Ca^{2+} has been alluded to in the previous sections. Increasing evidence suggests that NO, an ubiquitous free radical gas, may have an important influence on the development of brain injury following ischaemia, although the precise mechanism remains to be elucidated (Dalkara T and Moskowitz MA 1994).

NO is synthesised during the conversion of the essential amino acid L-arginine to L-citrulline by the enzyme NOS (Moncada S 1992). In the last few years it has become apparent that there are at least two isoforms of this enzyme (Moncada S 1992). The constitutive, cytosolic, Ca^{2+}/calmodulin dependent isoform releases NO for short periods in response to receptor or physical stimulation. NO released by this enzyme acts as a transduction mechanism underlying several physiological responses. The inducible Ca^{2+} independent NOS isoform (i-NOS), induced after activation of macrophages, endothelial cells and a number of other cells, once expressed, synthesizes NO for long periods (Faraci FM and Brian JEJ 1994). Upregulation of i-NOS can occur in the presence of certain cytokines including lipopolysaccharides, interferon gamma (IFN-γ) and interleukin-beta (IL-1β) (Asano K et al 1994).

In the adult brain, biochemical evidence of enhanced NO production following ischaemia has been obtained from studies using electron paramagnetic resonance spin trapping and porphyrinic microsensors (Tominaga T et al 1993; Malinski T et al 1993). In the fetal sheep, using microdialysis techniques, a delayed increase in extracellular cerebral citrulline concentration has been observed several hours after resuscitation (Tan WK et al 1995). As a product of NOS in the generation of NO from L-arginine, this finding suggests that increased NO production occurs many hours after the initial insult and maybe involved in the development of delayed cerebral injury.

Whether NO causes neuroprotection or neurodestruction following cerebral ischaemia is a subject of much debate. It is possible that the effect incurred depends on where NO is

produced and the biochemical milieu of the surrounding environment.

The neuroprotective effect of NO depends on the influence of NO on the cerebral vasculature. NO, released from the endothelium in response to a number of agonists, relaxes smooth muscle through the activation of soluble guanylate cyclase causing an increase in cGMP. In the brain, the release of NO is thought to be involved in the maintenance of basal cerebrovascular tone, and in cerebral vasodilation associated with a number of physiological changes (Horvath I et al 1994; Ichord RN et al 1994; Niwa K et al 1993; Northington FJ et al 1992). A beneficial effect maybe incurred when endothelial derived NO acts on the vascular smooth muscle to decrease vascular tone, and on platelets and neutrophils to inhibit aggregation and scavenge free radicals. This has been shown to be particularly important during early reperfusion and NOS inhibitors can limit recovery from ischaemia and increase the extent of histological injury (Prado R et al 1993).

The neurotoxic effects of NO have been recognised both from *in vitro* and *in vivo* studies. Indeed, NO has been implicated in Glut-mediated neurotoxicity through the stimulation of the NMDA (Dawson VL et al 1991). The effect is partly mediated through the reaction of NO with SO^{-}_{2} (Radi R et al 1991). This reaction can occur when NO is produced in the vicinity of SO^{-}_{2}, as may occur during reperfusion (Beckman JS et al 1990). The reaction of SO^{-}_{2} with NO is substantially faster than the reaction with SOD and results in the generation of the powerful oxidant peroxynitrite ($OHOO^{-}$) (Huie RE and Padmaja S 1993). This decays homolytically to form species with the reactivity of OH^{-} and nitrogen dioxide (NO_2) as intermediates by a series of reactions:

$$-ONOO + H^{+} \Leftrightarrow HOONO \Rightarrow HO^{-} + NO_2$$

Peroxynitrite is not a free radical and is stable enough to diffuse for upto several cell diameters. It can efficiently oxidise sulfhydryl groups, lipids, DNA and proteins such as low-density lipoprotein, surfactant apoproteins and α-1-antiprotease (Dawson TM et al 1993). DNA damage may be central to NO neurotoxicity and occurs through base deamination and direct

DNA fragmentation. Such damaged DNA activates poly (ADP-ribose) synthetase (PARS) which, in an effort to repair DNA, depletes cells of NAD and ATP. Toxic mechanism include mono-ADP-ribosylation of nuclear proteins and S-nitrosylation of glyceraldehyde-3-phosphate dehydrogenase. These cytotoxic effects cause depletion of energy metabolites secondary to alteration of glycolytic enzymes, and depletion of energy substrates after stimulation of ADP-ribosylation. Inhibitors of poly-ADP-ribosylation protect neurons in culture from NO mediated injury. Energy is consumed in the regeneration of NAD from nicotinamide and the depletion ultimately leads to cell death (Zhang J et al 1994).

Studies have been performed to determine the overall role of NO following cerebral ischaemia although, in the face of the divergent properties of NO, it is not suprising that the results are inconclusive (Iadecola C et al 1994). The role of NO on the cerebral vasculature, and the extent of cerebral injury following perinatal hypoxia-ischaemia has not been closely investigated, and it remains unclear whether the effect of increased NO production is favourable or detrimental. The effect of NO needs to be examined in a model in which delayed cerebral injury is observed and the changes in cerebral vasculature can be continuously monitored.

Figure 1.5 **Proposed model of neuroprotective and neurodestructive action of nitric oxide on neurons**

The NMDA receptor's redox modulatory site can be downregulated by NO group transfer (S-nitrosylation with nitrosium ion (NO^+) to form S-nitrosothiol (RS-NO)), which may aid disulphide bond formation. This reaction leads to less NMDA-evoked Ca2+ influx and thus neuroprotection, involves NMDA receptor thiol groups. In contrast, if the NO group is chemically reduced to $NO^•$, it can react with superoxide anion ($O_2^{•-}$) and become neurotoxic by peroxynitrite ($OHOO^-$) formation or decomposition products. Endogenous synthesis (by the Ca2+ activated enzyme, nitric oxide synthase (NOS)) supply NO in one of several redox states, for these reactions.

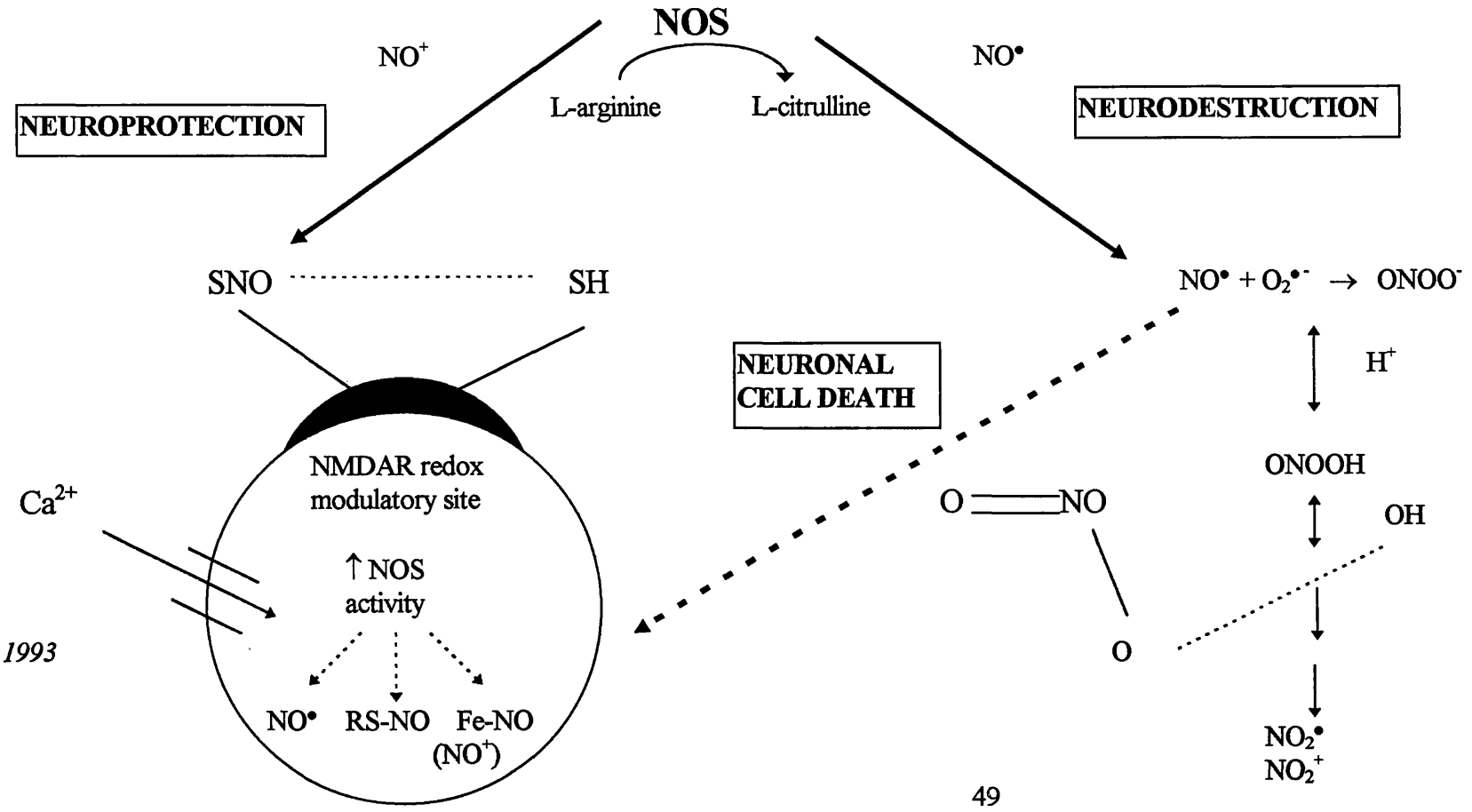

Adapted from :
Lipton SA et al 1993

1.6 Summary

Perinatal birth asphyxia remains a significant cause of subsequent neurodevelopmental impairment in the survivors. Of greatest prognostic importance is the neurological syndrome that accompanies birth asphyxia and progresses over the hours and days following resuscitation. From studies in asphyxiated infants and perinatal animal models of hypoxic-ischaemic brain injury, it is increasing clear that most neurons recovery the initial ischaemic event only to die subsequently as a consequence of the deleterious vascular, biochemical and cellular processes that are initiated. The principle pathophysiological mechanisms implicated include alterations in cerebral haemodynamics and oxygenation such that the compromised brain is subjected to further ischaemic episodes, and seizure activity that vastly increases the metabolic demands; cellular events principally involve mitochondrial dysfunction and the loss of intracellular survival signals and apoptosis; neurotoxic biochemical changes include the activation of Glu receptors, the accumulation of cytosolic calcium and the generation of free radicals, in particular NO.

The exciting conclusion is that the principle mechanisms of neuronal death in perinatal hypoxic-ischaemic encephalopathy operate after the termination of the initial insult. The implication concerning management is that interruption of this deleterious cascade, even after resuscitation from an asphyxial event, could perhaps prevent or ameliorate the extent of brain injury concurred.

Few studies have attempted to correlate the changes in cerebral perfusion and oxygenation to the secondary deterioration in cerebral energetics that occurs several hours after resuscitation from perinatal hypoxia-ischaemia. The principal difficulties in performing such studies relate to the previously employed methodology of measuring changes in cerebral perfusion and energetics. The techniques generally involve sacrificing the animals at different time points after the insult and examining the brain biochemically or histologically. Although the results of such studies have greatly improved our understanding of some of the principle mechanisms, the temporal relationship between the cascade of processes that are occurring remains unclear. This thesis is therefore directed towards combining techniques that continuously measure changes in cerebral perfusion and oxygenation, with those measuring changes in cerebral impedance and electrophysiology so that the critical role of disruptions in cerebral haemodynamics and perfusion can be related to the development of secondary deterioration.

1.7 Hypotheses

1. Changes in cerebral haemodynamics have been observed during the hours following cerebral ischaemia. Whether these changes further compromise cerebral perfusion within the already compromised brain is unknown. *The first hypothesis is that transient cerebral ischaemia in the perinatal brain, induces changes in cerebral perfusion and oxygenation that are temporally related to the early and delayed phases of cerebral injury.*

2. In asphyxiated infants, the extent of the delayed disruptions in cerebral energy metabolism correlate with neurodevelopmental outcome. *The second hypothesis is that the degree of delayed changes in cerebral perfusion and oxygenation following transient cerebral ischaemia correlate with the degree of cerebral injury.*

3. NO, possibly generated from the i-NOS or n-NOS isoforms, is thought to play an important role in the development of delayed cerebral injury. *The third hypothesis is that NOS expression is evident in the perinatal brain following ischaemia.*

4. It is unclear whether NO production is neuroprotective or neurodestructive in the perinatal brain following ischaemia. Increased NO production may cause cerebral vasodilation and improve cerebral perfusion. *The fourth hypothesis, raised from the results obtained from the first series of experiments, is that the late changes in cerebrovascular tone are mediated through an increased production of NO, and can be altered by NOS inhibition.*

5. However, NO can also generate highly potent oxidants which can promote neuronal death in culture. *The final hypothesis is that NOS inhibition alters the extent of perinatal cerebral injury following ischaemia.*

Chapter 2

Techniques employed in the experimental investigation of perinatal brain injury

2.1 Introduction

To address the hypotheses proposed in Chapter 1, techniques that continuously measure changes in cerebral perfusion and oxygenation need to be combined with those measuring the phases of cerebral injury following perinatal hypoxia-ischaemia.

Over the past decade, techniques have been developed that continuously measure these changes and therefore record the progression of hypoxic-ischaemic cerebral injury over a period of hours or days. These techniques play a major part in understanding the pathogenesis of hypoxic-ischaemic brain injury which is a cascade of processes initiated by the initial ischaemic insult and culminating in brain injury over a matter of hours or days.

Furthermore, the development of animal models of perinatal hypoxia-ischaemia have allowed the mechanisms of damage to be investigated under controlled conditions. Although a substantial extent of research has been performed on the perinatal rat model, the preparation has the disadvantage of small size which limits the extent to which the brain and systemic physiology can be investigated. The pathophysiology of hypoxic-ischaemic brain injury has been extensively investigated in the late gestation fetal sheep preparation of transient cerebral ischaemia. This preparation has the advantage of size and physiological stability, and has enabled the application of sophisticated techniques that can continuously record changes in electrophysiology, biochemistry and cerebral haemodynamics under stable conditions.

In this thesis, experiments were performed on the chronically instrumented, late gestation fetal sheep preparation of transient cerebral ischaemia. First described by Williams et al, perinatal cerebral ischaemia is induced *in utero* by bilateral carotid artery occlusion for thirty minutes (Williams CE et al 1990). The injury is associated with two phases of increased cortical impedance that represent the development of cytotoxic oedema (Williams CE et al 1991). An early phase occurring during the insult resolves following release of the occlusion; a late phase beginning 5-10 hours later and associated with the development of delayed cortical seizures, is thought to represent a progressive loss of membrane function. The advantages of this preparation over other perinatal preparations of hypoxia-ischaemia relate to the relative physiological stability associated with a fetal preparation; the developmental maturity; and the large body size of the fetal sheep by this stage of gestation.

The techniques employed in this study: near infrared spectroscopy, cortical impedance measurements and electroencephalography, are discussed in the following sections.

2.2 Near Infrared Spectroscopy

Near infrared spectroscopy (NIRS) is an optical technique which can provide crucial information concerning changes in cerebral perfusion and oxygenation continuously and repeatedly. The application of NIRS to the study of animal brain *in vivo* was initially shown most clearly by Jobsis in 1977 when he demonstrated that absorption of near infrared light of wavelengths between 700-1000 nm by soft tissue was low enough to allow spectral measurements to be made from brain when light was directed across the cranium (Jobsis FF et al 1977). Since this time, the non-invasive technique has been applied extensively to the investigation of a wide range of indices of brain oxygenation and haemodynamics in the newborn infant (Reynolds EOR et al 1988).

The NIRS method is based on 2 facts: The first is that light in the near-infrared range can pass with relative ease through skin, bone and other tissues to allow photon transmission to occur primarily through the brain. Secondly, by appropriate selection of near infrared wavelengths,

changes in light absorption that are characteristic of oxygenated and deoxygenated haemoglobin, and of oxidised cytochrome aa_3, can be used to monitor quantitatively changes in the amounts of oxygenated haemoglobin (HbO_2) and deoxygenated haemoglobin (Hb), and the oxidation-reduction status of cytochrome oxidase aa_3 ($CytO_2$), the terminal enzyme of the respiratory mitochondrial electron transport chain, which passes electrons to molecular oxygen for oxidative phosphorylation and ATP synthesis (figure 2.1).

Figure 2.1 **Schematic representation of cerebral oxygen delivery by haemoglobin and intracellular oxygen utilisation**

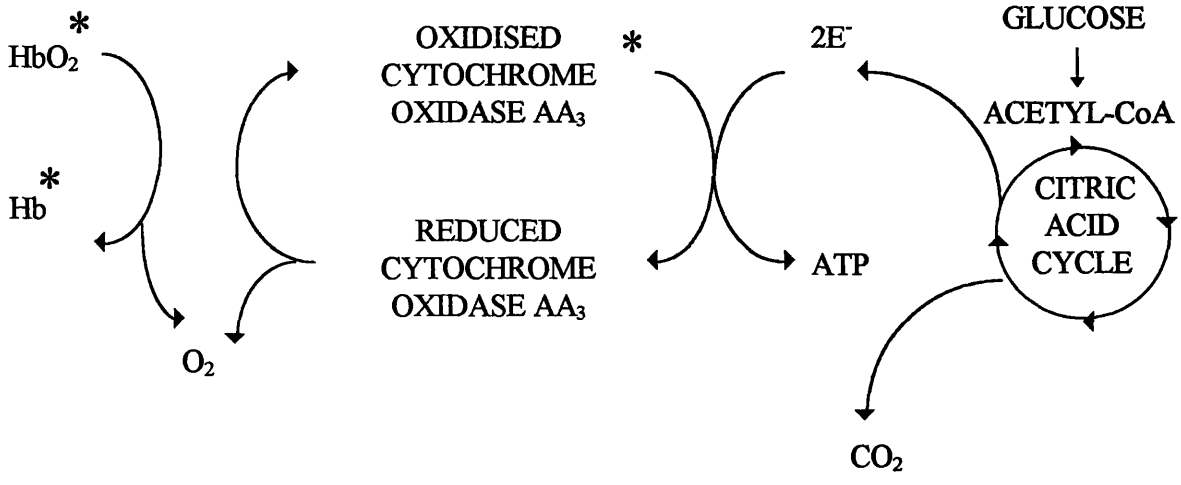

* Measured by Near Infrared Spectroscopy

There are only three chromophores with significant absorption bands in the near infrared region - oxyhaemoglobin (HbO_2), haemoglobin (Hb) and oxidised cytochrome oxidase aa_3, ($CytO_2$) the terminal enzyme of the respiratory electron transport chain. The chromophores absorb light in a characteristic manner and changes in the concentration of the chromophores can be calculated from changes in absorption of photons passing through tissue. The chromophores occupy key positions in cellular oxygenation and metabolism and by measuring changes in the concentrations of the chromophores, changes in cerebral perfusion and oxygenation can be observed over prolonged periods under normal and pathological conditions.

2.2.1 Principles of Near Infrared Spectroscopy

To obtain quantitative measurements of molar changes in HbO_2, Hb and $CytO_2$ in the brain, the following calculations are important (Cope M 1991; Cope M et al 1988). The calculation of chromophore concentration from absorption changes makes use of the Beer Lambert Law which, when describing optical absorption in a highly scattering medium, may be expressed as:

$$OD = a.c.L.B + G$$

where OD is the optical density, a is the absorption coefficient of the chromophore ($mM^{-1}.cm^{-1}$), c is concentration (mM), and L is the distance (cm) between the light entry and exit points. B is the pathlength factor that accounts for the increased optical pathlength caused by scattering and G is a geometric factor that accounts for loss of photons by scattering out of the line between the source and the detector. If L, B, and G remain constant, then changes in the optical density may be converted into changes in chromophore concentration by the relationship:

$$\Delta c = \Delta OD/(a.L.B)$$

If a, L, and B are known, it is possible to convert changes in optical attenuation (measured in OD) into changes in chromophore concentration (in $mmol.L^{-1}$) (Delpy DT et al 1988). In the presence of three chromophores measurements need to be made at a minimum of three wavelengths and, for accuracy, four wavelengths are employed by most commercially available spectrophotometers.

The extinction coefficients of HbO_2, Hb and $CytO_2$ have been determined and are shown in figure 2.2 (Wray S et al 1988). B, the pathlength factor has been derived by several methods, all of which give similar results. These include measurement of the time of flight of photons through tissues and absorption of light by tissue water (Delpy DT et al 1988; Delpy DT et al 1989; Hiraoka M et al 1993). In the brains of preterm infants, the value B has been determined by the "time of flight" method to be 4.39 (± SD 0.28) (Wyatt JS et al 1990). Quantification of spectroscopy data is possible when the end of fibreoptic fibres (optodes) are positioned at varying angles to each other on the head, with a distance between the optodes of greater than 2.5 cm (van der Zee P et al 1990).

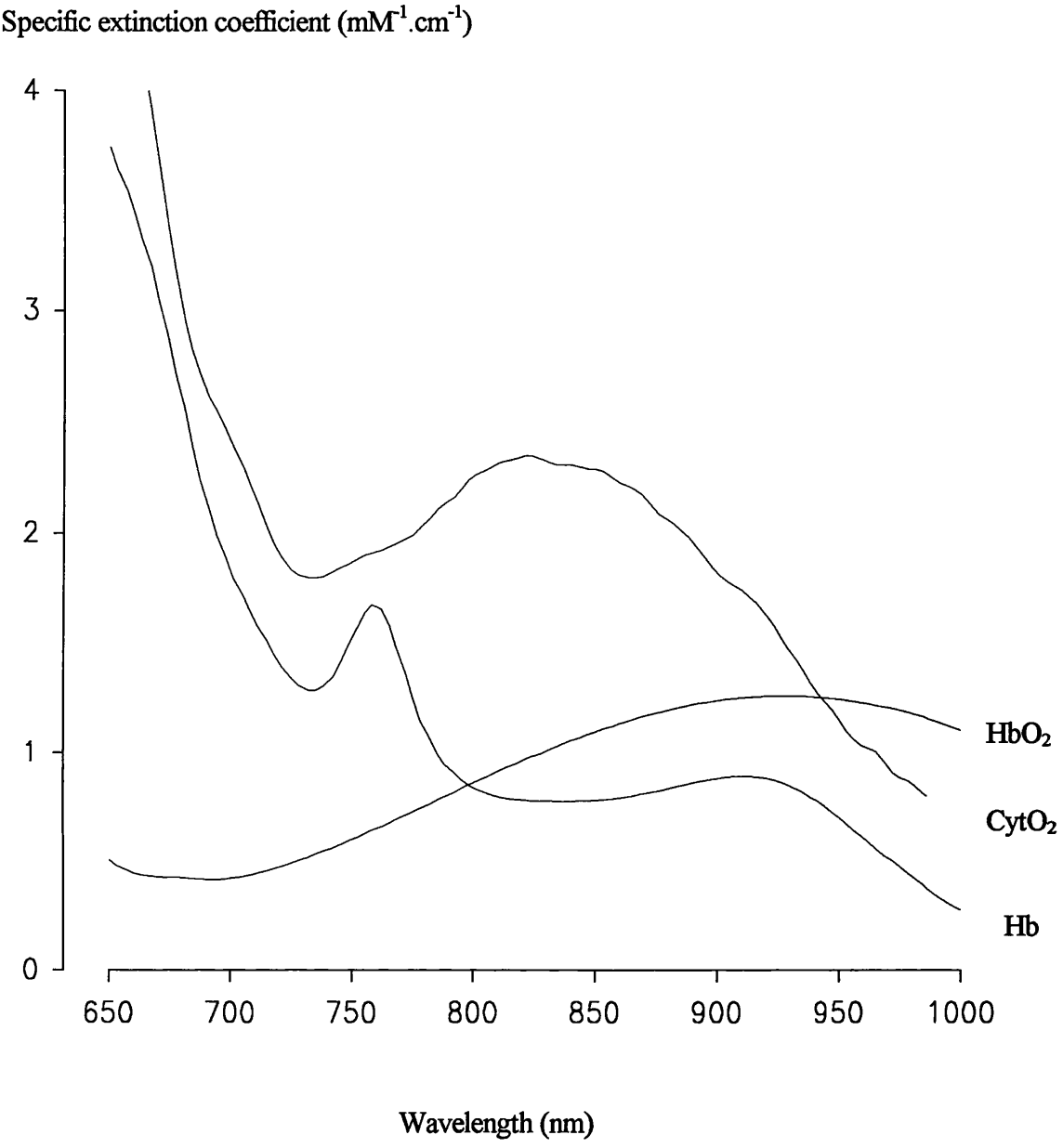

Figure 2.2 **Specific extinction coefficients of deoxyhaemoglobin (Hb), oxyhaemoglobin (HbO_2) and cytochrome oxidase difference ($CytO_2$) spectra**

Haemoglobin near infrared absorption spectra (measured as extinction coefficient $mM.cm^{-1}$) were obtained from lysed normal red blood cells fully oxygenated (HbO_2) and deoxygenated (HbR). Difference spectra for reduced and oxidised cytochrome aa_3 were obtained from rat brains following fluorocarbon exchange to remove all cerebral haemoglobin.

Adapted from: Cope 1991

2.2.2 Technical application of NIRS

The near infrared apparatus most commonly used (Hamamatsu Phototonics) employs a flexible fibreoptic bundle conveying near infrared light from laser diodes to and from the head at 4 wavelengths (774, 826, 844 and 910 nm). The ends of fibreoptic bundles or 'optodes', containing optical prisms, are applied to the skull and light transmitted across the head is conveyed to a sensitive photomultiplier tube.

Utilising the distance of optode separation derived from neonatal studies ensures that the signal detected contains an adequate component arising from brain tissue (van der Zee P et al 1990). In the neonate, with a biparietal diameter of approximately 7 cm, a minimum separation of 3 cm is advised and an even greater separation recommended (Cope M 1991). To detect a 10% change in the redox state of cytochrome oxidase, movement must be less than 0.3 mm throughout the study period, so secure fixation of the optodes is essential. A controlling computer calculates the changes in optical absorption at each wavelength and converts these into changes of [HbO_2], [Hb] and [$CytO_2$] (figure 2.3).

The detection of light transmitted from the brain is performed by a photon counting technique within a photomultiplier tube. Individual photons produce an electron at a photocathode which is subsequently amplified by accelerating the electron to hit "dynodes" where the single electron produces a number of secondary electrons. The electron current thus generated produces a voltage of adequate size to be detected electronically by a voltage comparator and converted into a digital pulse (Cope M 1991).

A safety feature built into the system detects changes in the light reflected from the surface to which the optodes are attached, and can be used to monitor the coupling between the transmitting optical fibre and the skull surface. If the signal indicates that the fibre is becoming detached (reflectance decreasing markedly), the laser diode drivers are automatically disabled.

Figure 2.3 **Application of Near Infrared Spectroscopy to measure changes in cerebral perfusion and oxygenation in the fetal sheep brain**

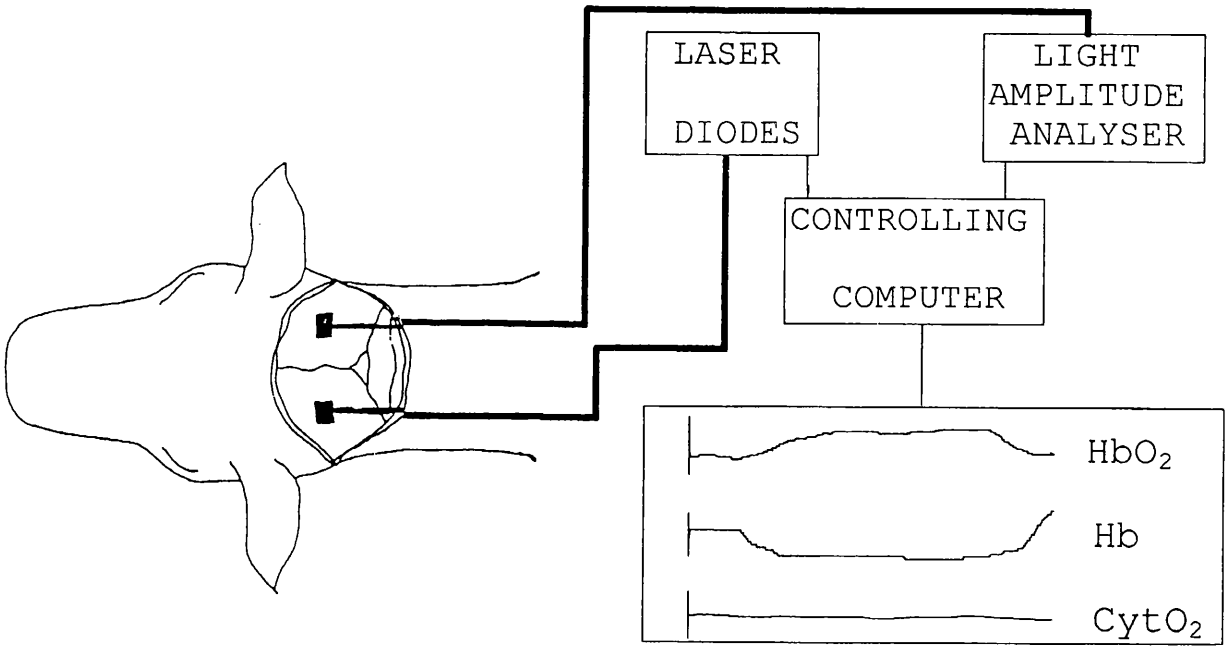

Near infrared light from laser diodes at four different wavelengths was transmitted along a fibreoptic cable to the fetal skull. The optode at the end of the cable was secured to the fetal skull with dental cement. A similar cable collected light transmitted through the fetal brain to a light amplitude analyser. The change in concentration of the chromophores oxyhaemoglobin (HbO2), deoxyhaemoglobin (Hb) and oxidised cytochrome oxidase were calculated from the changes in attenuation of the light by a controlling computer.

2.2.3 Analysis of NIRS measurements

A controlling computer is employed to calculate the changes in optical absorption at each wavelength from the near infrared light transmitted across the fetal skull. The changes in the concentration of the three chromophores Hb, HbO_2 and $CytO_2$ are then calculated using the modified Beer Lambert law. As there are three chromophores within the brain tissue (HbO_2, Hb, $CytO_2$) and light is generally transmitted at four different wavelengths, a standard curve-fitting analysis is used to increase the accuracy of the calculated concentration changes (Cope M et al 1991).

The algorithm employed in these studies is based on that published by Matcher et al 1995 from University College London (Matcher SJ et al 1995). This is a generalised algorithm determining concentration changes for Hb, HbO_2 and $CytO_2$. The concentrations are derived using multilinear regression given the specific absorption coefficients for Hb, HbO_2 and $CytO_2$ (oxidised minus reduced).

The Beer Lambert Law strictly applies to a non-scattering medium whereas light propagating through tissue is multiply scattered (the transport scattering coefficient of tissue is generally between 1-10 mm^{-1} whilst the geometrical pathlength is generally 3-5 cm). Quantification of NIRS measurements requires knowledge of the pathlength of the photons traversing the tissue, which is considerably longer than the distance between the sites of light entry and exit.

The scattering properties of brain tissue are mainly derived red blood cells (5%), mitochondria (20%) and lipoprotein membranes plus myelin sheath which constitute 50% solid contents of the immature brain. In addition to the scattering properties of a given tissue, the pathlength also varies according to wavelength and is increased as a result of increased scattering at shorter wavelengths.

The coefficients for each wavelength are scaled by the measured DPF at that wavelength. The algorithm has the matrix nomination form:

$$\begin{pmatrix} \Delta Hb \\ \Delta HbO_2 \\ \Delta CytO_2 \end{pmatrix} = \begin{pmatrix} 1.3564 & -0.9311 & -0.755 & 0.6918 \\ -0.7534 & -0.5030 & 0.0064 & 1.8817 \\ -0.1082 & 0.7928 & 0.4679 & -1.1034 \end{pmatrix} X \begin{pmatrix} \Delta OD_{774nm} \\ \Delta OD_{826nm} \\ \Delta OD_{844nm} \\ \Delta OD_{910nm} \end{pmatrix}$$

where ΔOD represents the change in detected optical density at the wavelength given in the subscript. The calculated concentration changes are then expressed in $mmol.L^{-1}$ multiplied by optical pathlength (L) for example for Hb:

$$L.[Hb] = 1.3564.\ \Delta OD_{774nm} + -0.9311.\ \Delta OD_{826nm} + -0.755.\ \Delta OD_{844nm} + 0.6918.\ \Delta OD_{910nm}$$

This algorithm therefore makes no assumptions about tissue scattering or geometry but takes into account the multiple scattering effects which make the relationship between absorption and attenuation non-linear.

2.2.4 Interpretation of results

2.2.4.1 Cerebral vascular tone and oxygenation measured by NIRS.

Haemoglobin (Hb), the most important naturally existing chromophore, is an iron containing protein with a molecular weight of 64 450 consisting of 4 subunits made up of 4 possible protein chains α, β, δ and γ. Each of the 4 subunits of Hb, in the active ferrous form (Fe^{2+}) form, can bind to a molecule of oxygen in a physical manner ie oxygenated rather than oxidised. 1 mole of Hb binds with 4 moles of oxygen to become HbO_2. The optical properties of Hb have been studied on ruptured red blood cells (Wray S et al 1988). Spectra on adult and fetal Hb indicate no perceptible differences in the NIR spectra between 650-1000nm .

Changes in concentration of total cerebral haemoglobin ([tHb]) can be calculated as a sum of the changes [Hb] and [HbO_2], and [tHb] is related to changes in CBV by the cerebral haematocrit:

$$\Delta CBV = \Delta[tHb] \times MW/([H] \times D \times R \times 10^5)$$

where MW is the molecular weight of haemoglobin, [H] is the large vessel Hb concentration in $g.dL^{-1}$, D is brain density in $g.mL^{-1}$, and R is the large vessel:cerebral haematocrit ratio (Wyatt JS et al 1991). CBV reflects the diameter of veins, arteries and the number of patent capillaries and, unlike CBF, is independent of changes in mean arterial blood pressure.

Changes in [tHb] measured by NIRS, reflect changes in cerebral vascular volume when arterial [Hb] and cerebral:peripheral haematocrit ratio remain constant. This reflects changes in cerebrovascular tone, which unlike measurements of CBF, can be interpreted without considering the arterial blood pressure. As NIRS does not determine whether vasodilatation occurs in arteries, capillaries or veins, it only offers an estimate of average vascular tone. The accuracy of NIRS in the measurement of the $paCO_2$ related changes in CBV and CBF has been confirmed by comparison with ^{133}Xe-clearance techniques in mechanically ventilated preterm infants (Pryds O et al 1990). Changes in vascular tone and blood oxygenation can readily be measured using NIRS and have been investigated extensively in the asphyxiated infant. The difference between [HbO_2] and [Hb] can be interpreted as a measure of cerebral blood oxygen saturation.

2.2.4.2 Cytochrome oxidase measured by NIRS

The histological techniques for measuring cytochrome oxidase activity in the brain all require examination of prepared brain tissue. NIRS however can monitor the changes in [$CytO_2$] *in vivo* and changes in the redox state of this respiratory enzyme may yield important information about the mechanism and timing of changes in mitochondrial oxygenation. However, the interpretation of changes in [$CytO_2$], as measured by NIRS, is complex and only reflects mitochondrial oxygenation under certain circumstances.

Cytochrome oxidase, a protein complex located in the inner membrane of the mitochondria, is the terminal enzyme of the respiratory electron transport chain. It catalyses the final electron transfer steps from cytochrome *c* to molecular oxygen, and is a member of the superfamily of haem-copper containing terminal oxidases. It is thought to consist of 2 haem groups (Cyt a, Cyt a_3) and 2 copper atoms (Cu_A, Cu_B) (Malmstrom BG 1990). The Cyt a site is closely associated with Cu_A and is described as the electron acceptor site receiving electrons from cytochrome c, whilst Cyt a_3 is closely associated with Cu_B and is the oxygen binding site (Chan SI and Li PM 1990). More recent evidence suggests that structure may be far more complex consisting of four protein subunits of which subunit 1 contains 12 membrane-spanning, primarily helical segments and binding haem a and the haem a_3-copper B binuclear centre where molecular oxygen is reduced to water. In addition two proton transfer pathways, one for protons consumed in water formation and one for 'proton pumping' have been identified (Iwata S et al 1995).

The oxidised form of cytochrome oxidase has an unusually strong absorption over a broad spectrum band within the NIR region centred at 830nm (Beinert H et al 1980; Edwards AD et al 1991). The absorption band is due to oxidation of the copper atom Cu_A at the electron acceptor site, and disappears when the enzyme is reduced and changes in the redox state of the enzyme can therefore be measured.

The rate at which electron pass down the respiratory chain is controlled by the rate of energy consumption and ATP usage. Each complex within the chain acts as an energy-conversion device and the energy generated with each step that the electrons take down the respiratory chain is stored by the pumping of protons out of the mitochondrion (Chan SI and Li PM 1990). This generates a proton motive force (Δp) across the mitochondrial membrane which is made up of an electrical gradient and pH gradient (figure 2.4).

Figure 2.4 **Energy conversion mechanism underlying oxidative phosphorylation**

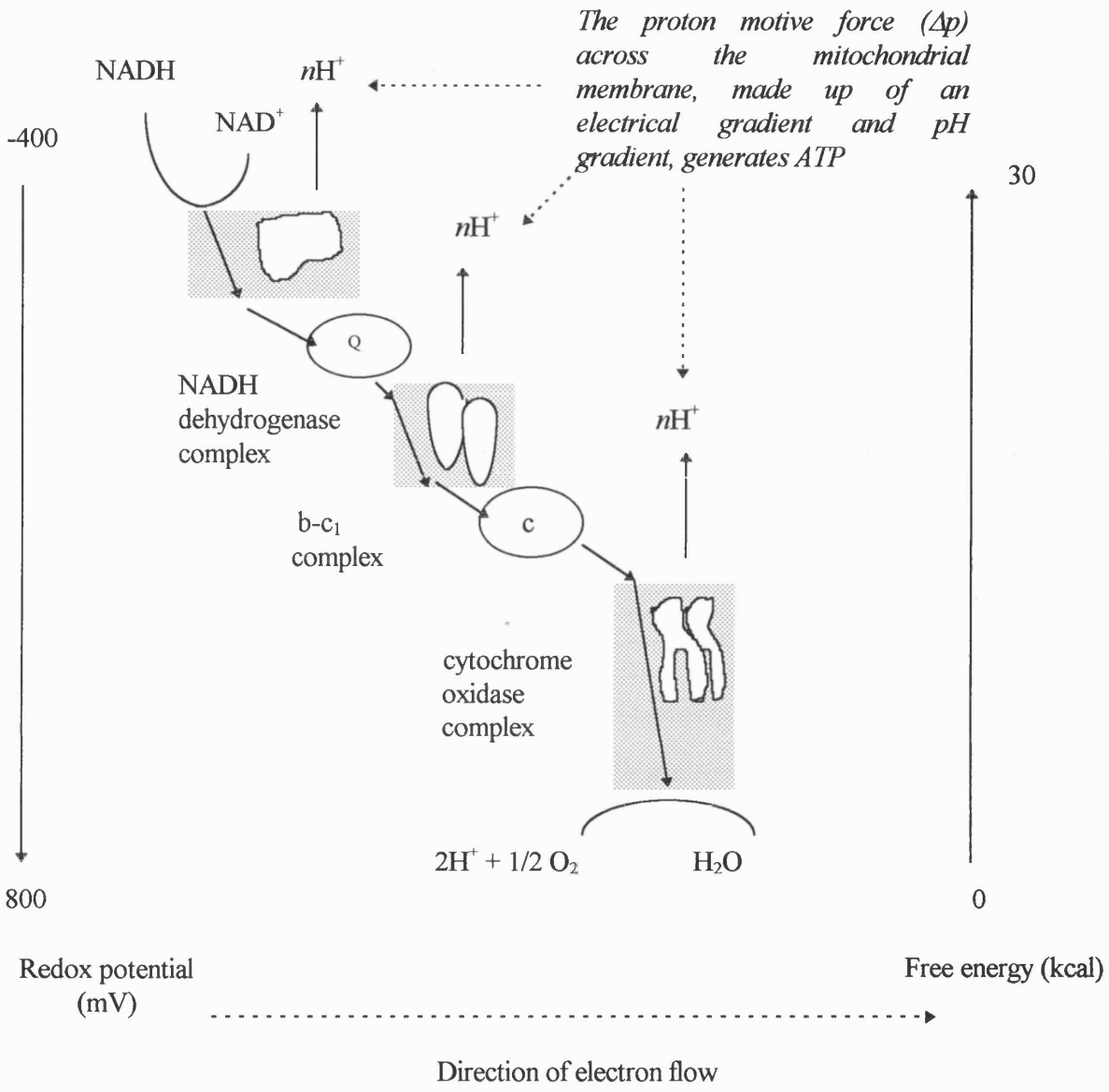

Figure 2.4 shows the energy conversion mechanism underlying oxidative phosphorylation. The redox potential drops 3 large steps, one across each major enzyme complex. The change in redox potential between any 2 electron carriers is proportional to the free energy released by an electron transfer between them. Each complex acts as an energy-conversion device and the energy generated is stored by pumping protons out of the mitochondria. The number of protons pumped per electron (n) is not known with certainty.

Δp has a strong controlling influence over respiration rate and an increased Δp leads to a decreased respiration rate. The magnitude of Δp is determined by the relative rates at which protons are pumped out of and return into the mitochondria. Increased energy utilisation results in a fall in ATP and increased cytosolic ADP. Protons pass into the mitochondria in the generation of ATP from ADP and Δp is decreased. This lowers the inhibition on the respiratory chain so that protons are again pumped out of the mitochondria and there is an increase in electron pumping down the respiratory chain. When Δp is thus increased, the respiratory chain is inhibited and protons flow back into the mitochondria with the generation of ATP from ADP. With a supply of electrons coming down the chain and in the absence of oxygen, all of the respiratory enzymes will become reduced. Alternatively, in the absence of electrons down the chain and in the presence of oxygen, all the enzymes will be oxidised. Under normal working of electrons moving down the chain, the electron donor will be at a more negative potential compared with the electron acceptor and changes in the redox state can be affected by NADH, succinate, oxygen or ATP concentration.

Changes in $[CytO_2]$ will therefore depend on the supply of oxygen; the availability of respiratory electrons; and the mitochondrial proton motive force which is determined by the rate of cellular ATP usage. Alteration in the rate of ATP utilisation; supply of reducing equivalents and mitochondrial dysfunction are all likely to have an influence on the final signal (Cooper CE et al 1994). However, alterations in $[CytO_2]$, as measured *in vivo* by NIRS, only reflect a change in mitochondrial oxygenation under certain circumstances.

In newborn infants, the NIR measurement of $[CytO_2]$ is relatively insensitive to changes in paO_2 and is most affected by changes in blood flow induced by changes in inspired CO_2 or by indomethacin, a prostaglandin synthase inhibitor used in the treatment of patent ductus arteriosus in premature infants (Edwards AD et al 1991; McCormick DC et al 1993). In these cases, regional heterogeneity may mean that small changes in the global oxygen delivery rate may cause a large change in the oxygen content of a portion of the brain, with concomitant changes in the $[CytO_2]$ signal. In mechanically ventilated rats, Cu_A redox state does not change with a reduction in the oxygen delivery rate until this is reduced below ~ 10ml $O_2.100g^{-1}.min^{-1}$ (Cooper et al. 1994). At these levels, oxygen delivery fails to reach the O_2 demand, resulting in

a fall in cerebral oxygen consumption and changes in the NAD redox state and lactate concentrations (Schlichtig R et al 1992).

In order to detect changes in cytochrome oxidase *in vivo*, the enzyme must be present in high enough concentrations to distinguish changes in its redox state from those of Hb. Studies in brain homogenates of rats have shown that the cytochrome oxidase concentrations range from 1 μM at birth to 5.5 μM upon maturity, but are significantly greater in the brains of newborn animals born at a more advanced stage of development (Brown GC et al 1991). The low concentration of cytochrome oxidase, compared with haemoglobin therefore raises the possibility of "cross-talk" when analysing the data. It is reassuring that studies in piglets and rats combining cyanide, to completely reduce cytochrome oxidase, with anoxia, to reduce Hb, suggest that the level of cross-talk is likely to be small (Tamura M 1992).

The contribution of other metals to the 830 nm band also needs consideration. Of the metal centres in the brain, cytochrome *c* is likely to interfere most with the Cu_A centre and, confusingly, the oxidised-reduced spectrum at 830 nm is almost exactly opposite for cytochrome *c* and cytochrome oxidase (Cooper CE et al 1994). It is likely that 10% percent of the signal ascribed to changes in the redox state of Cu_A are due to other redox centres/forms, and a 50% reduction in cytochrome *c* will induce a spurious 7.5% oxidation in cytochrome oxidase. Assuming a total cerebral cytochrome oxidase concentration of 5 μM, it is perhaps best to treat with caution 'cytochrome' changes significantly less than 1 μM.

A further source of error relates to changes in the scattering properties of immature brain tissue following ischaemia. These are unknown but may substantially interfere with the optical signal for $[CytO_2]$ because of the relative low concentration within the immature brain. Preliminary studies of the changes in optical pathway in newborn piglets suggest that the changes are probably small, although the final results of these studies is awaited (Wyatt, J.S. personnel communication).

In the application of NIRS to measurement of changes in cerebral oxygenation, it is best to consider changes in $[HbO_2]$ as changes in cerebral blood oxygen saturation and an indicator of

brain hypoxia, whilst changes in [$CytO_2$] reflect a wide variety of factors that alter the rate of cellular respiration.

2.3 Cortical Impedance

Cerebral oedema occurs as a consequence of perinatal HI brain injury, both in asphyxiated infants and in some perinatal animal preparations. In asphyxiated newborn infants, computerised tomography scanning and measurements of intracranial pressure suggest that brain swelling is maximal at 36-72 hours of age, and is associated with the development of cerebral necrosis which, in turn, implies a poor prognosis (Lupton BA et al 1988; Clancy R et al 1988). In the perinatal rat, cerebral oedema, determined by measuring brain water content at different time points following hypoxia-ischaemia, peaks 3 days post-ischaemia and is still present upto 6 days following the insult (Mujsce DJ et al 1990; Vannucci RC et al 1993).

Since 1956 cerebral impedance measurements have been used to measure the effect of hypoxia-ischaemia on the ion shifts between extracellular and intracellular compartments (de Boer J et al 1989). Increases in brain volume, as a consequence of increased intracellular water content, are predominantly due to intracellular swelling in the glial cells of the grey matter (Williams CE 1991). Intracellular swelling of these cells, due to failure of ionic pumps, reduces the extracellular space and thus increases tissue impedance. Persistent increases in impedance following hypoxia-ischaemia indicate tissue damage both *in vitro* and *in vivo* (Williams CE et al 1991).

In fetal sheep, studies have clearly demonstrated that there is a biphasic increase in cortical impedance (CI) following hypoxia-ischaemia (Williams CE et al 1991). A rapid early increase in CI occurs during the insult, and a delayed phase commences several hours later. The early increase occurs as a consequence of inhibition of oxidative phosphorylation causing energy failure, depolarisation and a loss of ion homeostasis. Failure to recover extracellular space after the initial insult indicates severe tissue damage and is directly related to histological outcome assessed at 3 days post-ischaemia (Tan WK et al 1993).

The delayed increased in CI is associated with a severe global ischaemic insult lasting for more than 20 minutes and is inevitably associated with the development of a significant degree of cerebral injury.

Histological evidence suggest that secondary intracellular swelling occurs when the injury is severe enough to cause tissue necrosis (Williams CE et al 1992). It indicates a delayed deterioration of membrane function suggestive of secondary tissue damage. Secondary cell swelling is coupled with cell death following transient ischaemia *in vitro* and is associated with loss of ionic homeostasis, oedema and neuronal death. Epileptiform activity is likely to contribute to the delayed increase in CI in fetal sheep by increasing the metabolic demand in an already compromised brain. However, even in the presence of MK-801, which completely abolishes delayed cortical seizures, a secondary increase in CI still occurs (Tan WK et al 1992). Continuous measurement of CI can therefore demonstrate the time course of intracellular oedema and this can be related to derangements in ionic homeostasis that occur as a consequence of alterations in cellular energy metabolism.

2.3.1 Principles of the technique

The principle of techniques measuring changes in tissue impedance depend on changes in extracellular space (Williams CE 1991). Intracellular swelling reduces extracellular space and increases tissue impedance, and the changes in impedance can therefore be used to estimate changes in extracellular space (Heroux P and Bourdages M 1994). Following cerebral hypoxia-ischaemia, increases in CI can be used to measure the time course of cytotoxic oedema that occurs as a consequence of derangements in energy metabolism and loss of ionic homeostasis across cellular membranes (Hossmann KA 1971).

Practically, tissue impedance can be measured by injecting a small electrical current through a pair of electrodes and measuring the potentials generated by a further pair of electrodes. The Maxwell relationship can then be utilised to determine the impedance or resistivity (R) of a tissue according to the electrode geometry (G), voltage signal (V) and the injected current (I) (Williams CE et al 1991). The relationship assumes tissue homogeneity:

$$R = G\,x\,V/I$$

With a constant current source and fixed electrode geometry the relationship becomes:

$$R = k\,x\,V$$

where k is a constant. With these assumptions, changes in tissue impedance are proportional to changes in voltage amplitude.

Given the heterogeneity of the brain, the assumption of the modified Maxwell equation fails, and the extent to which it fails depends, in part, on the size of the electrode array with respect to the structure investigated. A structure will appear homogenous if it is much larger than the dimensions of the electrode array.

Given the large size of the cortex as a whole and the high impedance boundaries, the changes of impedance will reflect the changes of resistivity of the parasagittal grey matter. A small electrode array with a defined geometric factor (G) would need to be used to accurately measure the absolute resistivity of the parasagittal grey matter.

2.3.2 Technical approach for measuring CI

A four electrode technique is used to measure changes in impedance that occur concomitantly with changes in extracellular space within the parasagittal cortex (Robillard P and Poussart D 1979; Williams CE et al 1991). The four electrode approach diminishes the artifacts arising from electrical polarisation at the medium-electrode interface induced by electrode contact in a two electrode system.

An isolated current source is used to inject a sinusoidal current of ±0.2 μA at 150 Hz bilaterally via one pair of electrodes through the parasagittal cortex. The other pair of electrodes record the subsequent voltage signal. The voltage recording electrodes are

connected to a high impedance amplifier (10^{12} ohm) to minimise currents at the electrode interface, that also generate polarisation artifacts. In addition, capacitive loading of the voltage electrodes is reduced by lowering the frequency of the current source. The subsequent impedance signal is superimposed on the unfiltered EEG signal, and an eighth order 30 Hz low pass filter is used to ensure that this does not contaminate the ECoG signal. The low amplitude impedance signal is then extracted with a powerful phase sensitive detection technique. This extracts the 'in phase' correlated impedance signal by averaging out the uncorrelated 'noise' (figure 2.5).

Spatial resolution is determined by the geometry of the electrodes, chosen to resolve impedance changes in the parasagittal cortex as a whole. The total measurement, as opposed to local measurement, is done to reduce the variability of the measurements as a consequence of the heterogeneity of damage within the parasagittal cortex. The high resistivity of white matter (700 ohm.cm^{-1}) compared to the grey matter (300 ohm.cm^{-1}) creates boundaries that further focal the impedance current through the parasagittal grey matter (Williams CE 1991).

Impedance techniques are limited in the estimation of absolute values of extracellular space. Fixed electrode geometry and an homogenous media are assumed and the changes in extracellular space are estimated from impedance measurements. Although the geometric factor for the electrodes is not known, it is taken to be constant for each study and similar between animals.

Figure 2.5 **Measurement of cortical impedance in the fetal brain**

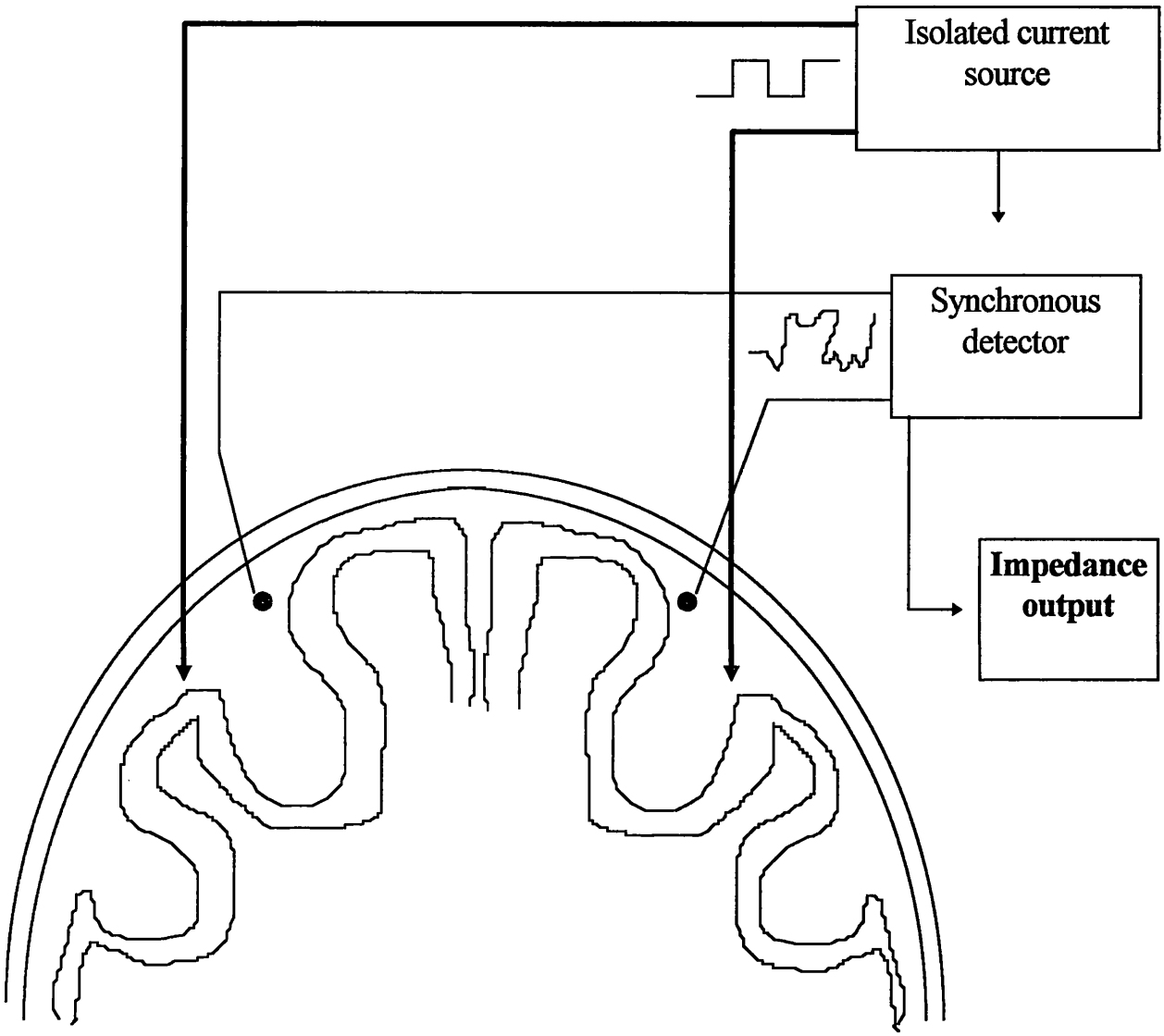

Figure 5 shows the technique of impedance measurements through the parasagittal cortex. A small 150Hz current (isolated) is injected through one pair of electrodes, the potentials generated by the resitivity of the tissue are measured by the second pair. To resolve the small signal obscured by electroencephalographic activity, a synchronous detector is utilised

Adapted from: Williams CE 1991

2.4 Electrocortical Activity

The response of the brain to injury is reflected by changes in the neuronal activity that evolve over a period of many hours. Electroencephalography (EEG) involves recording the electrical activity within the brain generated as a summation of potentials from synchronous neuronal activity. In the asphyxiated infant, EEG changes provide valuable information concerning the severity of the injury (see section 1.4.1). The multifocal or focal sharp waves or spikes observed on the first day following resuscitation progresses to a periodic pattern with more severe voltage suppression and fewer bursts, characterised by spikes and slow waves. This "burst suppression" pattern is particularly ominous and may evolve into an isoelectric tracing and a hopeless prognosis (Grigg Damberger MM et al 1989).

Continuous monitoring of EEG is particular useful in recording the progression from depressed amplitude and frequency, to intense seizure activity, to further voltage depression and isoelectric recordings. Neonatal seizures are an important prognostic feature of perinatal hypoxic-ischaemic brain injury and are associated with poor neurological outcome and the development of cerebral infarction when they persist for more than 30 minutes (Wical BS 1994).

After hypoxic-ischaemic injuries to fetal sheep, cortical cytotoxic oedema increases synchronously with the development of delayed cortical seizures, and may further compromise cellular metabolism (Williams CE et al 1992). Delayed seizures are therefore an important contributor to the secondary deterioration associated with severe cerebral hypoxia-ischaemia. In addition, seizure activity causes marked alterations in cerebral haemodynamics that may further compromises cerebral metabolism (Johnson DW et al 1993; Perlman JM and Volpe JJ 1983).

2.4.1 Physiological basis of the EEG signal

Both normal EEG and epileptiform activity are generated as a spatial summation of potentials (dipoles), generated by electrical activity in neurons (Williams CE et al 1990). In the cortex

these potentials are generated by electrical activity in pyramidal cells perpendicularly orientated to the surface of the cortex. All EEG recordings are bipolar and measure the potential difference between two recording sites (Williams CE et al 1991). To provide the necessary spatial resolution both recording electrodes must be situated close to the structure of interest. EEG is generated by synchronous activity of a population of cells and indeed in the brain electrical activity is synchronous over several centimeters (Williams CE 1991).

When a bipolar channel of parietal electocortical activity (ECoG) is recorded continuously, intensity spectra can be obtained by real time spectral analysis (Williams CE et al 1990; Williams CE and Gluckman PD 1990). Although intensity represents the activity of the neurons, the electrophysiological mechanism determining the ECoG frequency characteristics of the cortex are less clear. They are thought to derive from local circuit parameters especially the duration of inhibitory postsynaptic potentials. Recurrent collaterals from cortical pyramidal cells, feed back to stellate inhibitory cells that in turn inhibit the pyramidal cells. This feedback loop is likely to determine some of the global frequency characteristic of the cortex. The mechanisms regulating the frequency characteristics of the ECoG are unclear, so interpretations of changes in frequency characteristics should be restricted to those that correlate with well defined states of cortical activity.

2.4.2 Technical Application

Parasagittal EEG can be continuously quantified with real-time spectral analysis by a technique first applied in a fetal sheep preparation of cerebral hypoxia-ischaemia by Williams et al (Williams CE and Gluckman PD 1990). EEG activity is measured with extradural recording electrodes with coaxial leads placed at fixed positions on the dura overlying the parasagittal cortex. To minimise movement artifacts the electrode shields are actively driven to the electrode potential with voltage followers.

The system continuously analyses ECoG for intensity versus frequency content, and saves averaged 'data reduced' intensity spectra to disk at regular intervals. The ECoG signal is amplified 10,000 times, low pass filtered at 30 Hz and sampled at 256 Hz. For smoothing, an

eighth order Butterworth low-pass filter is used with the cut-off frequency set with the -3 decibels (dB) point at 30 Hz. ECoG intensity is logarithmically transformed as such data give a better approximation to the normal distribution (Gasser T et al 1982). The method has adequate frequency resolution for ECoG analysis and has the benefit of significant data reduction for long term ECoG studies.

2.5 Summary

The fetal sheep model of transient cerebral ischaemia provides a stable, unanaesthetised preparation in which the electrophysiological and haemodynamic changes can be studied over a period of several hours. In addition the large fetal sheep size at late gestation enables the application of sophisticated techniques for monitoring the responses of the fetal brain.

The technique of NIRS when combined with those measuring continuous changes in CI and ECoG allow for the temporal relationship between changes in cerebral perfusion and oxygenation to be related to the phases of cerebral injury following cerebral ischaemia. This is particular relevant for the investigation of perinatal hypoxic-ischaemic brain injury which is a progressive process over a period of hours to days in which the derangements that occur several hours following the initial injury are particularly critical in determining the extent of injury.

Chapter 3

General Methodology and Experimental Approach

3.1 Introduction

The studies in this thesis combined the technique of NIRS with those measuring changes in CI and ECoG in an *in utero* preparation of transient cerebral ischaemia induced in chronically instrumented late gestation fetal sheep. The principles of the techniques have been described in detail in the previous chapter, and the methodology and experimental protocol will be discussed in the subsequent sections.

As already described in chapter 2, the model of transient cerebral ischaemia developed by Williams et al in 1991 has the advantages of physiological stability particularly with regard to temperature control; developmental maturity; and the large body size which allows for complex instrumentation of the brain and the systemic circulation (Williams CE et al 1991).

The cerebral vascular anatomy of the sheep allows for restriction of cerebral blood supply to the carotid arteries by ligation of the anastomoses between the vertebral arteries and the carotid arteries. This is possible because the basilar artery is not supplied by the vertebral arteries but from the Circle of Willis, and therefore receives its blood supply only from the carotid arteries after the vertebro-carotid anastomoses have been ligated (Baldwin B and Bell F 1963). Therefore after surgical ligation of the vertebro-carotid anastomoses, occlusion of the carotid arteries induces global cerebral hypoperfusion to all regions of the fetal brain without systemic compromise.

Late gestation in the fetal sheep is considered to be any period beyond 119 days, where term is 146 days. At this time, the neuronal maturation and the degree of myelination reflect that observed in the term newborn infant. In addition, at this late stage of gestation, skin maturity, fused cranial sutures and overall large fetal size improves the risks associated with surgery and the accuracy of the techniques utilised in this study.

The experimental procedures conducted in these studies were performed some days after surgery, giving the fetus time to recover from the stresses of surgery and the influences of anaesthetic agents. Previous studies using this preparation have confirmed, with recordings of electroencephalographic activity, that normal sleep cycling is well established within a day of surgery (Dawes GS et al 1972). In addition, ready access to the fetal circulation allows for repeated measurement of arterial blood gases and mean arterial blood pressure so that the fetal 'well-being' can be repeatedly assessed throughout the subsequent days. All experiments were performed *in utero* so that brain and body temperature were maintained at a constant level according the maternal temperature. This is particularly advantageous in view of the critical influence of brain temperature on determining the extent of ischaemic brain injury in the immature brain (Yager J et al 1993)

Several hours after the carotid artery occlusion is released, secondary deterioration is a well recognized feature of the late, gestation fetal sheep preparation. A delayed increase in CI and the development of delayed cortical seizures can be measured from electrodes positioned on parasagittal cortex (Williams CE et al 1990; Williams CE et al 1991). The increase in CI is thought to represent a derangement of ionic homeostasis across cellular membranes (de Boer J et al 1989). Continuous measurement of changes in CI can be recorded and allows the temporal changes in energy metabolism to be related to other parameters.

The fetal sheep studies were conducted in the laboratories of Professor PD Gluckman in the Research Centre for Developmental Medicine and Biology at The University of Auckland, New Zealand during two lambing seasons. All studies were approved by the Animal Ethical Committee of the University of Auckland.

3.2 Surgical procedure

Romney Suffolk singleton fetal sheep from 119-133 days gestation were operated on under 2% halothane/oxygen general anaesthesia using sterile techniques. The ninety minute procedure involved externalization of the fetal head, neck and forelimbs and placement of polyvinyl catheters into two axillary arteries, brachial vein and amniotic cavity for measurement of mean arterial blood pressure (MAP), arterial blood sampling and antibiotic drug administration (Williams CE et al 1992). For experimental drug administration, an umbilical vein catheter was inserted into a tributary branch of the vein identified within any large cotyledon in the pregnant horn of the uterus.

The scalp was retracted to expose the fetal skull and through burr holes, three pairs of shielded stainless steel electrodes (AS636 1SSF, Cooner Wire Co., Chatsworth, CA, USA) were placed on the dura overlying the parietal cortex. Two pairs of electrodes recording ECoG were placed 10 mm lateral to bregma at 5 mm and 15 mm anterior to bregma. A third pair of stimulating electrodes was placed 15 mm lateral and 10 mm anterior to bregma for the measurement of changes in CI (Figure 3.1). A further pair of stainless steel wire electrodes (AS636 Cooner Wire Co., Chatsworth, CA) were sewn into the paraspinal nuchal muscle to record electromyographic activity (EMG).

Two fibreoptic cables transmitted near infrared light from laser diodes at 4 wavelengths (774, 826, 844 and 910 nm) to and from the fetal head. The ends of the fibre bundles or optodes, containing an optical prism, were surgically fixed onto each side of the parietal region of the skull with dental cement at least 3.5 cm apart and equidistant from the midline. The distance of optode separation, derived from neonatal studies, is critical to ensure that the signal detected contains an adequate component arising from brain tissue (van der Zee P et al 1990). Permanent fixture of the optodes to the skull was essential for measurement of the redox state of [$CytO_2$], as movement must be less than 0.3mm in order to detect a 10% change.

Figure 3.1 **Schematic illustration of the fetal head instrumentation**

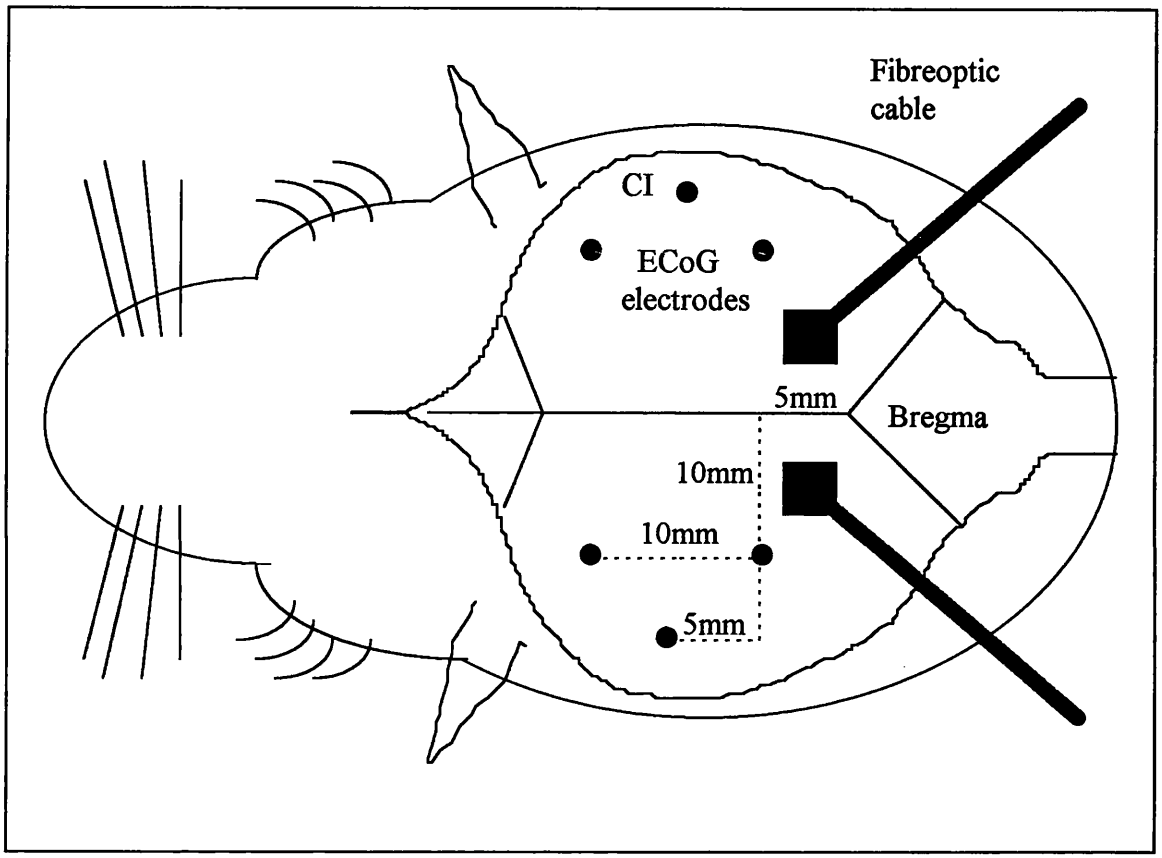

The figure shows the fetal head demonstrating the exposed fetal skull and the placement of 2 pairs of electrocortical (ECoG) electrodes and one pair of cortical impedance (CI) electrodes through burr holes onto the dura overlying the parasagittal cortex at fixed positions in relation to bregma (see text). A pair of fibreoptic cables transmitted and collected near infrared light to and from the fetal brain

After securing the electrodes and optodes onto the fetal skull, the neck was exposed and incisions of 5-8 cm were made longitudinally from the mandibular angle to expose the carotid arteries bilaterally. Lateral and medial vertebro-occipital anastomoses between the carotid and vertebral arteries were identified bilaterally and ligated.

The procedure eliminated all collateral blood supply to the carotids and restricted cerebral blood supply of the brain to these vessels. On each carotid artery, a double ballooned inflatable occluder was positioned and secured. The neck incisions were closed and the fetus was returned to the uterus; the connecting lines were externalised through a uterine and maternal lateral skin incision and muscle and skin layers were closed. A catheter was placed in a maternal vein within the hind leg for infusion of pentobarbital at the end of the study period.

After surgery, ewes were housed in metabolic wooden cages at a constant temperature (16°C) and humidity (50%) and given free access to hay and water supplemented by sheep nuts and alfalfa. Antibiotics (gentamicin 80mg intravenously to the fetus and penicillin 500mg intramuscularly to ewe) were administered daily for 3 days following surgery.

3.3 Techniques

3.3.1 Application of NIRS in the fetal sheep

The technique of NIRS has to date predominantly been utilised to investigate the cerebral haemodynamic responses in neonates. Therefore certain adaptions had to be made before the technique could be applied for the investigation of changes in cerebral perfusion and oxygenation in the chronically instrumented fetal sheep. Optodes and fibeoptic cables had to be developed that could be autoclaved between operations as the surgical procedures were all performed under strict sterile conditions. Furthermore, optodes and cables had to be constructed to tolerate continuous exposure to body fluids over a prolonged period of several days without decomposition or leakage.

In addition, a technique had to be developed for permanently fixing the optodes to the fetal head during surgery but allowing easy removal at post-mortem without damaging the delicate optode head or cable. Finally, ewes were awake and active, and maintained individually in wooden cages some distance from the computer equipment. Therefore the cables had to be long and flexible in order to allow maximum motility for the ewes and securely positioned so that they would not be damaged by movement or eaten. There was no problem of occluding ambient light as all experiments were performed *in utero*.

3.3.1.1 Construction of optodes and fibeoptic cables

The optodes and fibreoptic cables were made specifically for these studies by Idris Roberts according to the specifications described by Cope (Cope M 1991). The cables consisted of a bundle of glass fibres, each of 50 μm diameter (Eurotec Optical Fibres Ltd, U.K.). The bundles, which were made up of many thousands of small glass fibres to a diameter of 10 mm, were made to approximately 2 metres length. The end of the fibreoptic bundle was glued and then smoothed by delicate filing. Each bundle was then encased in a flexible, autoclavable, black polyvinyl chloride (PVC) sheath. At the proximal end of the cable, an optical prism which was employed to reflect transmitted light by 90° onto the skull surface, was glued to the smoothed end of the glass bundle. At the distal end, a connector was fixed to allow the cables to be attached to the commercial near spectrophotometer employed in these studies (NIRO 500 Hamamatsu Phototonocs KK, Hamamatsu City, Japan).

Prior to autoclaving, the optode heads were liberally coated with silcone glue. This ensured that any possible defect in the materials, that might allow leakage of body fluids into the cable, was blocked. In addition, the silicone glue allowed the cable heads to be readily removed from the fetal skull. The cables were thoroughly washed to remove all tissue debris between surgeries and then autoclaved.

3.3.1.2 Placement of the optode head on the fetal skull

Fixture of the optode heads to the fetal head had to guarantee no movement during the study period and easy removal at post-mortem so that the expensive cables could be recycled at least three times. This was best achieved by applying the optode heads directly to the fetal skull. The skull was exposed by retraction of the scalp and the area of skull overlying the parasagittal cortex bilaterally was then cleaned and dried. The 2 optode heads were secured within small metal holders and then glued to the fetal skull at an equal distance either side of the midline and a minimum distance of 3.5 centimetres using superglue. Having secured the optodes, the area was completely covered with dental cement. This technique secured the optodes to the fetal skull with no possibility of movement, even if the cranial sutures were not completely fused. Furthermore at post-mortem, the dental cement block containing the optodes in the metal holders could be detached complete from the fetal skull and the optodes removed undamaged by snapping the metal holder backwards.

3.3.1.3 Fixture of the fibreoptic cables

The cables were externalised through an incision in the left lateral abdominal wall of the ewe. They were then secured to the back of the ewe with a tie superficial positioned through the skin immediately adjacent to the spine. The cables were protected along their track by tunneling through the sheep's thick wool fur. The cable length between the sheep and the NIRO 500 was protected with foil and suspended form the wooden cage with elastic bands such that it was not trampled but allowed for maximum motility. Furthermore on recovering from the anaesthetic the ewes were loosely collared so that the cables were not within eating range.

The measurement of the changes in cerebral perfusion and oxygenation NIRS have been described in detail in chapter 2.

3.3.2 Cortical impedance

The four electrode technique described in chapter 2 was used to measure continuous changes in CI that are known to occur concomitantly with changes in extracellular space within the parasagittal cortex. This technique has been developed over the last 5 years by Dr. CE Williams at the Research Centre for Developmental Medicine and Biology, The University of Auckland. It has been repeatedly used to estimate the degree of cytotoxic oedema following transient cerebral ischaemia in fetal sheep. The two phases of increase CI that follow thirty minutes transient cerebral ischaemia in late gestation fetal sheep is thought to reflect disruptions in membrane function that occur as a consequence of disruptions in cerebral energetics. The measurement provides a means of following the phases during which perinatal brain injury develops.

CI is measured from electrodes placed through burr holes on the dura overlying the parasagittal cortex bilaterally, and reflects the changes that occur within the brain tissue that spans the electrodes. It is therefore primarily a reflection of parasagittal cortical impedance, and this placement reflects the fact that this region is most predominantly injured by the insult incurred.

The impedance signal is calibrated at the start of the study period, at 10 and 100 ohms such that the percentage change, rather than specific impedance, was measured. As with all techniques measuring impedance, the technique is limited to an estimation of absolute values of extracellular space. It was assumed in these studies that the electrode geometry was fixed and the media homogenous. Although the geometric factor for the electrodes is not known, it can be considered to be constant for each study and similar between animals.

Changes in CI were processed on-line and averaged over one and ten minute intervals and recorded on magnetic disc for later analysis using a data base acquisition programme (Labview for Windows Version 2.5.2, National Instruments, Austin, Tx).

3.3.3 Electrocortical activity

The measurement of ECoG intensity and frequency allows for confirmation of cerebral ischaemia induced by carotid artery occlusion and for continuous recording of the changes induced by a severe cerebral ischaemic insult. Again the technique, which is described in chapter 2, is well established in the investigation of transient cerebral ischaemia in the chronically instrumented late gestation fetal sheep.

Recording of ECoG activity is important in understanding the significance of changes in cerebral haemodynamics and oxygenation. Cerebral electrical activity is characteristically coupled with CBF such that blood flow is increased during periods of hyperexcitability. A bipolar channel of parietal ECoG was recorded continuously from the electrodes placed on the dura overlying the parasagittal cortex and intensity spectra are obtained by real time spectral analysis (Williams CE et al 1990; Williams CE and Gluckman PD 1990).

The system continuously analysed ECoG for intensity versus frequency content, and saved averaged 'data reduced' intensity spectra to disk at regular intervals. The method has adequate frequency resolution for ECoG analysis and has the benefit of significant data reduction for long term ECoG studies. The ECoG signal was amplified 10,000 times, low pass filtered at 30 Hz and sampled at 256 Hz. For smoothing, an eighth order Butterworth low-pass filter was used with the cut-off frequency set with the -3 decibels (dB) point at 30 Hz.

ECoG intensity was logarithmically transformed to give a better approximation to the normal distribution (Gasser T et al 1982). Elimination of short term fluctuations less than 20 minutes was accomplished by on-line smoothing with a digital Blackman filter with a cutoff of 0.1 cycles.point^{-1}. Cortical hyperexcitability, indicated by the development of intense low frequency activity, was defined as ECoG intensity of $\geq$ -5 dB with a shift towards the delta frequency band (1.25-4.50 Hz). Seizures were confirmed by inspection of EMG activity on the chart recorder.

3.3.4 Mean arterial blood pressure

Continuous recording of changes in MAP of the fetus were important for determining fetal well-being and for relating changes in cerebral perfusion to changes in the systemic circulation. MAP was recorded from catheters positioned in the axillary arteries of the fetus. Using a transducer to measure pressure, MAP was recorded from both arteries in parallel and adjusted electronically for changes in amniotic pressure (AP). Changes in AP occur in association with position of the ewe (standing or recumbent), and in the presence of uterine contractions. The AP changes need to be subtracted form the pressure trace of the fetus for accurate MAP recording. AP was recorded from a catheter fixed to the fetal hindlimb within the amniotic space.

3.3.5 Histological assessment

3.3.5.1 Neuronal scoring

The accuracy of the histological technique was important for determining the relation between the degree of disruptions in cerebral perfusion and oxygenation, to the extent of cerebral injury. The histological assessment employed involved a technique of neuronal scoring that is well established as an accurate method for comparing between groups of animals who have undergone comparable insults (Tan WK et al 1993; Tan WK et al 1992; Gunn AJ et al 1994).

After the brains had been fixed, blocks of tissue from one cerebral hemisphere were processed and embedded in paraffin wax. Coronal sections were cut at 8 μm thickness and stained with acid-fuchsin (Lees GJ 1989). For staining, sections of the brain were defatted with 95% ethanol and then incubated for two minutes with 0.1% acid-fuchsin solution acidified with acetic acid, washed three times with distilled water and dehydrated through ethanol, butanol and xylene. Fresh solutions of acid-fuchsin were prepared weekly, or after a maximum of ten batches of sections. Alternative sections were counterstained with Nissl dye (thionine) to provide anatomical markers.

Neuronal scoring is a well established technique for determining the extent of histological injury within the brain and for comparing between subjects. Neuronal score is determined on sections by light microscopy at a magnification of x 400. Based on previous studies using this experimental preparation, areas in the brain were selected to include those most susceptible to ischaemic injury (Gluckman PD and Parsons Y 1983). The regions of the parasagittal cortex examined coincided with the position of the electrodes and included all the gyri bordering the sagittal sulcus, and the medial half of the laterally adjacent gyrus. Lateral cortex, including all the most lateral gyri in the section, regions of the hippocampus, striatum, amygdala and thalamus were also examined. Each region was scored in multiple preselected areas for the proportion of dead neurons. The regions of brain examined are shown in figure 3.1.

Neurons with ischaemic cell change were identified according to the criteria of Brown and Brierley (Brown AW and Brierley JB 1966). Cells with acidophilic (red) cytoplasm and contracted nuclei or with just a thin rim of red cytoplasm with pyknotic nuclei were assessed as dead, whereas all others were considered viable. The mean values from two sections and from both right and left hemisphere were used. Each region was scored using a six point damage scale in which the nominal damage score was taken as the midpoint of the range as follows:

0 = no dead neurons, 5 = 1-10%, 30 = 11-50%, 70 = 51-90%, 95 = 91-99%, 100 = 100% dead neurons.

The neuronal scoring allowed animals within and between groups to be compared in order to determined the significance of delayed changes in cerebral perfusion and oxygenation. The brains were examined by the author and the findings confirmed by an independent assessor (Dr CE Mallard) who has extensive experience in the preparation and neuropathology.

Figure 3.2 **Diagram showing regions of the fetal sheep brain assessed for neuronal score after transient cerebral ischaemia**

The coronal sections shown in this figure are 15, 20, 24 and 29 mm anterior to the stereotaxic zero reference. Hippocampal damage was determined at 13 and 15 mm. Abbreviations: AA amygdaloid area; AM anteromedial nucleus; AV anteroventral nucleus; APT anterior pretectal nucleus; AV anteroventral nucleus; Cd caudate nucleus; AML external medullary lamina; LG lateral geniculate nucleus; MPt medial pretectal nucleus; Pul pulvinar of thalamus; Put putamen; Ret reticular nucleus; VA ventral anterior nucleus; VL lateral ventricle; VPL ventral posterolateral nucleus; VPM ventroposteromedial nucleus of the thalamus

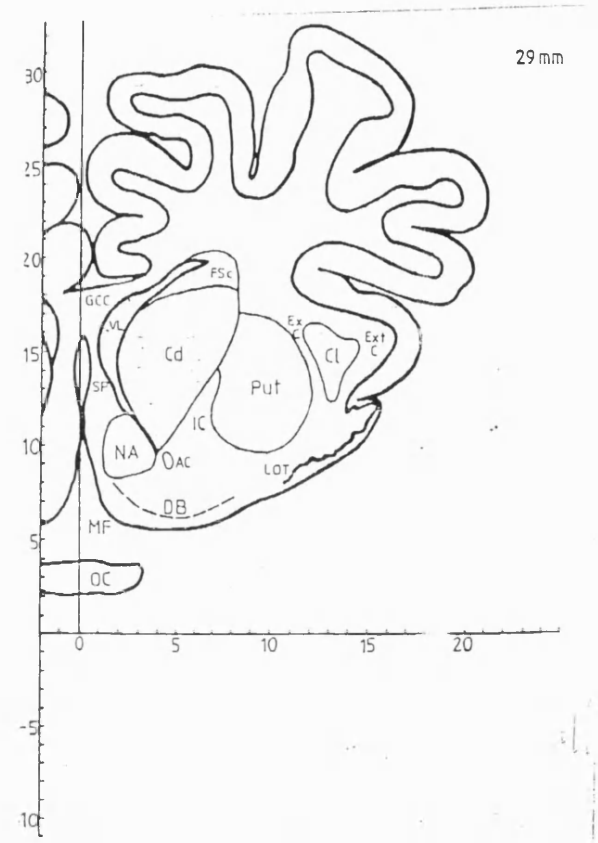
29 mm
FSc
GCC
VL
Cd
Put
Ex C
Cl
Ext C
SF
IC
NA
AC
LOT
DB
MF
OC

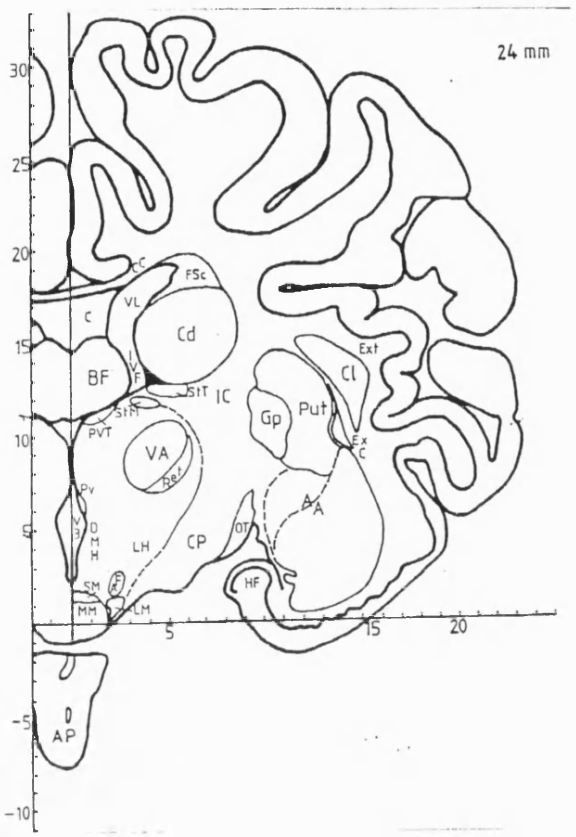
24 mm
FSc
VL
Cd
BF
IC
Ext
Cl
Gp
Put
Ex C
StT
StM
PVT
VA
Ret
LH
CP
OT
HF
LM
AP

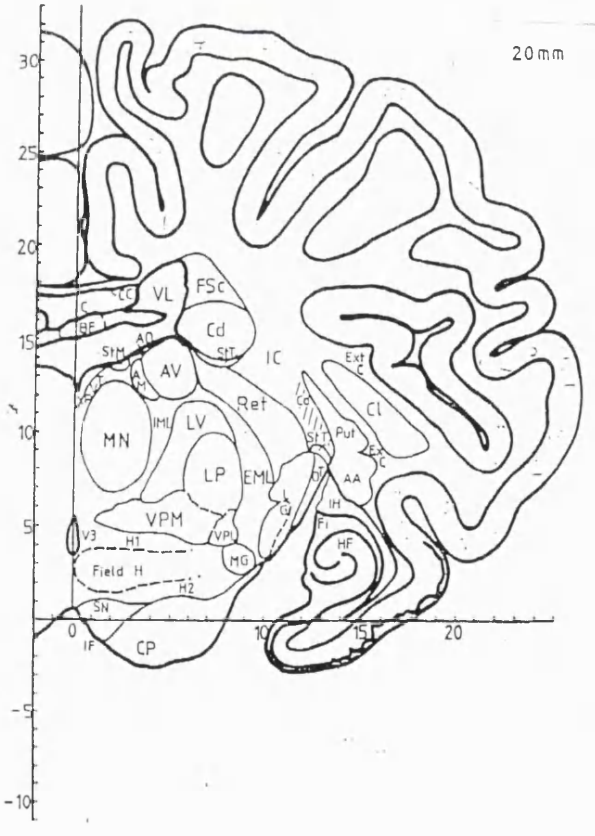
20 mm
VL
FSc
Cd
IC
AV
Ret
Ext C
Cl
MN
LV
Put
LP
EML
AA
VPM
VPl
MG
Field H
HF
SN
IF
CP

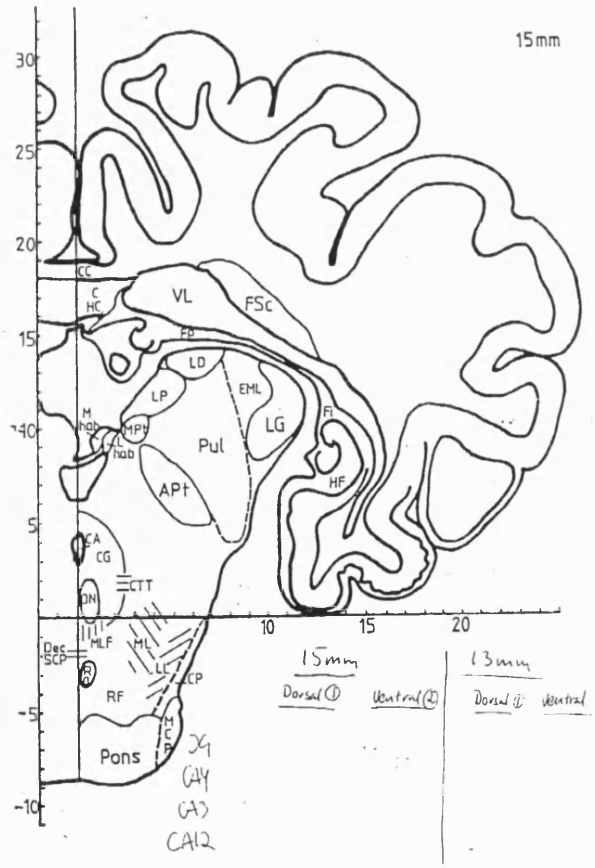
15mm
VL
FSc
LD
LP
EML
LG
Pul
APt
HF
CA
CG
CTT
DN
MLF
ML
LL
CP
RF
Pons
Dec SCP
15mm
Dorsal ①
Ventral ②
13mm
Dorsal ①
Ventral
CA1
CA3
CA4
CA1Q

3.3.5.2 Immunohistochemical Staining

Immunohistochemical techniques were employed to determine whether transient cerebral ischaemia in fetal sheep was associated with the development of increased NOS expression. The other hemisphere, not used for determining neuronal score as described in the previous section, was preserved in PBS sucrose at 4°C for three months; then blocked and mounted onto cork tiles, embedded in synthetic mounting media (Tissue Tek, Miles Laboratories, Elkhart, IN) and immediately frozen in melting dichlorodifluoromethane. Frozen tissue sections (10μm) were cut and thaw-mounted onto poly-L-lysine-coated glass slides and stained by immunohistochemistry.

Tissue sections were stained with the avidin-biotinylated-peroxide complex method and the antisera used to detect NOS isoforms were: (a) a polyclonal antibody raised against an extractable form of rat brain constitutive neuronal NOS (n-NOS); (b) a polyclonal antibody raised against a deduced peptide sequence of macrophage inducible NOS (i-NOS) and (c) monoclonal antibody to an extractable form of NOS from cultured and natural bovine aortic endothelial cells (e-NOS) (Hsu S et al 1981). The antisera were developed in the Department of Histochemistry, Royal Postgraduate Medical School, Hammersmith Hospital, London and specificity has been previously confirmed by Western blotting (Pollock JS et al 1993; Buttery LD et al 1994; Springall D et al 1992).

Endogenous peroxidase was blocked by immersing slides in 0.03% hydrogen peroxide in methanol for 30 minutes, followed by washing in PBS. After blocking nonspecific binding by incubating in 3% normal goat serum for 20 minutes, sections were blotted to remove excess serum and incubated overnight with antiserum, for n-NOS, e-NOS or i-NOS, diluted 1:1000 both in PBS containing 0.05% bovine serum albumen (PBS:BSA) and 0.1% sodium azide.

Sections were washed in PBS and then successfully incubated with biotinylated goat antiserum to rabbit immunoglobulin G diluted 1:100 in PBS containing 0.05% bovine serum albumin and freshly prepared avidin-biotin-peroxidase, for 30 and 60 minutes, respectively. Peroxidase activity was revealed using the glucose oxidase diaminobenzidine with nickel enhancement method (Shu S et al 1988). Sections were dehydrated, cleared in xylene and mounted in Pertex Mounting Media.

The brain sections were examined under light microscope to determine the presence of staining for the isoforms of NOS. The staining was compared with sham control brains that had not been exposed to cerebral ischaemia but had undergone similar surgical intervention.

3.4 Experimental protocol

Experiments were performed two to three days following surgery by which time normal physiological parameters and sleep patterning were re-established. Prior to each experiment, fetal arterial blood samples were obtained and only fetuses whose arterial partial pressure for oxygen (PaO_2) was greater than 2.27 kPa (17 mmHg), pH greater than 7.32 and lactate concentration less than 1.2 $mmol.L^{-1}$, were entered into the study.

Transient cerebral ischaemia was then induced by thirty minutes inflation of the bilateral carotid cuffs. This was achieved by inflating the balloons of the bilateral carotid cuffs with 0.5mls of saline injected by syringe and then clamping the catheters to maintain the pressure. Successful occlusion was confirmed by an isoelectric ECoG and a rise in CI. The electrophysiological changes were observed throughout the occlusion period and return of minimal electrical activity or failure of CI to progressively increase was remedied by further inflation of the cuffs and re-clamping. Fetuses were rejected if electrical activity was not abolished or CI failed to rise. This was usually the consequence of inadequate ligation of the vertebrocarotid anastomoses during surgery or mechanical failure of the carotid balloons.

Arterial blood samples were taken prior to and immediately following the end of the occlusion, and at frequent intervals thereafter throughout the study period. Blood samples of 1ml, kept in ice until measured, were used to determine arterial oxygen saturation (SaO_2), PaO_2, $PaCO_2$, lactate, glucose and haemoglobin (Hb).

At the end of the study period (96 hours for the first series of experiments; 72 for the second) ewes were sacrificed by an intravenous injection of at least 15 mls of pentobarbitone. Having detached all the connecting cables from the computers the ewes were speedily transferred to the post-mortem room and the fetuses were immediately removed. The carotid arteries of the fetuses were again exposed and catheterised bilaterally. The brain was perfused *in situ* initially with 500 mls of heparinised saline followed by 500 mls of either 4% paraformaldehyde (first series of experiments) or 10% formaldehyde (second series of experiments). The brains were then gently removed from the skull and preserved in the perfusate until ready for histological assessment.

3.5 Data collection

Continuous measurements were made of NIRS, CI and ECoG from the fetal brain; systemic fetal MAP and maternal amniotic pressure; and fetal nuchal EMG activity from at least twelve hours prior to the transient cerebral ischaemic insult and throughout the study period. All data were stored on computer hard disc for later analysis. In addition CI, MAP, filtered ECoG and EMG were displayed on an analogue ink-jet chart recorder at 5 $mm.min^{-1}$ and all data were continuously displayed on two computer screens throughout the study period.

Changes in concentration of the chromophores Hb, HbO_2 and $CytO_2$ were displayed on-line every 30 seconds during the study period and recorded on magnetic disc for later analysis. Changes in [tHb] were calculated on line as a sum of the changes in [Hb] and [HbO_2]. The distance between the optodes was determined during surgery and confirmed at post-mortem using measuring calipers.

A controlling computer calculated the changes in optical absorption at each wavelength from the near infrared light transmitted across the fetal skull and converted these into changes in the concentration of the 3 chromophores Hb, HbO_2 and $CytO_2$ using the modification of the Beer Lambert law, which describes optical absorption in a highly scattering medium. As there are three chromophores within the brain tissue (HbO_2, Hb, $CytO_2$), light was transmitted at four different wavelengths and standard curve-fitting analysis was used to increase the accuracy of the calculated concentration changes (Cope M et al 1991). Differential pathlength factor (DPF) through the fetal sheep head at postmortem was determined by Dr M Cope and Professor D Delpy at The Department of Medical Physics, University College London using a streak camera and was calculated to be 4.55.

CI, ECoG, EMG and MAP recordings were processed on-line, averaged over one and ten minute intervals and recorded on magnetic disc for later analysis using a database acquisition programme (Labview for Windows Version 2.5.1, National Instruments, Austin, Tx.).

3.6 Statistics

The specific statistical analysis techniques employed are described in chapters 4 and 5 in relation to the appropriate hypotheses. Changes in cerebral perfusion and oxygenation during and following cerebral ischaemia, were determined over the course of the study period from the changes in [HbO_2], [Hb], and the sum [tHb], and [$CytO_2$] by NIRS. To reduce error due to signal noise, data were median filtered over 500 seconds and on this data descriptive measurements were made. Data were averaged over fixed time period and then significant changes during the study period were determined by analysis of variance (ANOVA) with time as the repeated measure. Specific changes were then determined by Student Newman Keul's multiple comparison test.

Similarly changes in CI and MAP were determined and the relation between changes in the NIRS variables and other variables were determined with linear regression, according to the specific questions proposed before the start of each study.

Neuronal scores were obtained in the brain regions and percentage overall injury represented a summation of these scores. The univariate relation between changes in NIRS variables and histological outcome were determined.

Off line signal analyses were performed by Viewdac Data Acquisition, Version 2.1 (Keithley Data Acquisition Division, Keithley Instruments, Inc., Taunton, MA02780, USA) and statistics were calculated using the Statistical Analysis System, Version 1.02 (Jandel Scientific, Erkrath, Germay). All results are presented as mean ±SEM. All time points referred to relate to the end of the carotid artery occlusion as time zero.

3.7 Summary

The studies were performed on late gestation, singleton fetal sheep preparation of transient cerebral ischaemia. In this preparation, transient cerebral ischaemia was induced by bilateral carotid artery occlusion for thirty minutes following ligation of the vertebro-carotid anastomoses. The insult is associated with the development of delayed cerebral injury, indicated by the presence of a delayed increase in CI. Delayed cortical seizures occur several hours after the insult has terminated and can be recorded continuously with ECoG.

The technique of NIRS, which depends on the transmission of NIR light through the brain and it characteristic absorbance by the chromophores Hb, HbO_2 and $CytO_2$, was adapted to measure continuous changes in cerebral perfusion and oxygenation in the fetal sheep brain following transient cerebral ischaemia and these changes were temporally related to the phases of cerebral injury recorded simultaneously by CI and ECoG.

Continuous monitoring of MAP and arterial blood gases contributed to an understanding of the observed changes as it is well known that hypoxia and hypercarbia are both potent mediators of cerebral vasodilation. In addition, changes in MAP may well alter cerebral perfusion if the cerebrovascular system becomes pressure passive due to endothelial injury although this would not necessary influence the measure of CBV.

Histological analysis enabled the extent of neuronal loss to be determined so that the importance of changes in cerebral perfusion and oxygenation on the development of hypoxic-ischaemic brain injury in the immature brain could be established. Furthermore the application of histochemical techniques was used to determine the presence of NOS isoforms within the ischaemic brain.

Chapter 4

Delayed Vasodilation and Altered Oxygenation Following Cerebral Ischaemia

4.1 Introduction

In this chapter the changes in cerebral perfusion and oxygenation were related to the phases of cerebral injury and histological evidence of brain injury in the fetal sheep brain using the techniques described in chapter 2 and the methods described in chapter 3. The hypotheses addressed in this chapter were that delayed cerebral injury in fetal sheep was associated with changes in cerebral perfusion and oxygenation, and that the degree of these changes correlated with the degree of cerebral injury.

Cellular dysfunction was observed by measurements of CI and ECoG, and the overall severity of cerebral damage was assessed histologically. Cerebral vascular tone was assessed by observing changes in [tHb] with NIRS. Mean cerebral oxygen saturation was assessed by examining the relative changes in [Hb] and [HbO_2] in relation to [tHb], and an estimate of cerebral mitochondrial oxygenation was made using NIRS to detect changes in [$CytO_2$].

4.2 Materials and methods

The techniques and general methodology for this study is described in detail in chapters 2 and 3 and will only be briefly described here.

4.2.1 Surgical procedure

Fourteen singleton fetal sheep of known gestational age (range 119-133 days) were operated on under general anaesthesia using sterile techniques. Two of these animals were studied as sham operated controls. Six experiments were rejected: 3 due to inadequate carotid artery occlusion, 2 due to premature labor and 1 due to sepsis before the end of the study period. The general experimental approach has been described in chapter 3.

4.2.2 Experimental protocol

Fetuses whose arterial blood gas tensions and lactate concentration were normal 2 days after surgery were entered into the study. NIRS, CI, MAP and filtered ECoG recordings were commenced 12 hours prior to the ischaemic insult, continued for a further 4 days and stored on computer hard disc for later analysis. Transient ischaemia was induced by 30 minutes inflation of the bilateral carotid occluders with saline and confirmed by an isoelectric ECoG and a rise in CI. Arterial oxygen saturation (SaO_2), PaO_2, $PaCO_2$, lactate, glucose and haemoglobin were measured prior to and immediately following the end of the occlusion, and at 6 hourly intervals during the study period.

Ewes were sacrificed with an overdose of pentobarbital four days after the ischaemic insult. The brain was perfused through the common carotid arteries with 4% phosphate buffered paraformaldehyde at 4°C. The brain was divided into the hemispheres and one half was preserved in phosphate buffered saline (PBS) containing 0.45M sucrose, whilst the other half was preserved in 10% formalin for neuronal scoring.

4.2.3 Data Collection

ECoG was recorded continuously and intensity spectra were obtained by real time spectral analysis as described in chapter 2. NIRS recordings of changes in [tHb], [HbO_2], and [$CytO_2$] were displayed on line every 10 seconds during the study period and recorded on magnetic

disc for later analysis. The distance between the optodes was determined during surgery and confirmed at post-mortem using measuring calipers.

4.2.4 Data analysis and statistics

Changes in [tHb], [HbO_2] and [$CytO_2$] were calculated from alterations in optical attenuation by least-squares multilinear regression using the algorithm described in chapter 2. ECoG intensity data were log transformed and analysed to determine the onset of epileptiform activity as indicated by the development of intense low frequency activity.

Descriptive measurements were made on data that had been median filtered over 500 seconds. Significant changes during the study period were determined by analysis of variance (ANOVA) with time as the repeated measure. Specific changes were then determined by Student-Newman-Keul's multiple comparison test.

Linear regression analyses were applied to determine the univariate relation between changes in NIRS variables and those in CI and ECoG, to determine the temporal relationship. The degree of the early and delayed changes in cerebral perfusion and oxygenation were related to the phases of cerebral injury and histological outcome, using univariate linear regression, to determine the implications of the observed alterations. All results are presented as mean ±SEM. All time points referred to relate to the end of the carotid artery occlusion as time zero.

4.3 Results

4.3.1 Subjects

The 6 fetuses fulfilling the study entry criteria and the 2 control subjects were comparable in gestational age (126±2 days), weight (3.3±0.2 kg) and biparietal diameter (5.4±0.1 cm).

Changes observed in the NIRS and electrophysiological variables are expressed conventionally as change from a baseline obtained from the 12 hours pre-insult recordings. For the NIRS variables and ECoG log-transformed data, the baseline was normalised with respect to the mean value of pre-insult recordings and changes are recorded in $\mu mol.L^{-1}$ and dB respectively. CI measurements were expressed as percentages of pre-insult values.

4.3.2 Evidence of cerebral injury

4.3.2.1 CI and ECoG

Figure 4.1 shows CI and ECoG in the study group, and demonstrates the delayed changes seen in previous studies using this preparation (Williams CE et al 1991). There are two periods when CI increased above baseline: (I) during ischaemia, and (II) a delayed phase commencing 17.5±2.3 hours post-ischaemia, peaking at 42.3±2.4 hours and lasting 66.0±4.9 hours.

ECoG was depressed during and after ischaemia, and increased in amplitude at 13.6±3.0 hours due to seizures, confirmed by inspection of raw ECoG, that persisted for 25.4±3.2 hours. Values for CI and ECoG during and after ischaemia related to changes in [tHb] are shown in table 4.1. Worse histological outcome was related to a more depressed ECoG amplitude at 96 hours post insult ($r=0.93$; $p<0.01$) and a lesser recovery of CI to baseline following the insult ('residual') ($r=0.82$; $p<0.05$), as shown in figure 4.2.

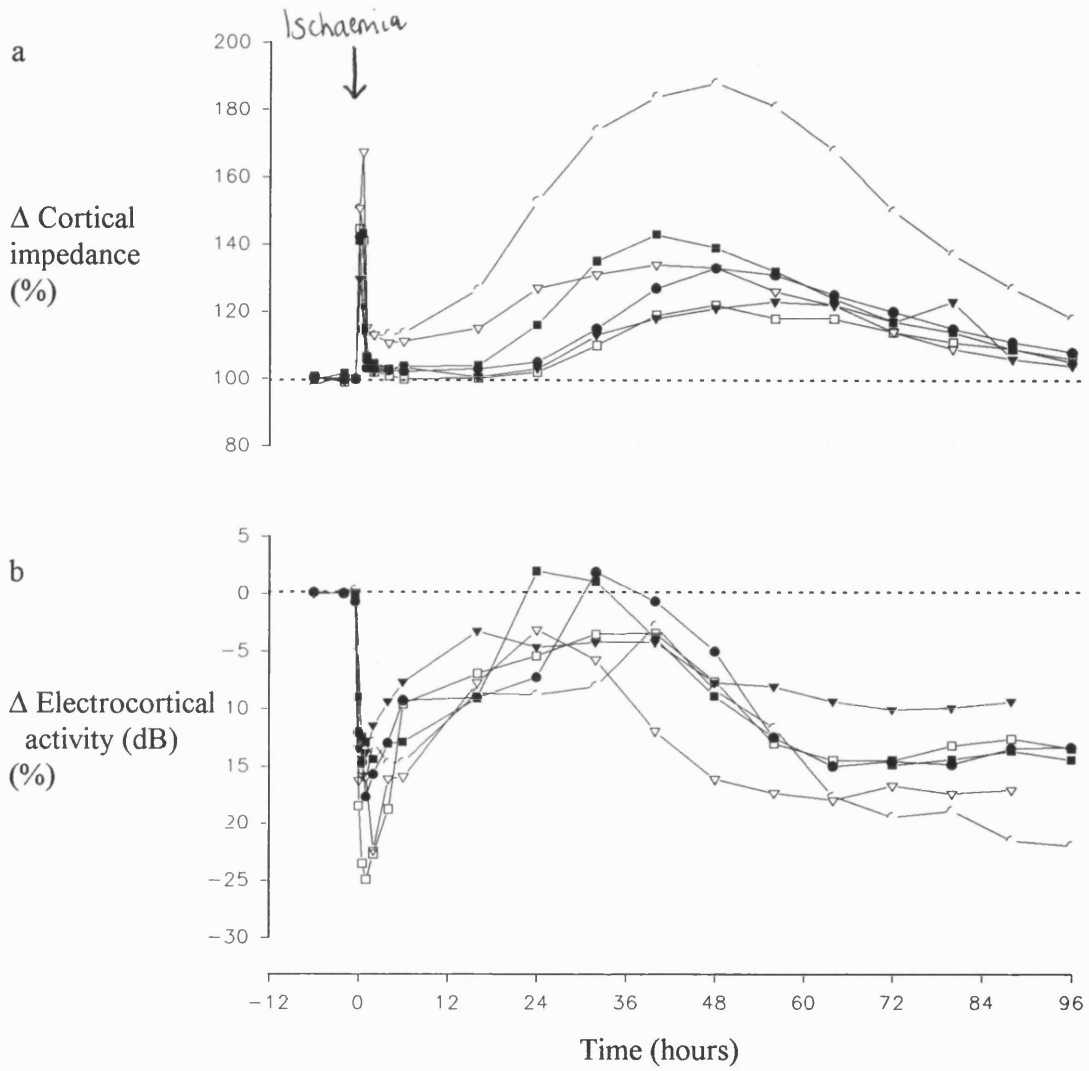

Figure 4.1 a, b **Changes in *(a)* cortical impedance and *(b)* electrocortical activity following transient cerebral ischaemia**

(a) shows the changes in cortical impedance (CI) over 96 hours during and following transient cerebral ischaemia (n=6). Symbols represent mean of averaged data for each fetus as a percentage (%) change from pre-ischaemic baseline (100%). There was an increase in CI during the insult, a period of recovery and a delayed increase commencing several hours later.

(b) shows the changes in electrocortical activity (ECoG) in decibels(dB) from the pre-ischaemic zero baseline. ECoG is depressed during and following cerebral ischaemia; recovers towards baseline, and then is finally depressed to an extent that relates to the severity of the histological outcome

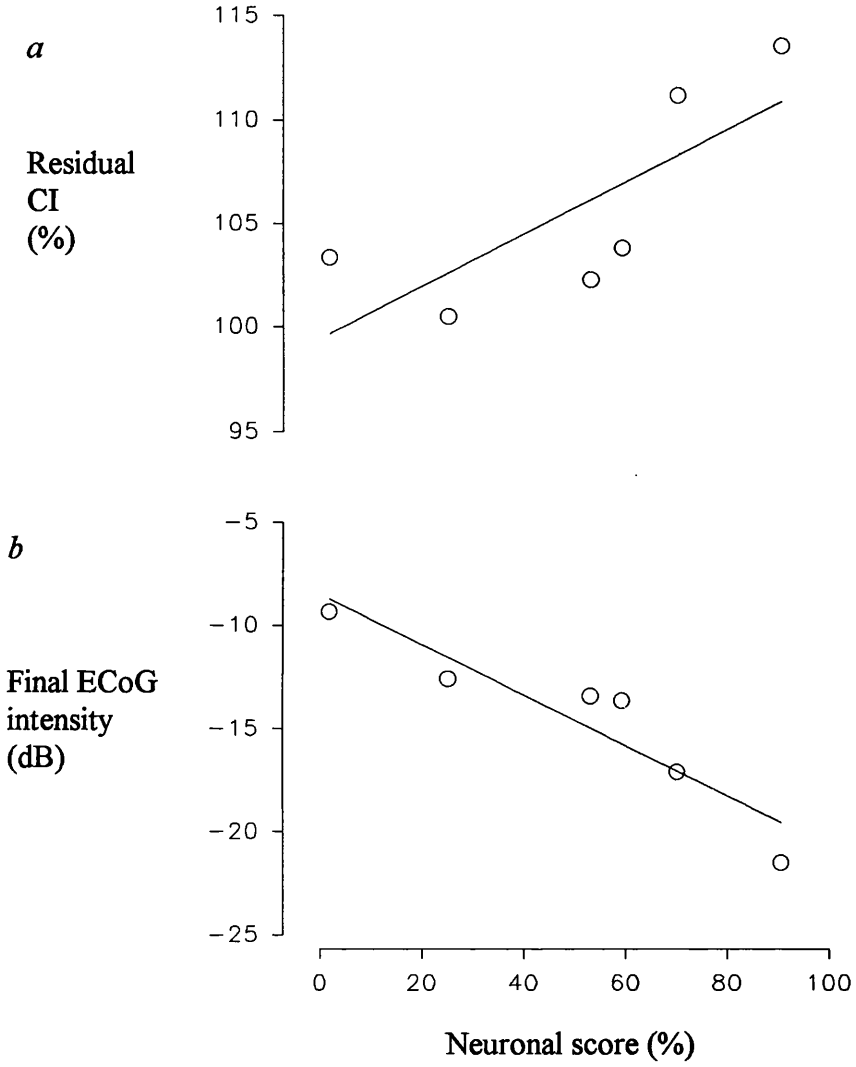

Figure 4.2 a, b **Relation between (*a*) residual cortical impedance and (*b*) final electrocortical intensity and histological outcome assessed 4 days following transient cerebral ischaemia**

The figure shows the relation between neuronal score and (a) residual cortical impedance (CI) measured immediately following reperfusion. Residual CI directly related to neuronal score ($r=0.82$; $p<0.05$) and a greater residual CI was associated with a greater extent of cerebral injury. Final ECoG intensity (b) was inversely related to neuronal score and was more depressed with a more extensive cerebral injury ($r=0.93$; $p<0.01$)

4.3.2.2 Neuronal score

Figure 4.3 gives histological results. Damage was seen in a similar distribution in all subjects, but the severity of damage was variable. Laminar necrosis was observed in the parasagittal region of the cortex with a lesser degree of injury in the hippocampus, lateral cortex, striatum and dentate gyrus.

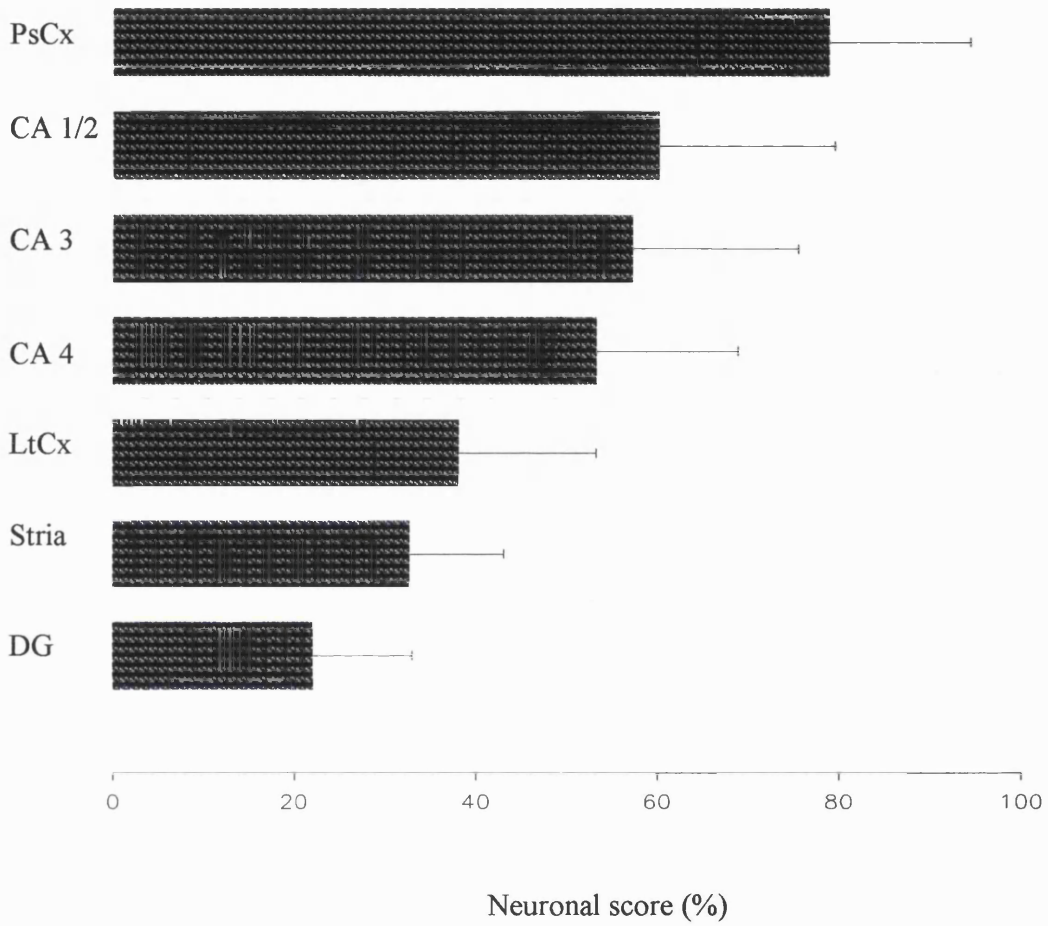

Figure 4.3 **Neuronal loss assessed four days after transient cerebral ischaemia**

The bar chart shows the histological outcome in the parasagittal cortex (PsCx), hippocampal regions (CA1/2,3), lateral cortex (LtCx), striatum (Stria) and dentate gyrus (DG). Each bar represents the mean neuronal score ±SEM. Neuronal score represents the proportion of dead cells to total number of cells assessed in each region. Neuronal scoring is described in the text.

4.3.3 Cerebral haemodynamics and oxygenation

4.3.3.1 Total cerebral haemoglobin concentration

Figure 4.4a shows changes in [tHb] during and following transient cerebral ischaemia. Inspection of these data revealed a characteristic pattern in all subjects, with two increases of [tHb] above baseline. Changes in [tHb] could be defined *post hoc* into 5 phases, here given with mean time of onset and the duration of each phase ±SEM:

0	Pre-ischaemic baseline.	(-12; 11.5 hours)
1	Fall in [tHb] during carotid artery occlusion	(-0.5; 0.5 hours)
2	First post-ischaemic increase in [tHb]	(0.5±0.1; 2.3±0.4 hours)
3	[tHb] returned to baseline	(2.7±0.4; 10.0±2.4 hours)
4	Second post-ischaemic increase in [tHb]	(12.8±2.0; 43.1±5.2 hours)
5	Return towards baseline at end of study period	(55.9±5.2; 7.0±4.6 hours)

Table 4.1 shows the changes in [tHb] and other variables during these phases.

Phase	Change in [total cerebral haemoglobin] ($\mu mol.L^{-1}$)	Change in cortical impedance (%)	Change in electrocortical activity (dB)	Mean arterial blood pressure (mmHg)	Lactate ($mmol.L^{-1}$)	Glucose ($mmol.L^{-1}$)	Arterial Haemoglobin ($g.dl^{-1}$)
0	0	100	0	29.8±1.6	0.9±0.1	0.8±0.1	11.4±0.5
1	-41.9±3.4*	143±3.2*	-12.7±1.6*	38.0±2.3‡	1.9±0.4‡	1.5±0.1‡	11.5±0.6
2	19.9±2.2*	107±1.7	-16.8±1.7*	30.3±1.6	2.3±0.5*	1.1±0.1	11.1±0.3
3	-2.8±1.2	105±2.2	-10.8±1.4*	30.4±2.2	1.3±0.2	1.2±0.1	10.9±0.4
4	43.0±3.8*	141±9.8*	-7.3±0.7‡	35.5±2.7‡	1.4±0.4	1.0±0.1	10.8±0.8
5	12.4±5.6	120±6.9‡	-13.6±1.0*	35.4±4.7	1.0±0.2	1.2±0.1	11.4±0.6

Table 4.1 **Changes in total cerebral haemoglobin ([tHb]) and other variables during and following cerebral ischaemia**

The 5 phases of changes in total cerebral haemoglobin[tHb] from zero baseline that occurred during and following transient cerebral ischaemia are defined in the text. Values are peaks ±SEM, or mean ±SEM in phases 3 and 5 when there was no peak change. (Significant changes from baseline ‡ $p<0.05$; * $p<0.01$).

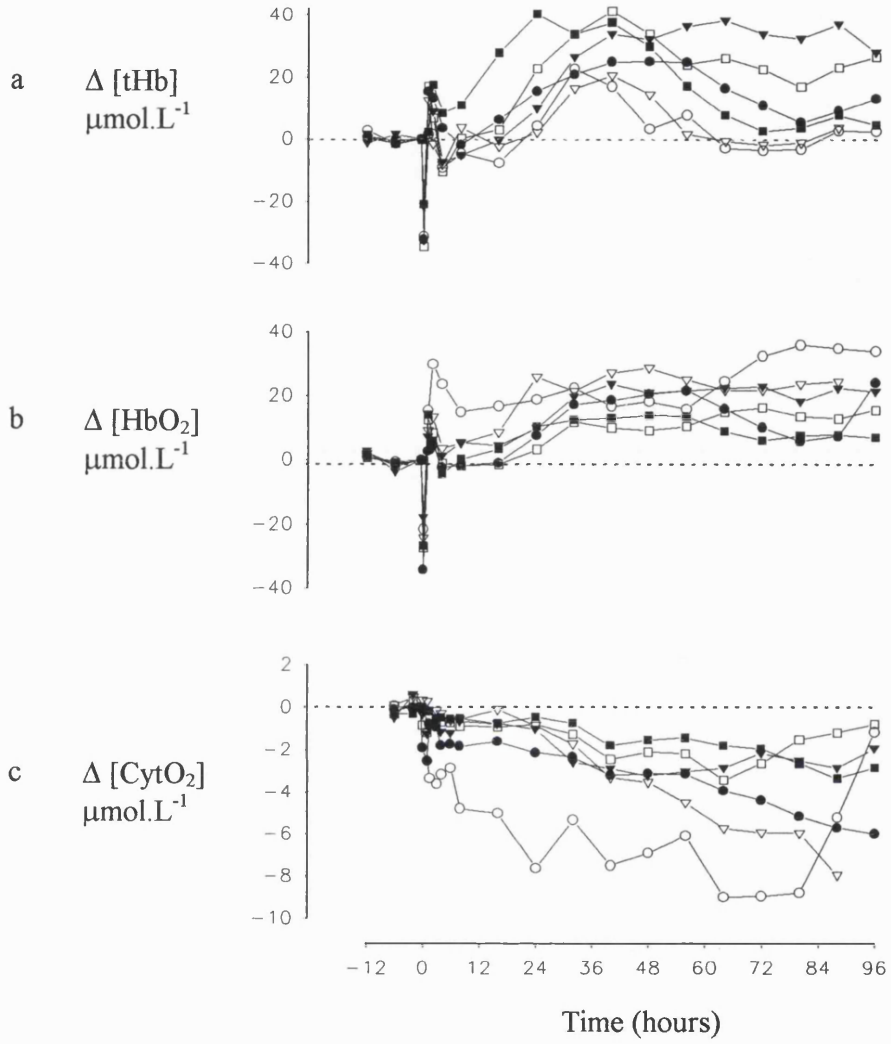

Figure 4.4 a,b,c **Changes in NIRS variables following transient cerebral ischaemia**

Changes in (a) total cerebral haemoglobin (Δ[tHb]), (b) oxyhaemoglobin (Δ[HbO_2]) and (c) oxidised cytochrome oxidase (Δ[$CytO_2$]) from pre-ischaemic normalised baseline (n=6). In each graph, different symbols represent data from each fetus. A fall in [tHb] during ischaemia is followed by a first post-ischaemic increase in [tHb], then a return to baseline, and a second post-ischaemic increase in [tHb] commencing several hours later. [tHb] returns towards baseline at the end of the study period. In figure 4.4b Δ[HbO_2] demonstrates similar changes although the persistent increase in [HbO_2], when [tHb] returns to baseline, demonstrates an increase in mean cerebral saturation. Figure 4.4c demonstrates a fall in [$CytO_2$] during the insult, a period of relative stability and then a progressive fall until 72-80 hours post-ischaemia.

Linear regression analysis relating [tHb] to other variables showed that:

a) The duration of the first rise in [tHb] was longer in fetuses with more severe histological outcome ($p<0.05$) (Figure 4.5a).

b) The time of onset of the second increase in [tHb] was earlier in subjects with more severe histological outcome ($p<0.01$) (Figure 4.5b).

c) The duration of the second rise in [tHb] was shorter in subjects with more severe histological injury ($p<0.01$) (Figure 4.5b).

d) In all animals the onset of the delayed increase in [tHb] preceded the onset of the second increase in CI ($p<0.05$).

e) MAP increased during ischaemia and during phase 4, but linear regression analysis showed no significant relation between [tHb] and MAP.

f) Arterial PaO_2, SaO_2 $PaCO_2$ and haemoglobin concentration were constant throughout. Arterial pH, glucose and lactate concentration altered during ischaemia, but not during the later phases of the experiment. No other significant relations were found (tables 4.1 and 4.2).

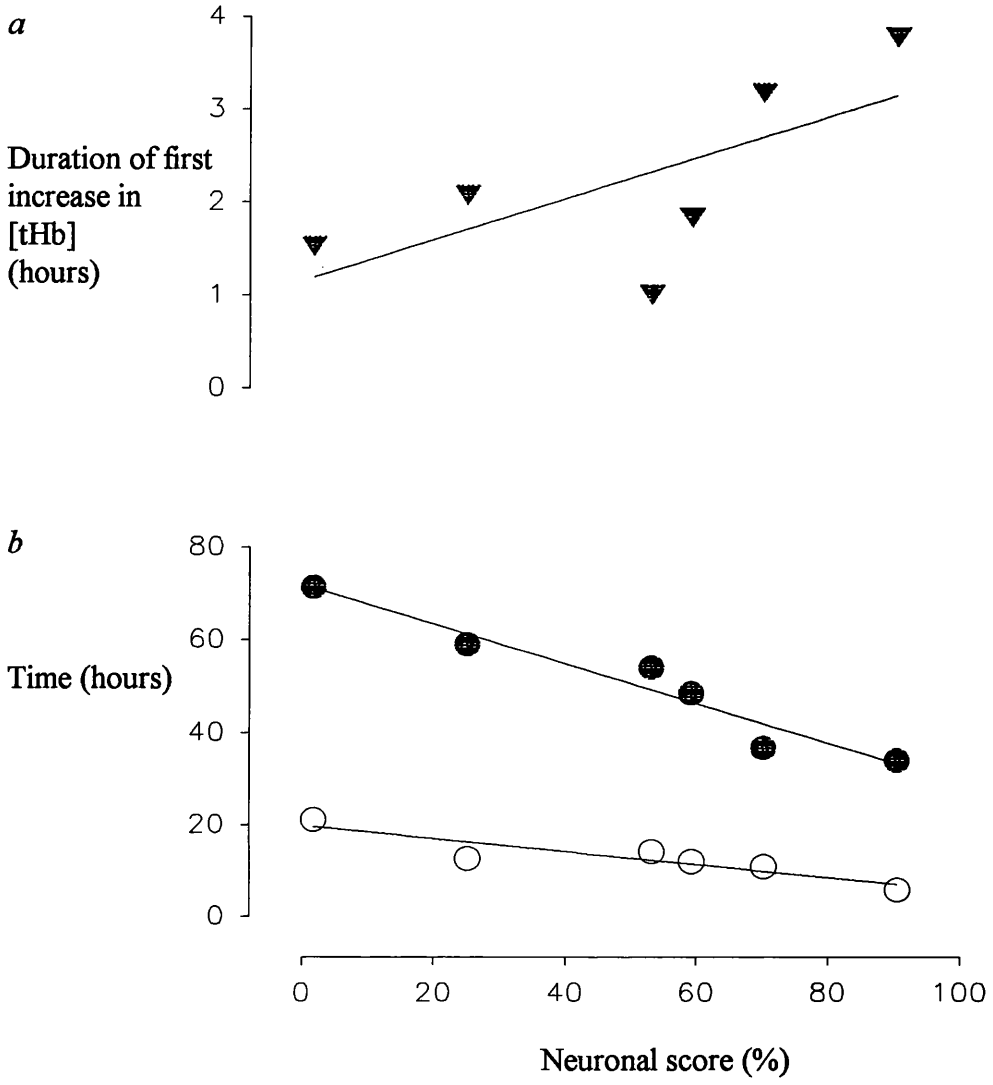

Figure 4.5 a, b **The relation between Δ [tHb] and histological outcome following transient cerebral ischaemia**

(a) shows the linear relation between the duration of the first increase in [tHb] ($r=0.82$; $p<0.05$) and overall neuronal score, and (b) shows the relation between time of onset (●) ($r=0.93$; $p<0.01$) and duration (○) ($r=0.97$; $p<0.01$) of the second post-ischaemic increase in [tHb] and overall neuronal score. A worse histological outcome is associated with a prolonged first increase in [tHb] and a second post-ischaemic increase in [tHb] that commences earlier and is short lived.

4.3.3.2 Cerebral oxygenation

Figure 4.4 shows the changes in concentration of (b) [HbO_2] and (c) [$CytO_2$] in the 6 fetuses. Changes in [HbO_2] and [$CytO_2$] during the 5 phases in [tHb] are given in table 4.2. During phase 5, [HbO_2] remained increased although [tHb] returned towards baseline, demonstrating an increase in the mean cerebral oxygen saturation.

The optical signal attributed to [$CytO_2$] declined during the insult and immediately following. It then showed no significant change until 28-30 hours post-insult when it fell progressively to a minimum of -5.0±2.8 $\mu mol.L^{-1}$ at 78-80 hours. The maximal fall was variable among the subjects and a greater maximum fall in [$CytO_2$] at 78-80 hours was related to a greater residual CI following the insult ($r=0.90$; $p<0.05$); greater depression of final ECoG amplitude ($r=0.83$; $p<0.05$) (figure 4.6b) and worse histological outcome ($r=0.84$; $p<0.05$) (figure 4.6c).

Phase	Change in [cerebral oxyhaemoglobin] ($\mu mol.L^{-1}$)	Change in [oxidised cytochrome oxidase] ($\mu mol.L^{-1}$)	PaO_2 (kPa)	$PaCO_2$ (kPa)	SaO_2 (%)
0	0	0	20±2.0	46±3.8	48±4.3
1	-29.2±1.9*	-0.7±0.2‡	20±3.0	45±7.5	48±7.5
2	17.9±3.0*	-1.5±0.2‡	20±2.1	45±3.5	44±4.1
3	3.6±2.6	-0.8±0.2‡	22±2.6	47±4.6	46±3.3
4	28.0±3.3*	-2.5±0.9‡	20±2.6	46±5.8	45±4.6
5	18.1±2.5*	-3.6±0.8*	23±2.8	47±4.1	46±5.2

Table 4.2 **Changes in oxyhemoglobin ($[HbO_2]$), oxidised cytochrome oxidase ($[CytO_2]$) and arterial blood gases during and following cerebral ischaemia**

*Changes in variables in relation to 5 phases of changes in [tHb] defined in the text. Values are peaks±SEM, or mean±SEM in phases 3 and 5 when there was no peak change. (Significant changes from baseline ‡ $p<0.05$; * $p<0.01$).*

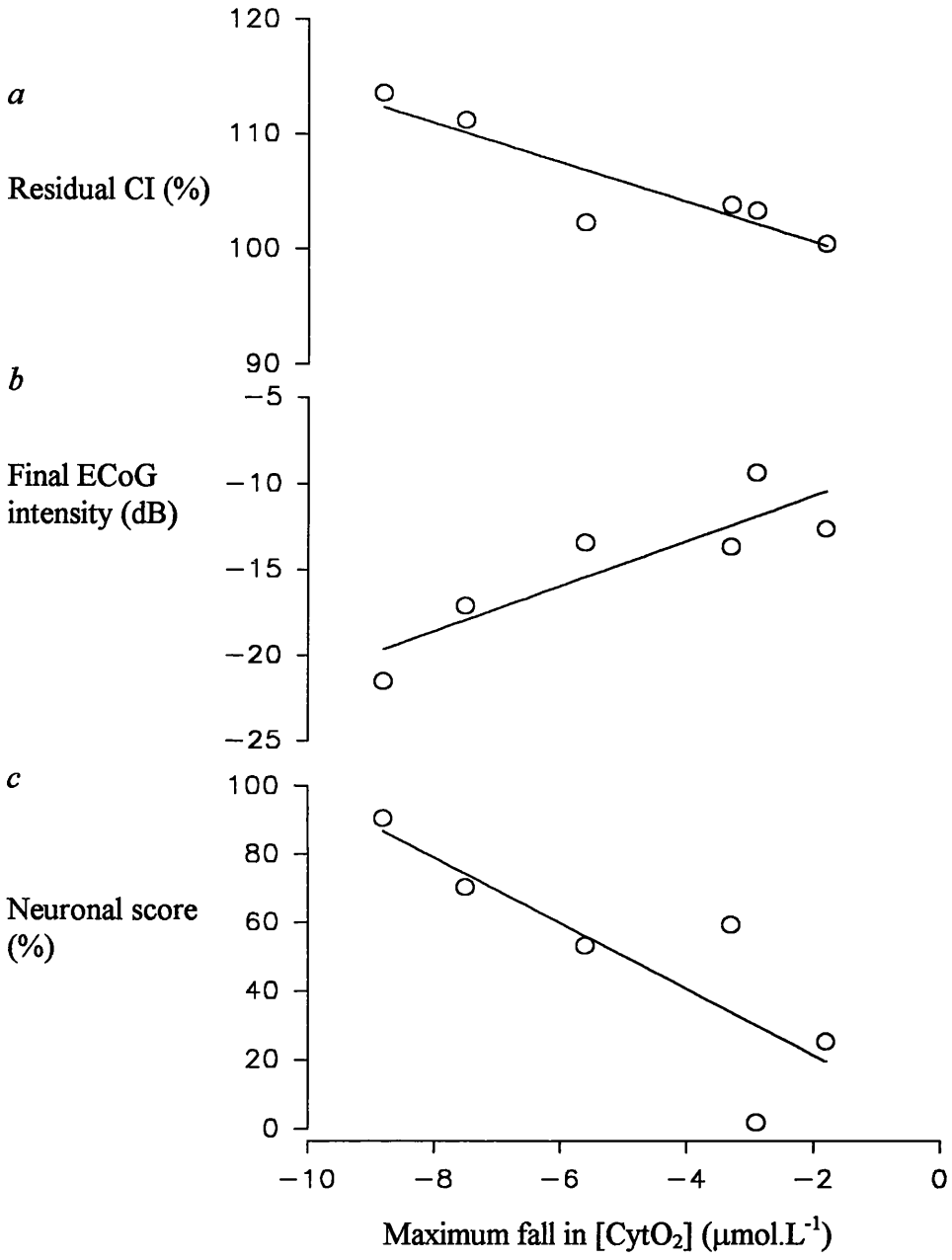

Figure 4.6 a,b,c **The relation between maximum fall in oxidised cytochrome oxidase and outcome following transient cerebral ischaemia**

Figure 4.6 shows the relation between maximum fall in oxidised cytochrome oxidase ([$CytO_2$]) and (a) residual cortical impedance (CI) ($r=0.90$; $p<0.05$); (b) final electrocorticographic activity (ECoG) ($r=0.87$; $p<0.05$) and (c) neuronal loss ($r=0.84$; $p<0.05$). A greater final fall in [$CytO_2$] is associated with higher residual impedance immediately following the ischaemia; a more depressed final ECoG intensity; and a worse histological outcome. Each symbol represents averaged data from each fetus studied.

4.4 Discussion

In this study, the cerebrovascular changes and the alterations in cerebral oxygenation that occurred during and following cerebral ischaemia were measured in fetal sheep with NIRS. As has been described in some detail in chapter 2, the technique can accurately detect changes in the concentration of Hb, HbO_2 and $CytO_2$. The erroneous effect of movement on optical pathlength was eliminated by surgical fixation of the optodes onto the fetal skull. However, the changes in the scattering properties of the brain following cerebral ischaemia have not been investigated and must be considered when interpreting the results.

When arterial haemoglobin and the cerebral:peripheral haematocrit ratio are constant, changes in [tHb], measured as a sum of [Hb] and [HbO_2], are a precise measure of changes in cerebral vascular volume. Change in [HbO_2] is a measure of the overall oxygenation of the cerebral blood, whilst changes in the signal attributed to [$CytO_2$] reflects the oxidation-reduction balance within the mitochondria. Compared to haemoglobin, the concentration of cytochrome aa_3 in the fetal brain is likely to be very low and therefore changes in the [$CytO_2$] measured by NIRS are far more susceptible to subtle changes in tissue optics and can only be interpreted with caution at present.

There was an increase in [tHb] during two discrete periods following cerebral ischaemia and the increases were not contingent upon alterations in arterial haemoglobin concentration, MAP or arterial blood gases and were too large and rapid to be ascribed solely to alterations in cerebral:peripheral haematocrit ratio. The changes therefore represent periods of cerebral vasodilation and demonstrate that following ischaemia, delayed cellular dysfunction is accompanied by vasodilation.

The excellent time resolution of NIRS allowed precise definition of the time course of the cerebrovascular changes. The first increase occurred immediately following the end of the ischaemia, and may be related to the reactive hyperaemia that has been observed in both adult and perinatal animals following hypoxia-ischaemia. The increase was short-lived and then

[tHb] returned to preischaemic baseline.

The second period of vasodilation occurred several hours later and preceded the delayed increase in CI, suggesting that the vascular changes occurred before cellular dysfunction was sufficiently deranged to disrupt ionic homeostasis. The results of this study suggest that following ischaemia, delayed cellular dysfunction is accompanied by vasodilation rather than vasoconstriction.

The duration and pattern of the cerebrovascular changes were related to the severity of cerebral damage such that a more severe injury was associated with a larger first increase in [tHb]; an earlier onset of the second increase; and a shorter duration of the second period of increased vascular volume. The results may suggest that a common chemical mediator induced both the cerebral vasodilation and the delayed increase in CI. The mediators of the second period of vasodilation are not known but the phase may reflect an endogenous protective mechanism.

Observation of the changes in [HbO_2] and [Hb] demonstrated that [tHb] declined after reaching its second peak, and most of the fall was accounted for by a decrease in cerebral [Hb]. Thus relatively more of the haemoglobin remaining in the brain was oxygenated, and this reflects an overall increase in mean cerebral oxygen saturation. However, the NIRS estimation of [$CytO_2$] also declined progressively from about 20 hours following reperfusion.

In chapter 2, the difficulties in interpreting the changes in [$CytO_2$] as measured by NIRS were discussed. Firstly, the concentration of cytochrome aa_3 within the fetal brain is probably low and the unknown changes in scattering properties of the brain during and following ischaemia will effect the measurement of [$CytO_2$] during the ischaemic insult.

Furthermore, changes in the redox state of [$CytO_2$] reflects the rate of ATP utilisation; supply of reducing equivalents and the mitochondrial proton force and can only be considered to reflect mitochondrial oxygenation under certain circumstances.

However, despite the caution that must be taken when interpreting Δ[CytO2] as measured by NIRS, the larger, late fall in [$CytO_2$] closely related to independent measures of the severity of brain injury. This may well indicate that the measurement represents a true biological change that warrants closer investigation.

4.5 Summary

In summary, a complex biphasic pattern of vasodilation accompanied the early and delayed changes in CI. There was a late increase in the oxygenation of cerebral blood although [$CytO_2$] apparently declined following ischaemia. The degree of the early and delayed changes in cerebral perfusion and oxygenation were related to the extent of cerebral injury assessed histologically. The possible involvement of NO in these processes is addressed in the next chapter.

Chapter 5

Role of Nitric Oxide following cerebral ischaemia in the perinatal brain

5.1 Introduction

The role of NO production during and following cerebral ischaemia is thought to be important in the development of cerebral injury following ischaemia. However whether the role is destructive or beneficial in the perinatal brain remains unclear.

NO is a potent vasodilator and has been implicated as improving cerebral perfusion in the immediate post-ischaemic phase. During early reperfusion following cerebral ischaemia in adults rats, NO donors and L-arginine, the precursor of NO, have been shown to increase CBF and improve cerebral outcome. However, in combination with SO^{-}_{2} radicals, NO can generate highly potent oxidants in particular peroxynitrite which is thought to promote cell death. Indeed, the neurotoxic effects of the EAA, Glut, have been shown to be mediated by NO through this mechanism (see section 1.5.3.4).

The role of NO in the development of cerebral injury in the perinatal brain has not been established. Only 2 experiments investigating the role of NO are presented in the literature (Hamada Y et al 1994; Trifiletti RR 1992). Both have been performed in perinatal rats and employed NOS inhibitors to determine the effect on histological outcome following hypoxia-ischaemia. A protective role has been observed with low doses whilst high doses appear to be less effective. The effect on cerebral haemodynamics has not been demonstrated in any of these investigations.

In chapter 4 the results of the previous experiments are described and show that severe transient cerebral ischaemia in fetal sheep is followed by two periods of cerebral vasodilation: an early period that occurs immediately after the insult and lasts for one or two hours; and a second episode that begins about 12 hours later and continues over a prolonged period.

The second period of increased cerebral perfusion was coincident with a phase of delayed cerebral injury, demonstrated by a delayed increase in CI and cortical seizures. The changes in CI imply that cellular membrane function was impaired and ionic homeostasis across cellular membranes was disrupted causing cytotoxic oedema to develop.

The increased production on NO has been implicated from microdialysis studies measuring changes in the extracellular cerebral concentration of EAA's in fetal sheep following cerebral ischaemia (Tan KMW et al 1995). The studies demonstrated that during the delayed phase of increase in CI, there was an increase in the extracellular concentration of L-citrulline, which is produced by NOS in the generation of NO from L-arginine. NO mediates cerebral vasodilation in the developing brain through cGMP, but can also induce neuronal death through the generation of peroxynitrite and activation of poly (ADP-ribose) synthetase (Dawson VL et al 1991; Zhang J et al 1994).

In this chapter the role of NO is described by a series of experiments that were conducted to determine the presence of isoforms of the enzyme NOS within the ischaemic brain; and demonstrate the effects of NOS inhibition on cerebral perfusion and oxygenation, histological outcome and electrophysiology. The presence of NOS isoforms was determined using immunohistochemical techniques in the fetal sheep brain following cerebral ischaemia. The role of NO production on the delayed changes in cerebral perfusion and oxygenation were investigated using N^G-nitro-L-arginine (L-NNA), a competitive inhibitor of NOS. CI was recorded to determine the severity of the initial injury and the course of the delayed cerebral injury; and NIRS was employed to continuously measure changes in cerebral perfusion. The severity of cerebral injury was determined histologically at 3 days.

5.2 Presence of NOS isoforms

5.2.1 Materials and Methods

Seven fetal sheep brains, five exposed to transient cerebral ischaemia and two sham controls were obtained from the experiments described in the previous chapter. According to experimental protocol the brains were perfused with 4% paraformaldehyde and then one hemisphere was maintained at 4°C in phosphate buffered sucrose for 3 months.

In collaboration with The Department of Histochemistry, Royal Postgraduate Medical School, the avidin-biotinylated-peroxidase complex method was used to detect NOS isoforms binding to:

(a) a polyclonal antibody raised against an extractable form of rat brain constitutive neuronal NOS (n-NOS);
(b) a polyclonal antibody raised against a deduced peptide sequence of macrophage inducible NOS (i-NOS) and
(c) monoclonal antibody to an extractable form of NOS from cultured and natural bovine aortic endothelial cells (e-NOS) as described in chapter 3.

Staining was performed by Lee DK Buttery

5.2.2 Data Analysis

Using light microscopy the brain sections were examined for the presence of the NOS isoforms indicated by the appearance of dark brown staining. The parasagittal and lateral cortex, regions of the hippocampus, striatum and dentate gyrus were all inspected.

5.2.3 Results

Immunostaining was performed on frozen sections obtained from 5 fetal sheep brains four days following transient cerebral ischaemia and on 2 sham-operated control brains in which the ballooned cuffs had failed to induce carotid artery occlusion. Photomicrographs 5 demonstrate n-NOS (*a*) and *(b)*, e-NOS (*c*) and i-NOS (*d*) staining in a fetal sheep brain following ischaemia.

5.2.3.1 n-NOS

Neuronal cells bodies exhibiting NOS immunoreactivity were found scattered throughout the cerebral cortex, caudate, putamen, amygdala and hippocampus. Neuronal cell types were non-pyramidal cells of the brain cortex, and medium-sized neurons in the other regions. Generally, the cell cytoplasm and dendritic processes were most prominently stained and stained neurons demonstrated different intensity of reaction. Dendritic processes and synapses also demonstrated dark staining within the cerebral cortex. There was minimal background staining within the myelin. Diffuse brown staining was noted within the dentate gyrus and the hippocampal regions and this did not have the granular appearance noted within the neuronal cell bodies within the cortex.

5.2.3.2 e-NOS

Staining was localised in the endothelial layers of the large and medium-sized vessels of the cerebral cortex and within the ependymal vessels within the choroid plexus and lining the ventricular space. The dark brown granular staining was most prominent within the cytoplasm of the endothelial cells.

5.2.3.3 i-NOS

i-NOS staining ranged from being sparse to being completely absent. Staining was brown, diffuse and non-granular within the subependymal and ependymal layers of the cortex. No neuronal cell bodies or processes were stained in any of the subjects, although in one brain where the microglial reaction was prominent microglia stained occasionally within the cortex.

Photomicrograph 5

Photomicrograph of (a and b) n-NOS; (c) i-NOS and (d) e-NOS staining using immunohistochemistry in the parasagittal cortex of a 133 day old fetal sheep brain 4 days after transient cerebral ischaemia

(a) Brown n-NOS staining was observed in the cell bodies and dendritic arbors of neuronal cells most prominently within the cerebral cortex. (b) Granular staining was evident within these regions at high power magnification (x800)

(c) i-NOS staining was light brown, diffuse and poorly defined within the subependymal region of the parasagittal cortex. Furthermore staining within cell bodies was observed occasionally (arrow)

(d) e-NOS staining was confined to endothelium of cerebral vessels within the brain parenchyma and the ependymal vessels within the ventricular space

Haemotoxylin and eosin staining was employed to define brain region. (Magnification x400)

a

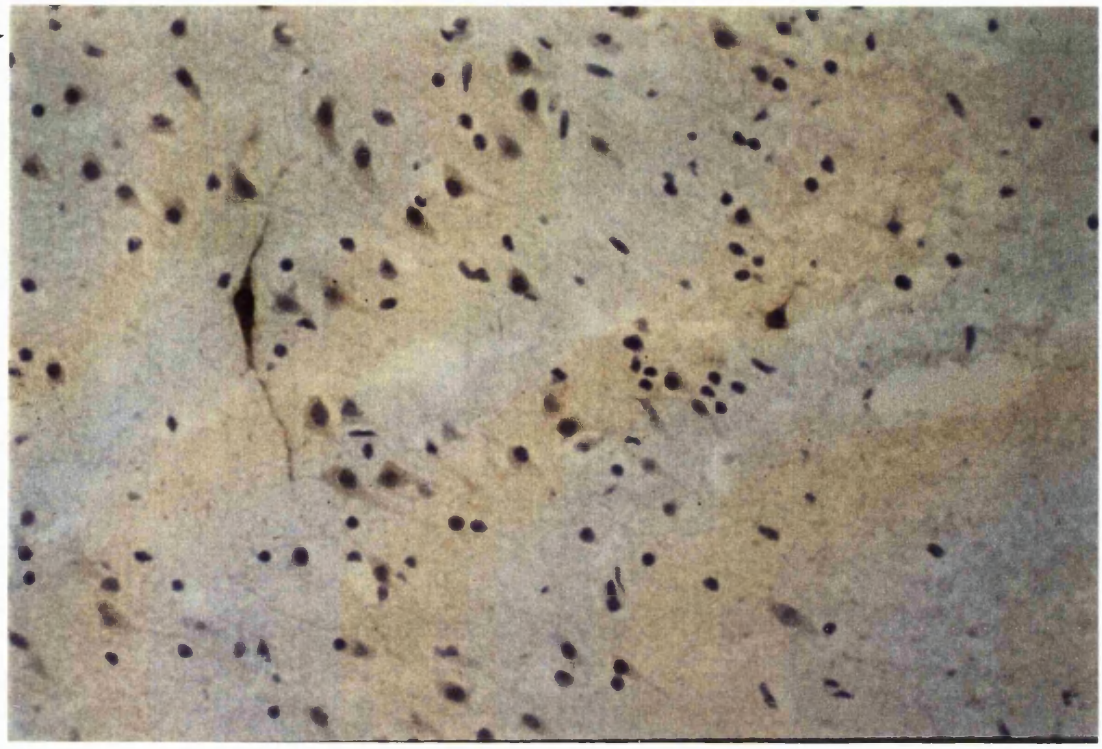

b

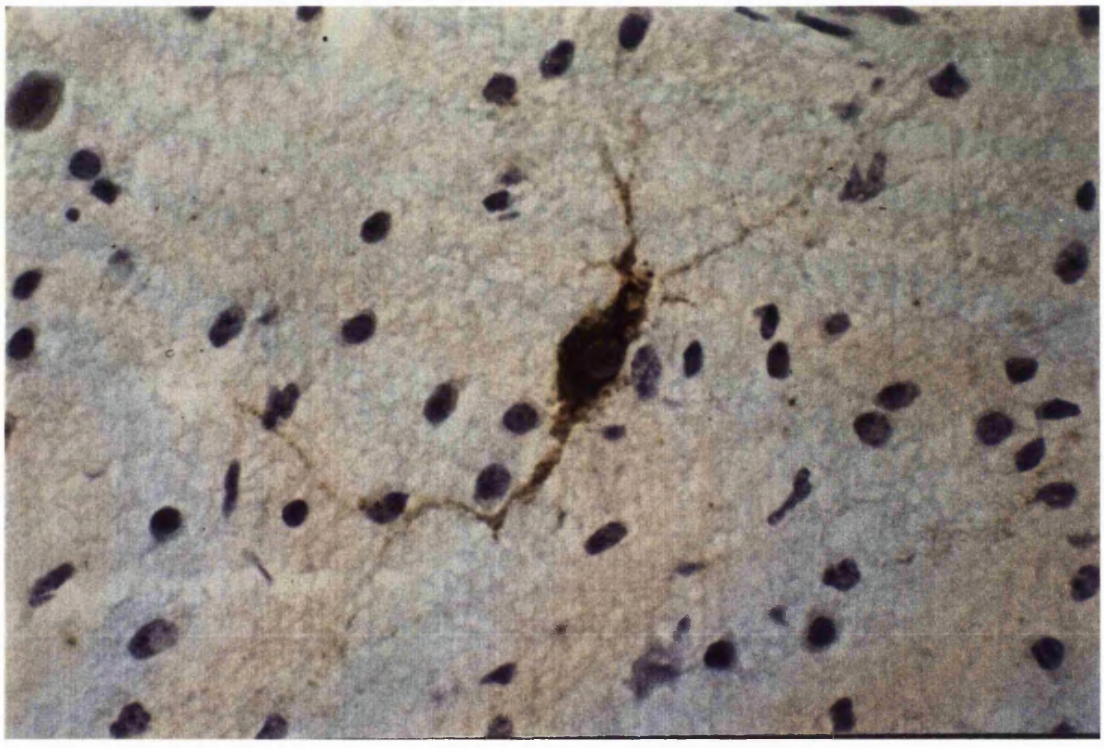

c

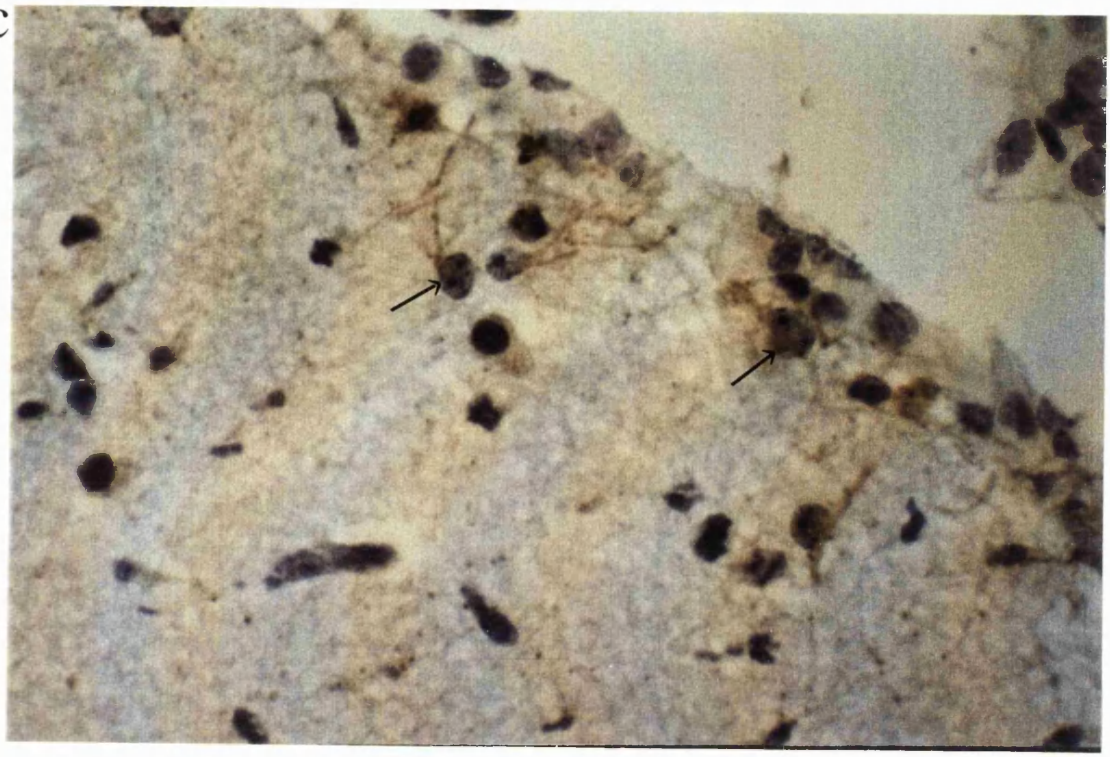

d

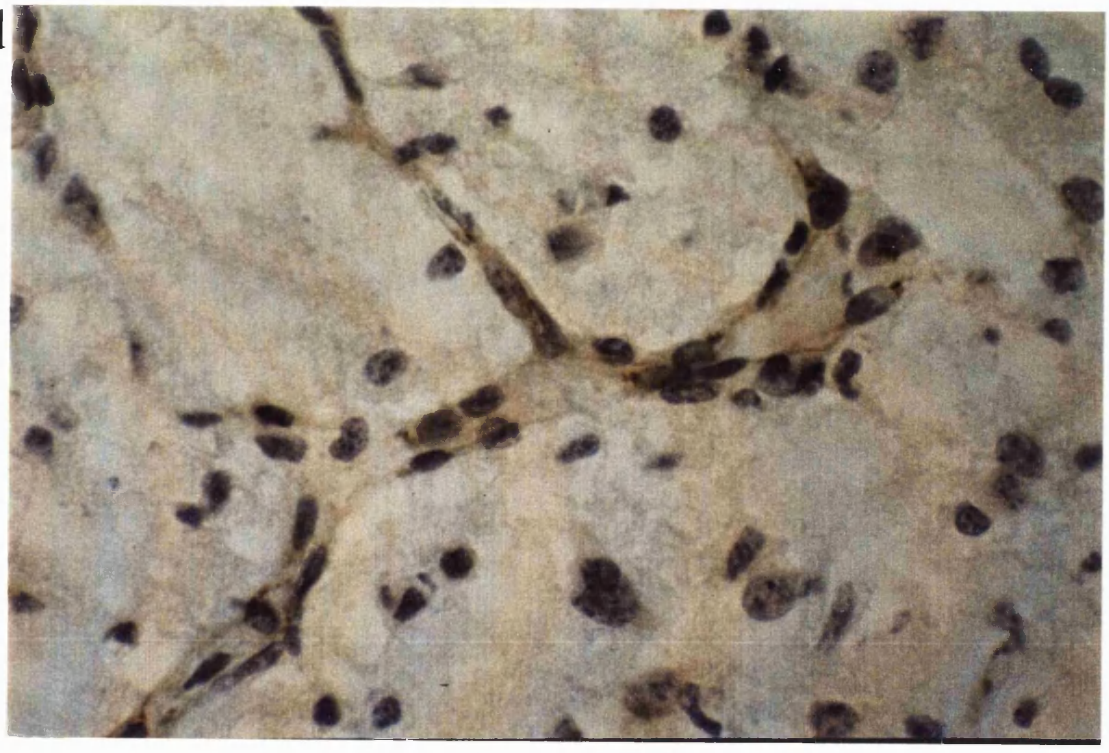

In 2 control animals the carotid arteries were not occluded, but the subjects were observed for the full 96 hour study period. There was no significant acute or delayed change in CI, ECoG, NIRS variables, MAP or blood gases during the study period.

n-NOS: In a similar intensity and frequency, prominent neuronal immunoreactivity was evident within cell bodies predominantly in the cerebral cortex, but also in the regions of the hippocampus, striatum and dentate gyrus.

e-NOS: Again there was staining within the endothelial layer of the cerebral vessels and the choroid plexus. Immunostaining was located within the cytoplasm of these cells.

i-NOS: No i-NOS immunoreactivity was found in the control brains. Diffuse background staining within the myelin was sometimes noted but was thought to be artifact.

5.3 Effect of NOS inhibition

5.3.1 Methods and Materials

Nineteen singleton Romney Suffolk fetal sheep of known gestational age (119-133 days) were operated on under 2% halothane/oxygen general anaesthesia using sterile techniques. The techniques employed and general experimental approach has been described previously in chapter 2 and 3. An additional polyvinyl catheter was placed in the umbilical vein for drug administration.

5.3.2 Drug Preparation

Acetylcholine was employed to confirm NOS inhibition as described in the next section. Acetylcholine chloride (Ach) (Sigma Chemical Co.,St. Louis, MO) was diluted with sterile 0.9% normal saline (10 $\mu g.mL^{-1}$). N^G-Nitro-L-arginine (L-NNA) (Sigma Chemical Co.,St. Louis, MO), employed to induce NOS inhibition, was dissolved in 0.1M HCl and diluted with 1M phosphate buffered saline (5 $mg.mL^{-1}$) to a pH of 2.8-3.4 as L-NNA is insoluble at neutral pH.

5.3.3 Experimental protocol

Prior to the ischaemic insult, the hypotensive effect of a bolus intravenous injection of Ach (2 μg) was measured. Five doses of Ach were rapidly injected into the umbilical vein and the effect on systemic MAP was recorded with measurements obtained every 0.5 seconds.

Transient cerebral ischaemia was then induced by 30 minutes inflation of the bilateral carotid cuffs as described in chapter 3 and confirmed by an isoelectric ECoG and a rise in CI.

Two hours post-ischaemia, fetuses were randomly assigned to treatment or control group. The treatment group received a continuous infusion of L-NNA into the umbilical vein at a dose of

50 mg.hour^{-1} for the first 4 hours followed by 20 mg.hour^{-1} over the subsequent 3 days. The dose was shown to attenuate the hypotensive effects of Ach and attenuation was confirmed daily throughout the study period in all the experimental animals. The control group received equal volumes of 1M phosphate buffered saline (pH 2.8-3.4), and Ach.

SaO_2, paO_2, $paCO_2$, lactate, glucose and Hb were measured prior to and immediately following the end of the occlusion, and at frequent intervals during the study period. Three days post-ischaemia ewes were sacrificed with an overdose of pentobarbital.

5.3.4 Histological assessment

Brains were fixed in 10% formalin and embedded in paraffin. Histological sections were stained with acid fuchsin and scoring was performed on both hemispheres on coronal subserial sections (8 μm) by an independent neuropathologist experienced in the preparation. Dead cells were recognized by an acidophilic (red) cytoplasm and contracted nuclei, or just a small rim of red cytoplasm with a pyknotic nuclei, whereas all other cells were considered viable. The proportion of dead cells was assessed and scored and a mean value obtained from both hemispheres which was expressed as a percentage (neuronal score).

5.3.5 Data analysis and statistics

For analysis of NIRS variables, changes in the chromophore concentration were calculated from alterations in optical attenuation by least-squares multilinear regression using the algorithm described chapter 2. ECoG intensity data were log transformed and the onset of epileptiform activity was indicated by the development of intense (>-5db), low frequency activity.

The number of seizures were counted from the data displayed on the chart recorder and were recognized as episodes of high intensity ECoG activity associated with increased EMG activity and MAP. Status epilepticus was scored as 60 seizures.hour^{-1}.

Changes in CBV were calculated from [tHb] according to the arterial Hb which was measured throughout the study period. Within each group, changes in CBV over time were determined using repeated measures ANOVA. Differences between the groups were determined by ANOVA and Student-Newman-Keuls multiple comparisons test.
Linear regression analysis was used to determine the relation between

i) the magnitude and duration of the delayed increase in CBV;
ii) the final CBV at 66-72 hours post-ischaemia;

and outcome measured histologically. Significant results (p value of <0.05) are presented as mean ±SEM. The end of the carotid artery occlusion is referred to as time zero.

5.3.6 Results

5.3.6.1 Study Groups

Nineteen subjects were investigated of which 8 were rejected: 3 due to premature labour and 5 who died before the end of the study period. There was no difference in mortality between treatment and control group. 11 fetuses were allocated to control (n=6) and treatment (n=5) groups and were similar for gestational age (127±1.2 days), weight (3.9±0.2 Kg) and head circumference (5.8±0.1 cm). Table 5.1 shows the physiological parameters throughout the study period. In both groups there was a rise in glucose and lactate and a fall in pH during the insult ($p<0.05$) and there were no differences between the groups during the study.

5.3.6.2 Evidence of NOS inhibition by L-NNA

5.3.6.2 i) Effect of L-NNA on the response to Ach

Figure 5.1 shows the change in MAP induced by 2 μg Ach. In both groups Ach induced a fall in MAP prior to L-NNA treatment. In the control group, this effect was maintained throughout the study. However it was suppressed in the treatment group following the administration of L-NNA ($p<0.001$).

5.3.6.2 ii) Effect of L-NNA on MAP

Changes in MAP throughout the study period are shown in figure 5.2. There was a rise in MAP during the insult in both groups ($p<0.001$). This resolved in the control group following release of the occlusion and persisted in the treatment group following the commencement of L-NNA until 24 hours post ischaemia ($p<0.05$). MAP was greater in the treatment compared to control group throughout the study period ($p<0.05$).

Table 5.1 **Changes in arterial blood indices, mean arterial blood pressure and cortical impedance in control and N^G-nitro-L-arginine groups during and following cerebral ischaemia**

*Table 5.1 shows the changes in arterial pH, oxygen tension (paO_2), carbon dioxide tension ($paCO_2$), oxygen saturation (SaO_2), lactate, glucose and hemoglobin (Hb), mean arterial blood pressure (MAP) and cortical impedance (CI) during and following cerebral ischaemia. There was a rise in lactate and glucose during the ischaemia in both groups. MAP increased during ischaemia in both groups and remained elevated above baseline in the treatment group during the subsequent 24 hours. CI increased during the insult; residual CI 2-6 hours shows no different between the groups; a delayed increase in CI commenced later and was of equal magnitude in both groups. Each time point represents mean ±SEM for each group; ‡ $p<0.01$ and * $p<0.05$.*

	Control group							N^G-Nitro-L-arginine treated group						
Time (hours)	-2	0	2	6	24	48	72	-2	0	2	6	24	48	72
pH	7.37 ±0.01	7.28 * ±0.04	7.36 ±0.02	7.37 ±0.02	7.36 ±0.01	7.38 ±0.01	7.35 ±0.01	7.39 ±0.01	7.28* ±0.01	7.35 ±0.02	7.38 ±0.02	7.37 ±0.01	7.35 ±0.01	7.37 ±0.02
PaO_2 mmHg	19±1	16±1	20±1	20±2	19±2	19±1	21±1	22±3	21±2	22±2	23±3	20±3	19±3	21±3
$PaCO_2$ mmHg	44±2	48±3	41±3	47±2	45±2	44±2	44±1	48±2	52±1	48±1	49±3	49±1	49±2	52±3
Lactate $mmol.L^{-1}$	1.0 ±0.2	2.9* ±0.6	2.1 ±0.8	1.4 ±0.4	2.3 ±0.7	1.5 ±0.4	0.8 ±0.1	0.9 ±0.1	3.2* ±0.1	3.2 ±0.7	1.5 ±0.3	1.0 ±0.2	1.1 ±0.2	0.8 ±0.1
Glucose $mmol.L^{-1}$	1.1 ±0.2	1.6* ±0.2	1.4 ±0.3	1.2 ±0.2	1.6 ±0.3	1.1 ±0.1	0.9 ±0.1	0.9 ±0.1	1.7* ±0.1	1.4 ±0.1	1.3 ±0.1	1.0 ±0.1	0.9 ±0.0	0.8 ±0.0
Hb g.dL	12±1	13±1	11±1	12±1	12±1	12±1	12±1	11±1	12±1	11±1	12±1	11±1	11±1	12±1
SaO_2 %	51±3	39±4	53±4	51±6	49±5	48±4	55±3	60±4	51±4	57±3	59±3	52±6	46±6	54±6
MAP mmHg	29±0.4	43±2.3‡	36±3.0	32±2.2	34±1.8	33±1.4	31±1.6	31±0.4	48±5.2	41±3.1	41±3.1	40±2.1	35±1.3	33±0.9
CI %	100±0.0	128±7.6‡	112±3.2	108±2.7	118±3.9*	133±4.4*	123±6.1*	100±0.0	138±2.5‡	106±1.2	105±1.4	111±2.1*	132±3.3*	126±5.8*

Table 5.1 **Physiological parameters in control and treatment group.**

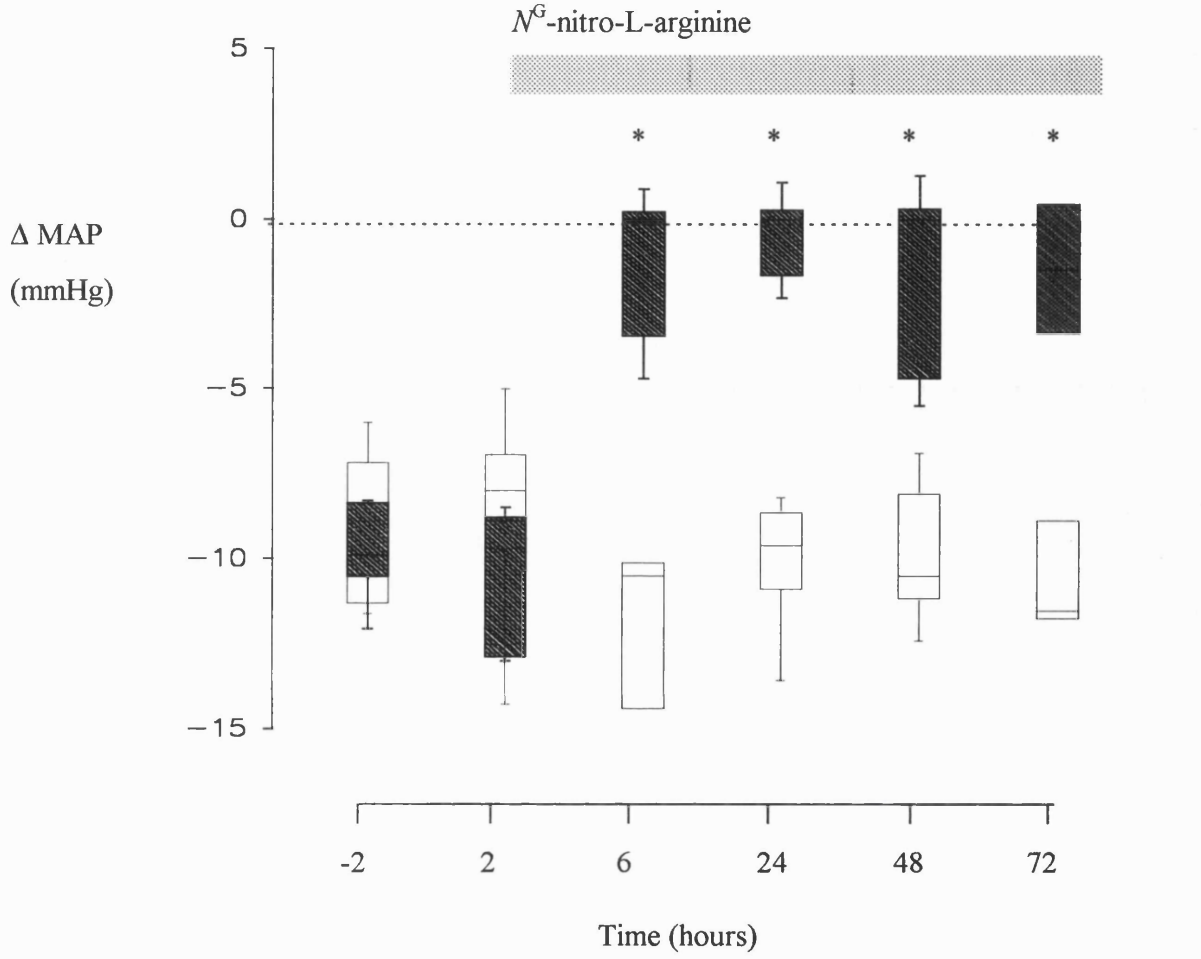

Figure 5.1 **Changes in mean arterial blood pressure induced by acetylcholine in control and N^G-nitro-L-arginine treated group prior to and following cerebral ischaemia**

The figure shows the changes in mean arterial blood pressure (MAP) induced by the administration of 2μg acetylcholine (Ach). Ach causes vasodilation and a fall in MAP through the release of NO and the effect is attenuated in the treatment group (filled bars), following the commencement of N^G-nitro-L-arginine at 2 hours ($p<0.01$). Each bar represents the range and median at each time point for each group.*

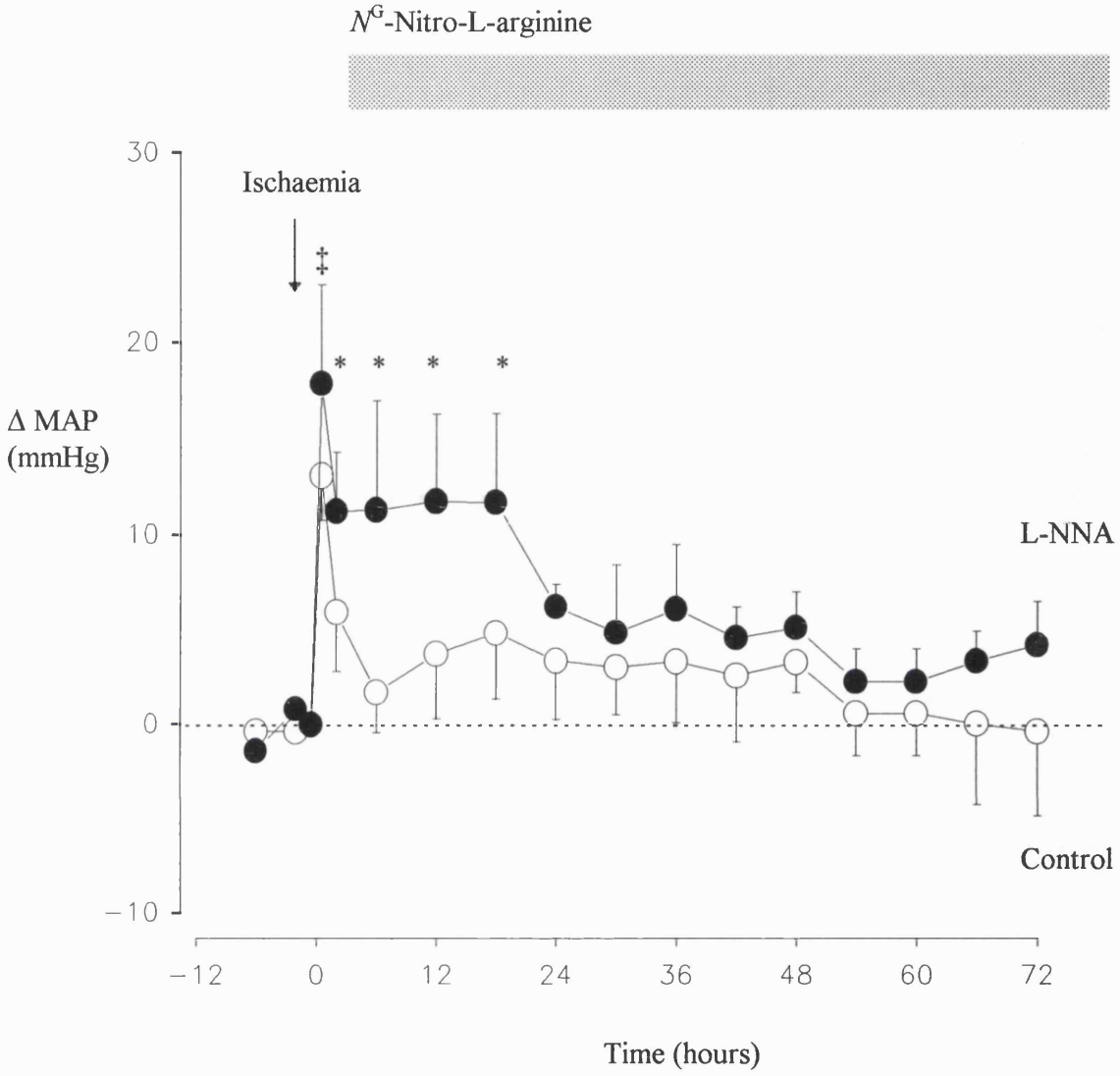

Figure 5.2 **Changes in mean arterial blood pressure in control and N^G-nitro-L-arginine treated fetuses during and following cerebral ischaemia**

The figure shows the changes in mean arterial blood pressure (MAP) during and following cerebral ischaemia in control (○) and N^G-nitro-L-arginine treated (●) fetuses. In both groups there was an increase in MAP during the ischaemic insult (‡ $p<0.01$). MAP returned to baseline in the control group following release of the occlusion but remained elevated above baseline in the L-NNA treated group

($p< 0.05$). Each symbol represents the mean ±SEM of averaged data in each group.*

5.3.6.3 Cerebrovascular Effects of L-NNA

Figure 5.3 shows the changes in CBV during and following cerebral ischaemia. As previously shown, following transient cerebral ischaemia there were 2 phases of increased CBV above pre-ischaemic baseline (1). The first phase immediately followed the insult and was similar in peak height and duration in the 2 groups.

The second phase commenced at 13.1±1.0 hours post-ischaemia in the control group and 12.7±2.3 hours in the treatment group. However, the increase was attenuated in the treatment group ($p<0.01$) and the maximum increase at 30-36 hours was significantly different between control (1.2±0.2 $mL.100g^{-1}$) and treatment group (0.5±0.1 $mL.100g^{-1}$) ($p<0.05$). Duration of the second increase in CBV was 43±4 hours in the control and 33±2 hours in the treatment group ($p=0.09$). At the end of the study period (66-72 hours post-ischaemia), CBV was depressed below pre-ischaemic baseline in the treatment (-0.7±0.2 $mL.100g^{-1}$;$p<0.05$), but not in the control group (-0.1±0.3 $mL.100g^{-1}$)

Linear regression analysis indicated that worse histological outcome was related to:

a) Shorter duration of the second increase in CBV ($r=0.8$; $p<0.01$). Figure 5.5a.
b) Lower final CBV ($r=0.8$; $p<0.01$). Figure 5.5b

There was no relation between the maximum increase in CBV at 30-36 hours and outcome.

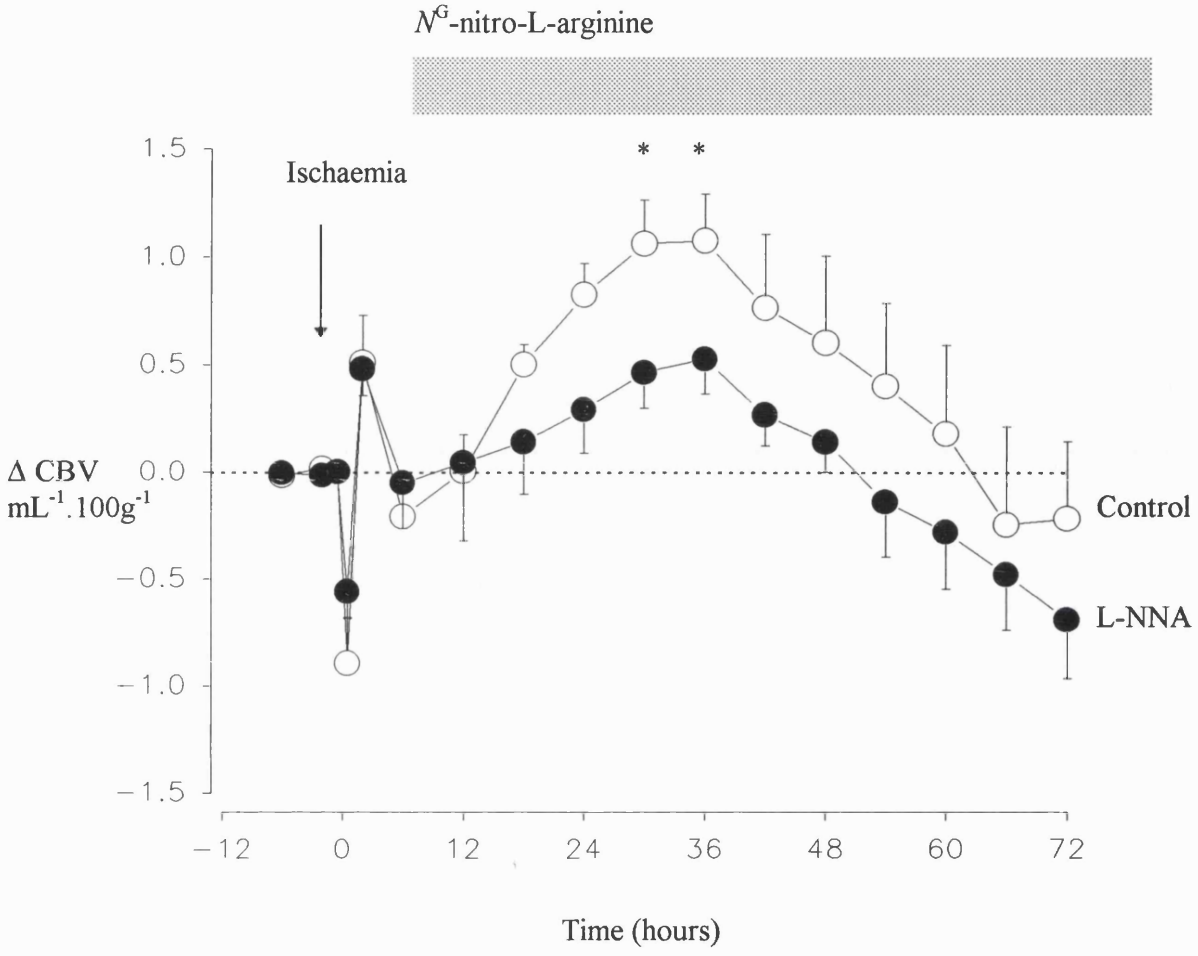

Figure 5..3 **Changes in cerebral blood volume in control and N^G-nitro-L-arginine treated fetuses during and following cerebral ischaemia**

*The figure shows the changes in cerebral blood volume (CBV) during and following cerebral ischaemia in control (○) and N^G-nitro-L-arginine (L-NNA) treated fetuses (●). There were 2 phases of increased CBV: i) an early phase immediately following the end of ischaemia and ii) a delayed phase commencing some hours later. There was no difference in the early phase, however the delayed phase was attenuated in the treatment group (* $p<0.05$). Each symbol represents the mean ±SEM of averaged data for each group*

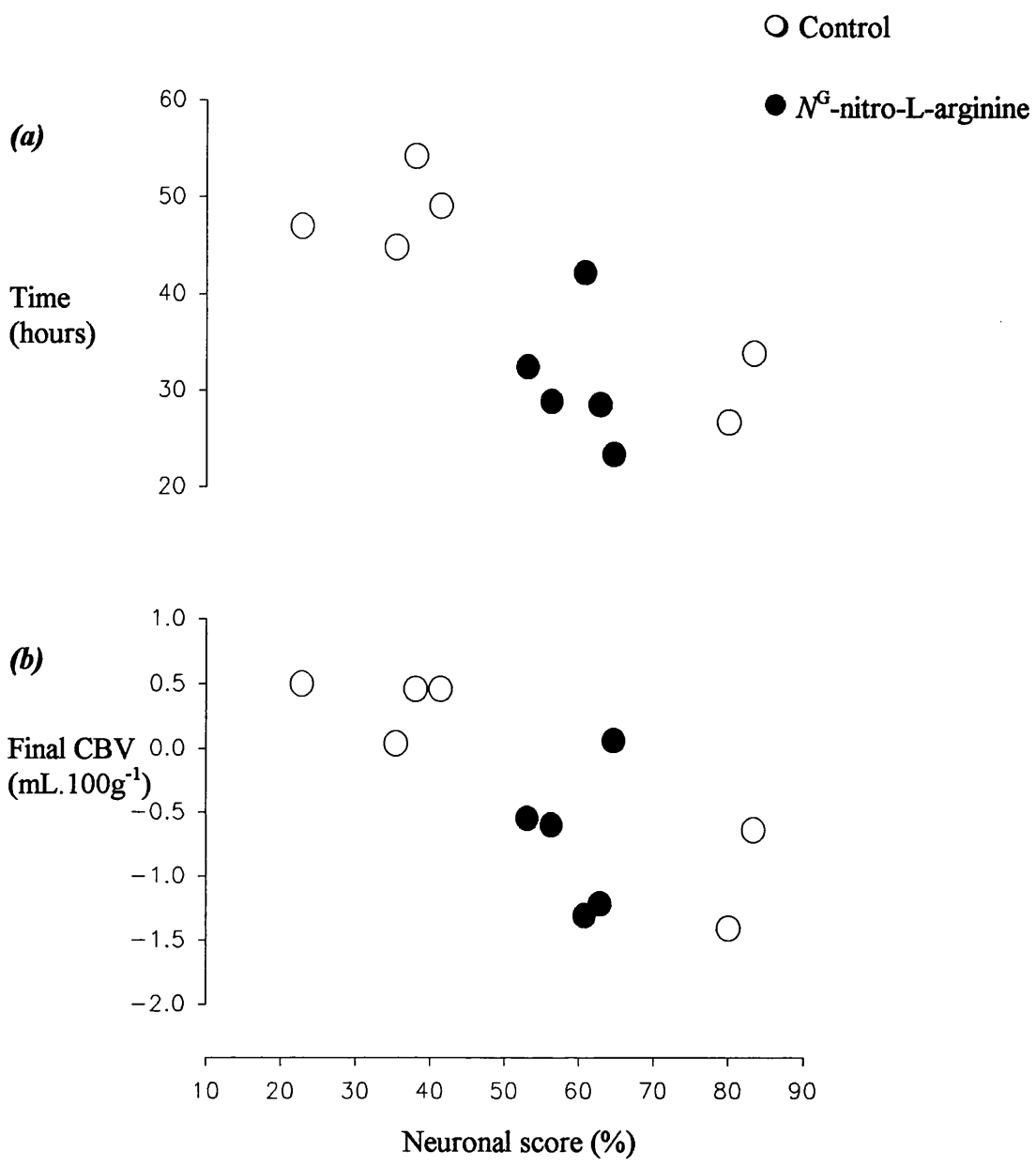

Figure 5.4 *(a), (b)* **The relation between the changes in cerebral blood volume and histological outcome following transient cerebral ischaemia in control and N^G-nitro-L- arginine treated fetuses**

(a) shows the relation between the duration of the delayed increase in cerebral blood volume (CBV) ($r=0.7$; $p<0.05$) and (b) final CBV at the end of the study period ($r=0.8$; $p<0.01$) and neuronal score. A worse histological outcome was related to a short-lived delayed increase in CBV and a more depressed final CBV.

5.3.6.4 Electrocortical activity and cortical impedance

5.3.6.4.i) ECoG Activity (Figures 5.5 -5.7)

Representative examples of the changes in ECoG intensity (a) and frequency (b) in control and treatment group is shown in Figure 5.5. ECoG intensity was depressed during and following ischaemia. In both groups delayed cortical seizures were indicated by intense, low frequency ECoG activity and persisted for 20 ±5 hours in the control and 16 ±3 hours in the treatment group.

Figure 5.6 shows the ECoG intensity in control and L-NNA treated group during and following cerebral ischaemia. In both groups ECoG intensity was depressed below pre-ischaemic baseline by the end of the study period and was more depressed in treatment (-19 ±1 dB) compared to control group (-10 ±2.0 dB) ($p<0.05$).

Figure 5.7 shows the seizure count (number of seizures.hour^{-1}) in the control and treatment group. There was an increased duration of seizures in the treatment group (18-48 hours) as compared to the control group (24-30 hours) ($p<0.05$).The duration of seizures did not relate to histological outcome. However, a more depressed final ECoG intensity at 66-72 hours related to a lower final CBV ($r=0.8$; $p<0.01$) and a worse histological outcome ($r=0.9$; $p<0.01$).

5.3.6.4 ii) Cortical impedance (Figure 5.7)

Figure 5.7 shows the two phases of increased CI above baseline: (I) during ischaemia and (II) commencing at 15±3 hours post-ischaemia in the control group and 14±4 hours in the treatment group. There was no difference in magnitude of the rise in CI during ischaemia between the groups. Recovery CI at 2-6 hours was 108±2.7% in the control and 105±1.4% in the treatment group indicating no difference in the severity of the initial cerebral insult. The delayed increase in CI peaked to 140±9% at 36±2 hours post-ischaemia in the control group and 140±6% at 42±3 hours in the treatment group.

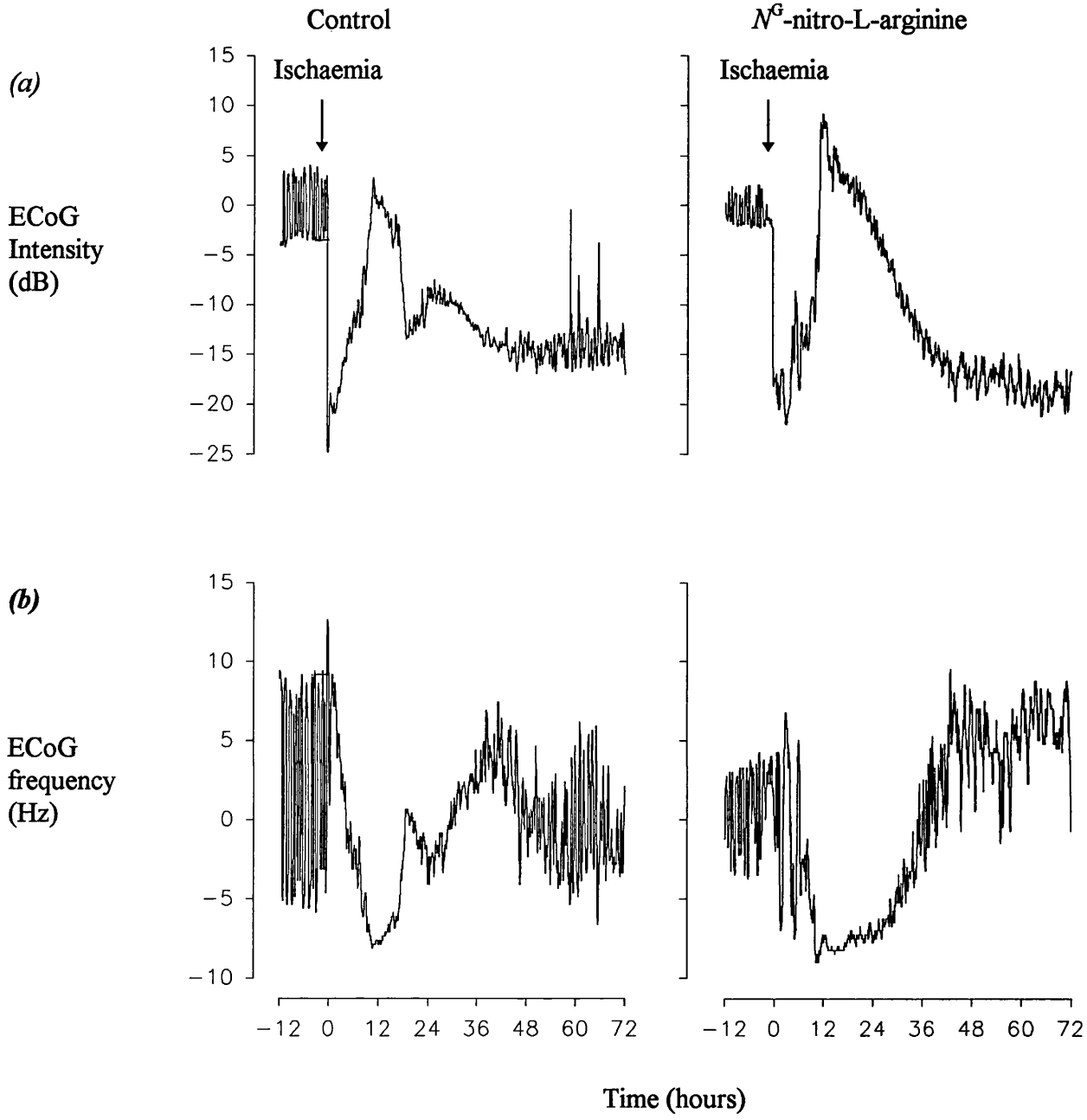

Figure 5..5 *a, b* **Changes in electrocorticographic intensity and frequency following transient cerebral ischaemia in a representative control and N^G-nitro-L-arginine treated fetus**

The time course of the changes in (a) electrocortical intensity (ECoG) and (b) frequency are shown in representative examples of a control fetus (left panel) and N^G-nitro-L-arginine treated fetus. In both there is depression of ECoG intensity during ischaemia. Delayed cortical seizures occurred in both groups, indicated by the presence of intense, low frequency epileptiform activity

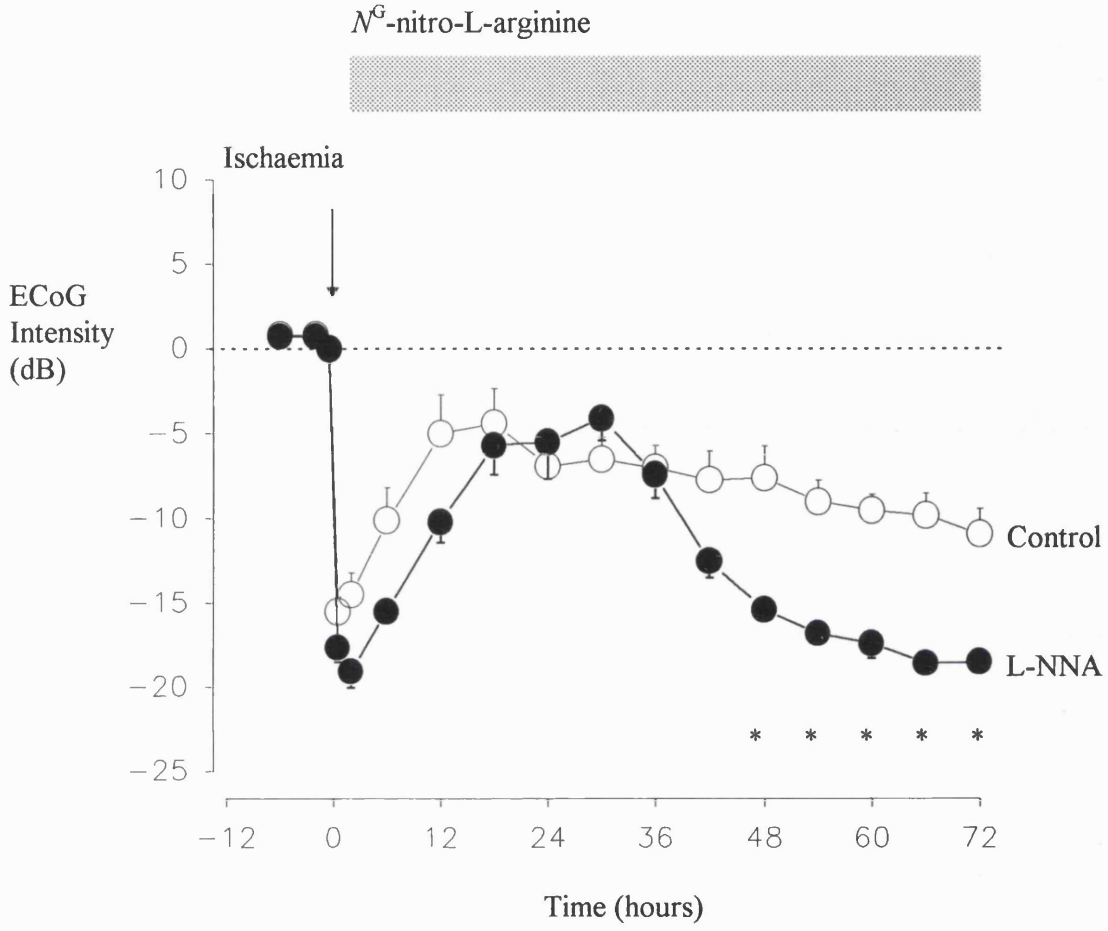

Figure 5.6 **Changes in ECoG intensity during and following cerebral ischaemia in control and N^G-nitro-L-arginine treatment group**

The figure shows the changes in electrocorticographic (ECoG) intensity during and following cerebral ischaemia in control (○) and treatment (●) group. In both groups there was a fall in intensity during and following the insult. A delayed increase in ECoG intensity indicated the presence of intense, low frequency epileptiform activity. Following seizures ECoG intensity was depressed below baseline in both groups and significantly more depressed in treatment compared to control group ($p<0.05$). Each symbol represents the mean ±SEM of averaged data in each group.*

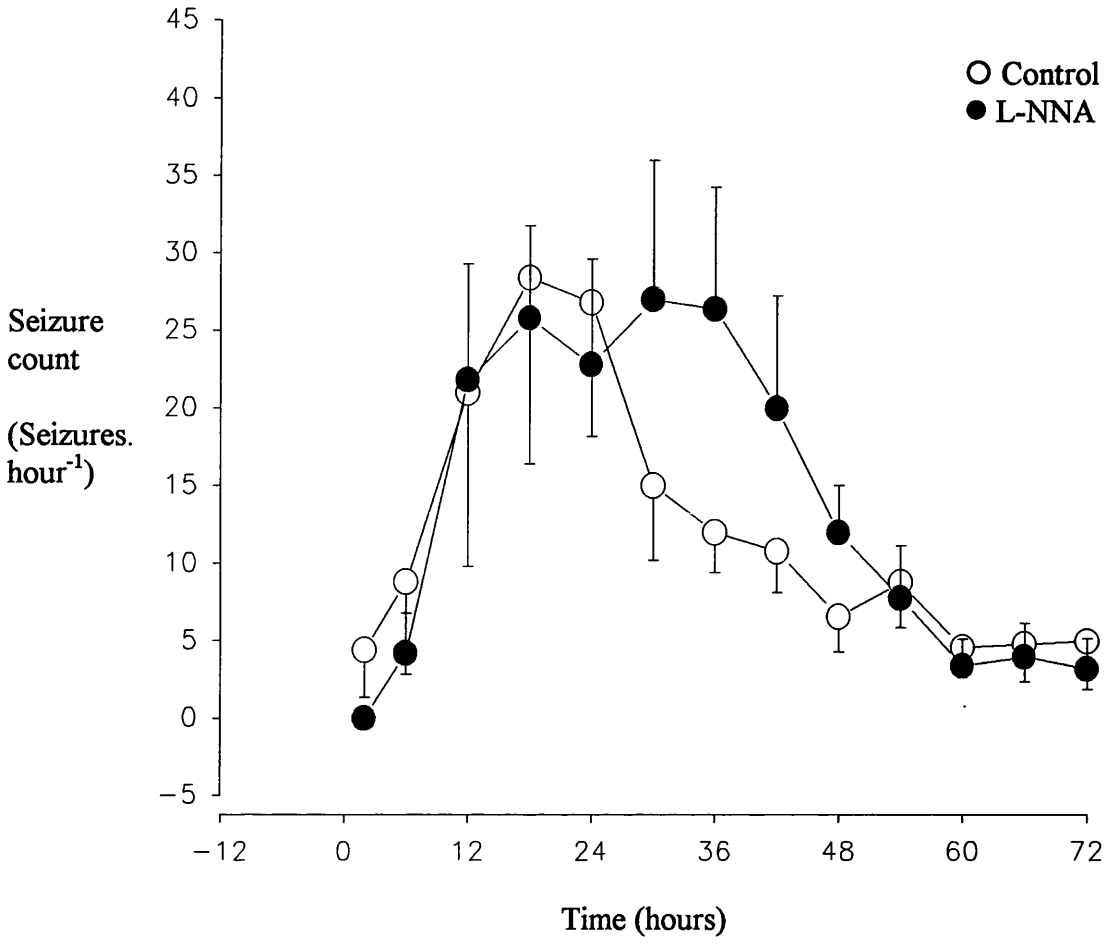

Figure 5.7 **Number of seizures following transient cerebral ischaemia in control and N^G-nitro-L- arginine treated fetuses**

Seizure count was assessed following transient cerebral ischaemia in control (O) and N^G-nitro-L- arginine (L-NNA) (●) treated fetuses. The number of seizures were counted on the analogue chart recorder, identified by the electrocortical intensity and electromyographic activity (status epilepticus was scored as 60.hour^{-1}). In the control group, seizure count was increased between 24-30 hours and in the treatment group between 18-48 hours ($p<0.05$)

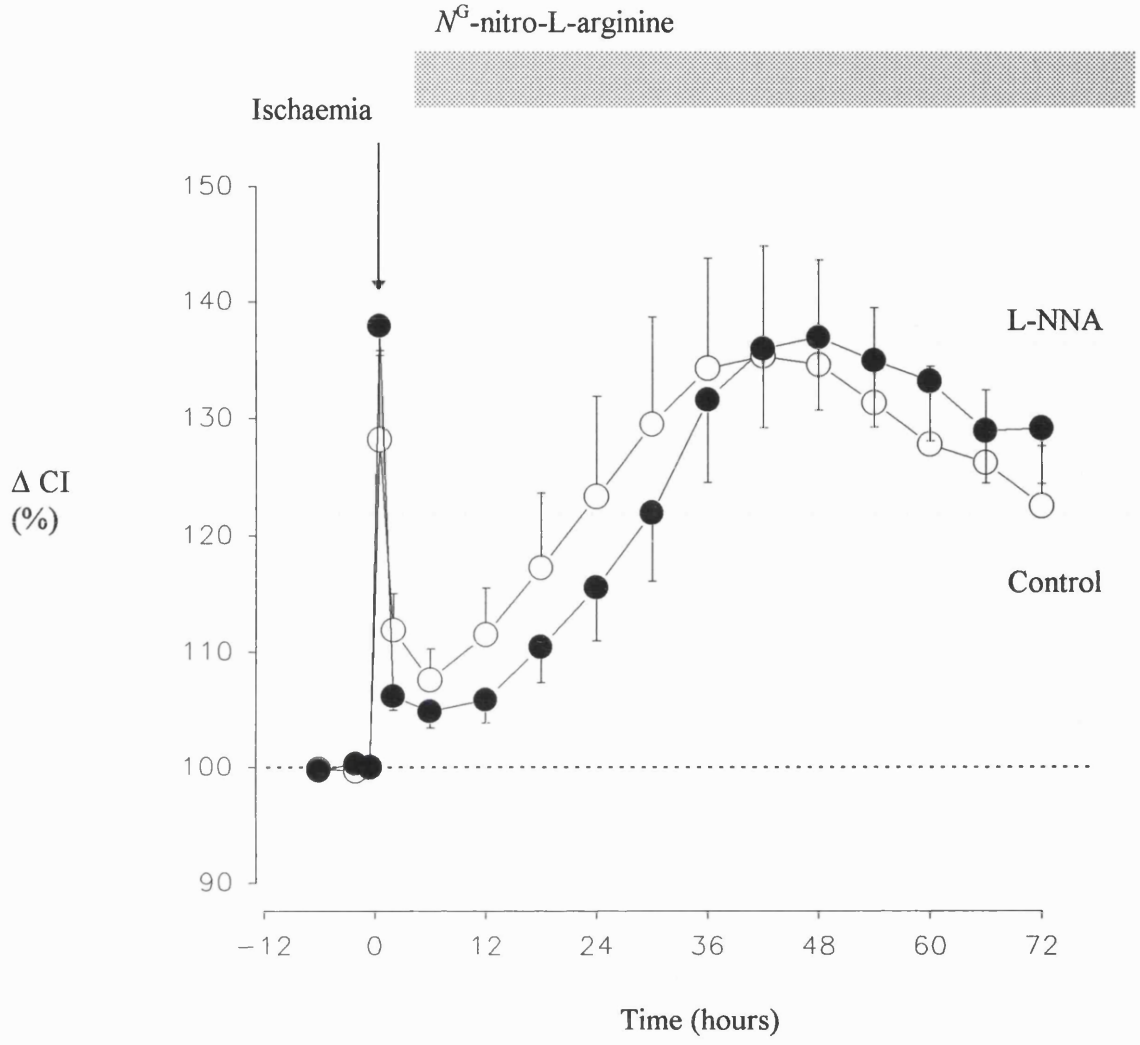

Figure 5.8 **Changes in cortical impedance during and following transient cerebral ischaemia in control and N^G-nitro-L-arginine treatment group**

The figure shows the changes in cortical impedance (CI) during and following cerebral ischaemia in control (O) and N^G-nitro-L-arginine (L-NNA) treated fetuses (●). There were 2 phases of increased CI - i) during the ischaemic insult; and after a period of recovery, ii) a delayed phase commencing several hours later. There was no difference between groups in the early or recovery CI indicating similar severity of the initial injury. An increase in CI reflects altered energy metabolism such that ionic homeostasis across cellular membranes is impaired and cytotoxic oedema develops. Each symbol represents mean ±SEM of averaged data in each group.

5.3.6.5 Histological Outcome

Figure 5.8 gives the histological results. The distribution of damage was similar in the 2 groups with laminar necrosis in the parasagittal region of the cortex and a lesser degree of injury in the lateral cortex, hippocampus, striatum and thalamus. There was increased cerebral injury in the treatment group in all regions assessed ($p<0.05$).

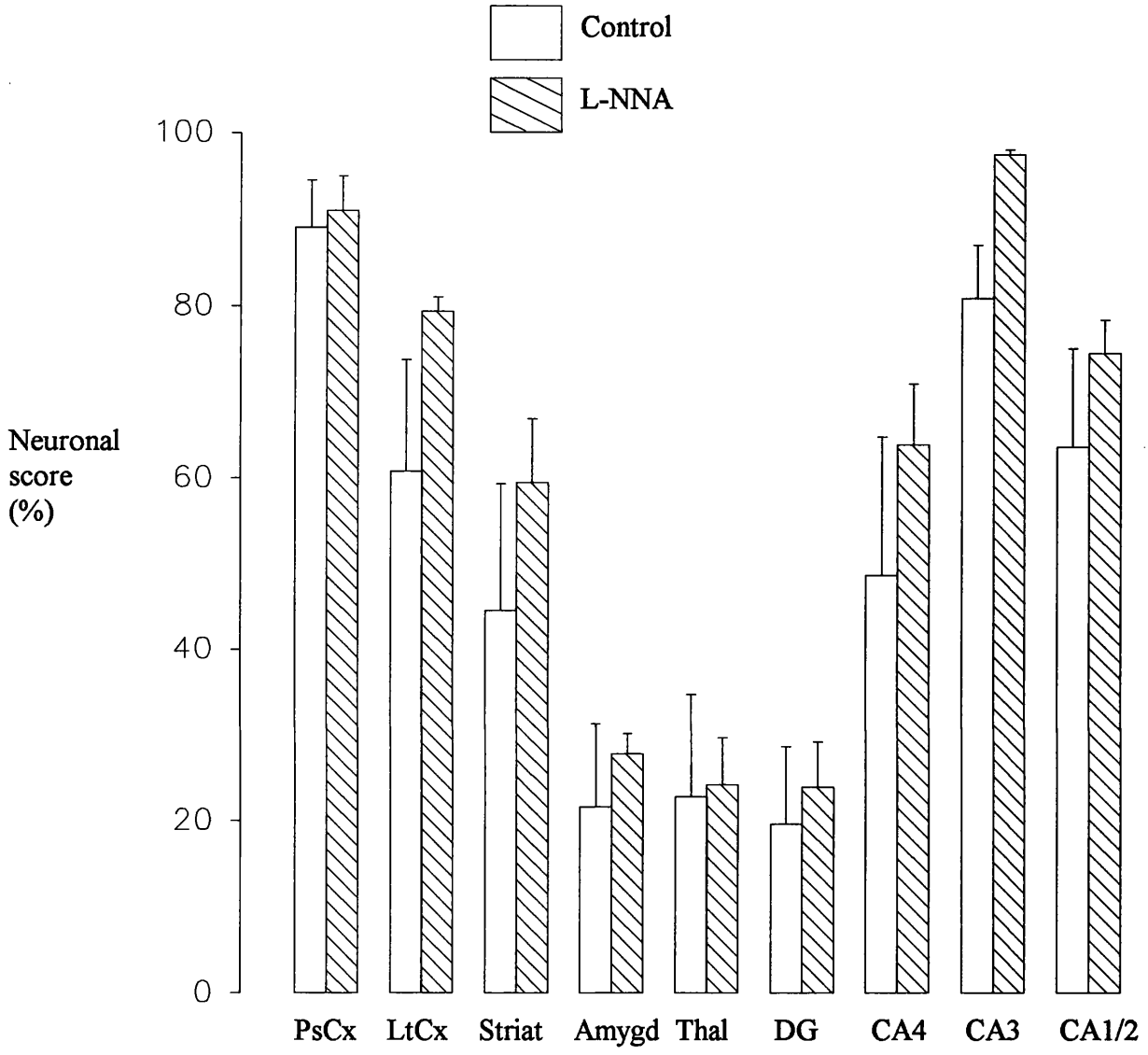

Figure 5.9 **Histological outcome 3 days following transient cerebral ischaemia in control and N^G-nitro-L-arginine treated fetuses**

Neuronal loss was scored 3 days following transient cerebral ischaemia in the parasagittal cortex (PsCx), lateral cortex (LtCx), striatum (Striat), amygdala (Amygd), thalamus (Thal), dentate gyrus (DG) and subfields of the hippocampus (CA1/2, 3, 4) in control (□) and treated animals (□). There was increased damage in the treated animals ($P<0.05$). Each bar represents mean ±SEM in each group.

5.3.6.6 Cerebral Oxygenation

Figure 5.10 shows the changes in [HbO_2] and [tHb] in (a) control and (b) L-NNA treated groups. In the control group, [HbO_2] remained elevated towards the end of the study period although [tHb] returned towards baseline demonstrating an increase in mean cerebral saturation. In the treatment group, a similar relationship was observed between [HbO_2] and [tHb] although the final [HbO_2] returned to baseline in the presence of a fall in [tHb] below baseline.

Figure 5.11 shows the changes in the optical signal attributed to [$CytO_2$] in the (a) control and (b) treatment groups. In the control group there was a fall in [$CytO_2$] following the insult to -0.3±0.1μmol.L^{-1}. A further fall commenced at 54 hours post-ischaemia and reached a minimum of -2.2 ±0.2 at 72 hours. In the treatment group [$CytO_2$] did not fall during or immediately following the insult. A progressive fall also commenced at 54 hours to reach a minimum of -2.0 ±0.4 μmol.L^{-1} at the end of the study period.

Figure 5.12 shows the relation between maximum fall in [$CytO_2$] and measures of outcome: *(a)* residual CI immediately following the insult; *(b)* final ECoG intensity; and *(c)* neuronal score. Maximum fall in [$CytO_2$] related to residual CI immediately following the insult ($r=0.76$; $p=0.01$) although did not relate to final ECoG ($r=0.12$; $p=0.744$) or neuronal score ($r=0.6$; $p=0.058$).

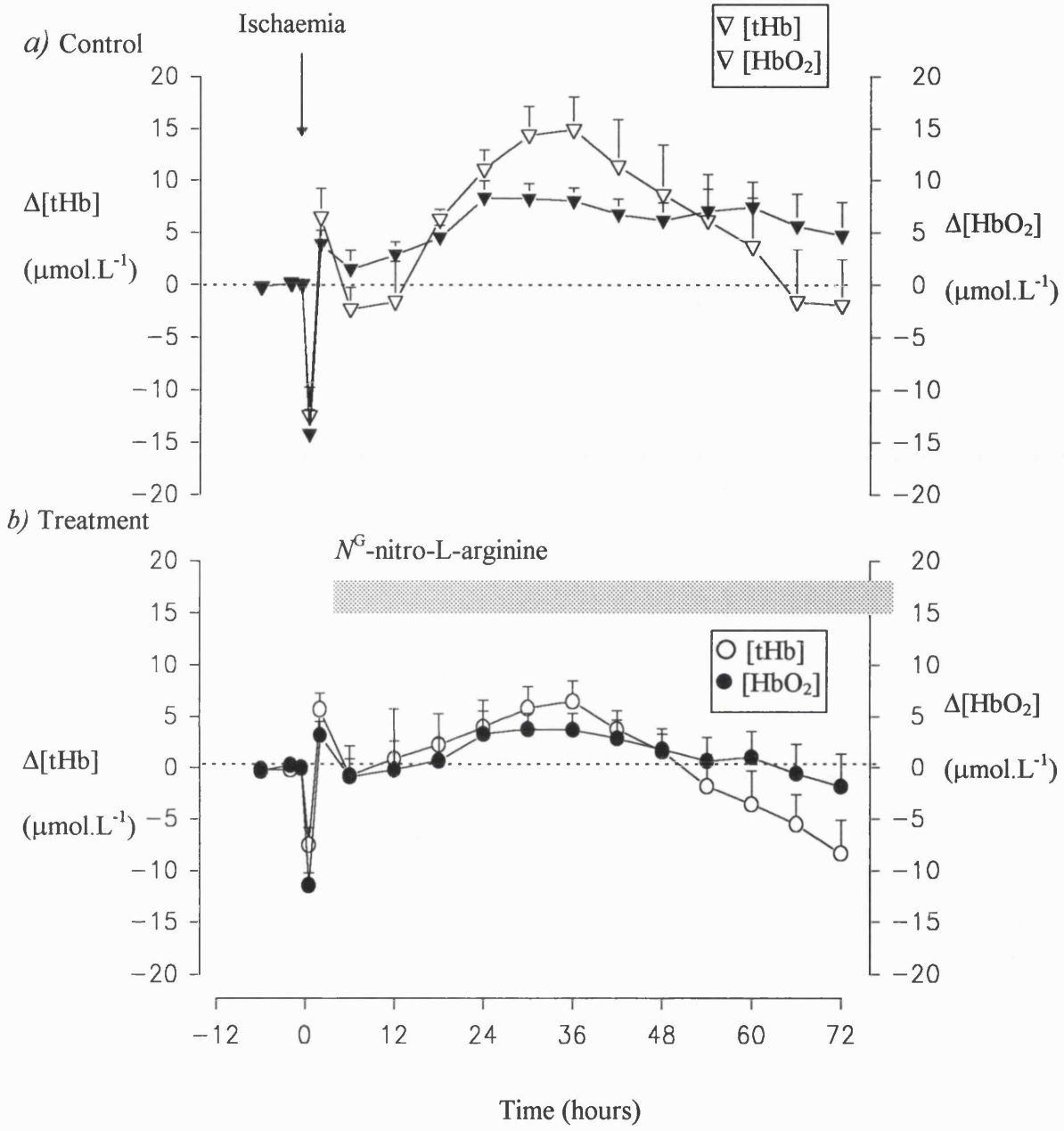

Figure 5.10 **Changes in oxyhaemoglobin and total cerebral haemoglobin in *(a)* control group and *(b)* N^G-nitro-L-arginine during and following cerebral ischaemia**

The changes in oxyhaemoglobin ($\Delta[HbO_2]$) and total cerebral haemoglobin ($\Delta[tHb]$) following ischaemia are shown in (a) control (∇) and (b) treatment group (○). In both groups, an increase in $[HbO_2]$ relative to [tHb] towards the end of the study period indicated an increase in mean cerebral saturation . Each symbol represents the mean ±SEM of averaged data in each group.

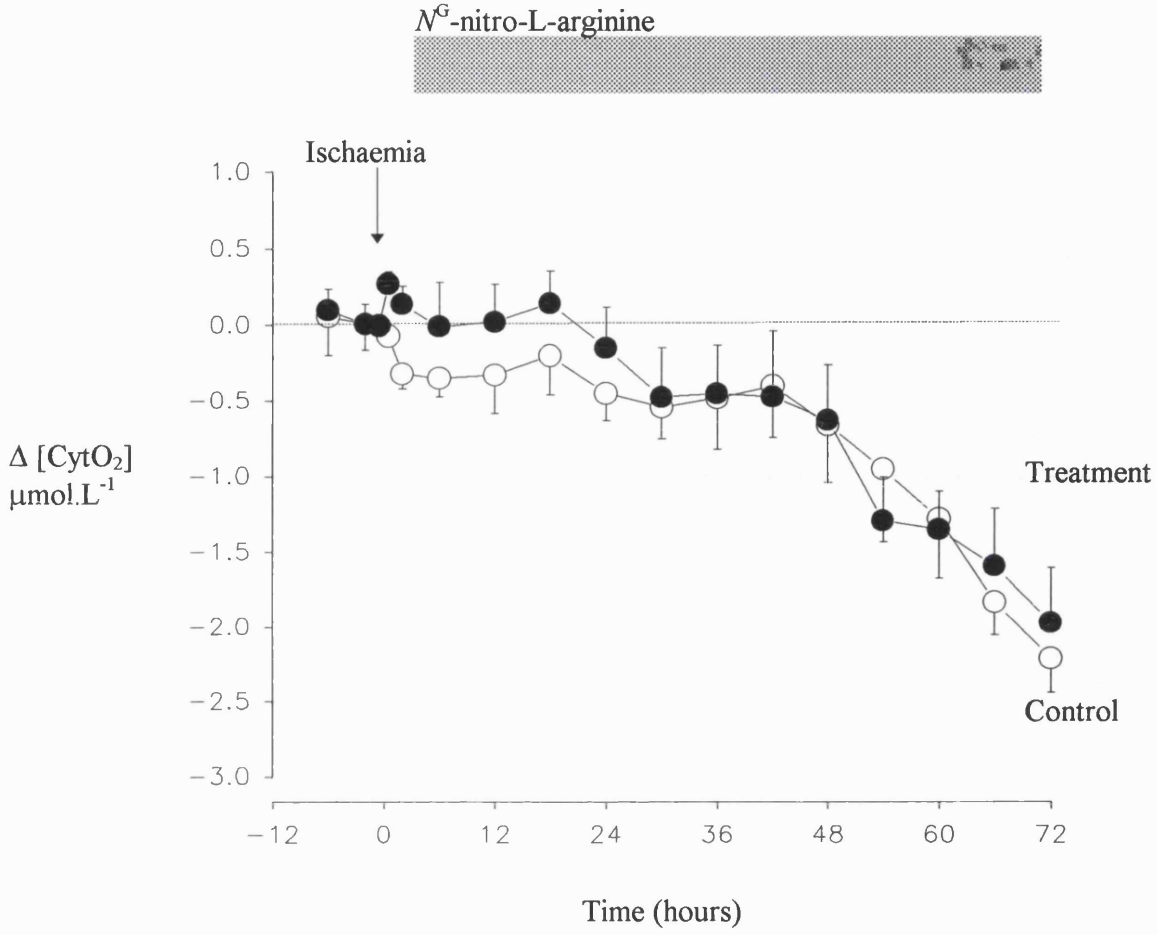

Figure 5.11 **Changes in the concentration of oxidised cytochrome aa_3 in control and N^G-nitro-L-arginine treatment groups during and following cerebral ischaemia.**

The figure shows the changes in oxidised cytochrome oxidase concentration (Δ [$CytO_2$]) in control (○) and N^G-nitro-L-arginine (L-NNA) treatment (●) groups. In the control group there was a fall following the ischaemic insult ($p<0.05$) and then a further fall that commenced 54 hours and then fell progressively until the end of the study period ($P<0.05$). In the treatment group there was no fall during or immediately following the insult. A progressive fall commenced at 54 hours until the end of the study period ($p<0.05$). There was no difference between the groups. Each symbol represents the mean of averaged data for each group ±SEM.

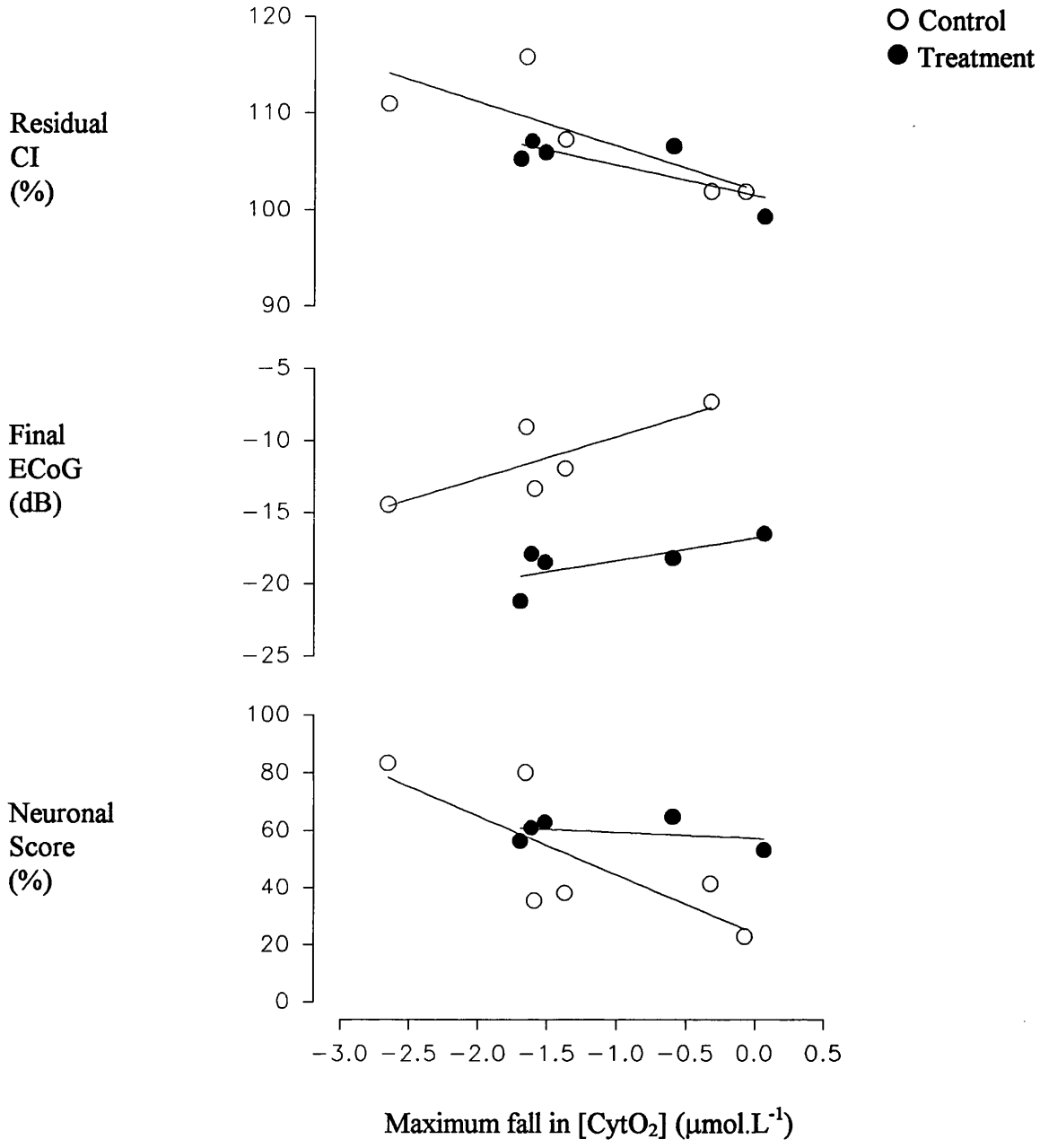

Figure 5.12 **Relation between maximum fall in oxidised cytochrome aa_3 and *(a)* residual cortical impedance; *(b)* final electrocortical intensity; and *(c)* neuronal score in control and N^G-nitro-L-arginine treated fetuses**

The figure shows the relation between oxidised cytochrome aa_3 ($[CytO_2]$) and measures of outcome. Figure 4.11 (a) shows that the maximum fall in $[CytO_2]$ was greater with an increased residual cortical impedance (CI) immediately following reperfusion ($r=0.76$; $p=0.01$). There was no significant relation between maximum fall in $[CytO_2]$ and (b) final electrocortical intensity (ECoG) or (c) neuronal score in either group. Each symbol represents averaged data obtained from each fetus in control (O) and (●) N^G-nitro-L-arginine treated fetuses.

5.4 Discussion

The aims of the studies described in this chapter were to determine the presence of NOS expression in the ischaemic perinatal brain; demonstrate a role for NO production within the phase of delayed cerebral injury; and alter histological outcome by NOS inhibition in a way that may indicate the role of NO production.

Immunohistochemistry staining revealed the presence of n-NOS and e-NOS in the ischaemic brain. However, i-NOS staining was sparse and only clearly identified within the glial cells of one severely damaged sheep brain. There was no evidence of i-NOS staining within the control brains.

The results of the second series of studies indicate that treatment with the NOS inhibitor, L-NNA, attenuated the delayed cerebral vasodilation following transient cerebral ischaemia, and caused cerebral vasoconstriction, but did not decrease the extent of the cerebral injury.

L-NNA is an analogue of L-arginine with a chemically altered guanidino moiety. The synthesis of NO involves oxidation of a guanidino-nitrogen moiety of L-arginine and L-NNA produces competitive and enantiomerically specific inhibition of the oxidation both *in vitro* and *in vivo* (Rees DD et al 1990). L-NNA does not have the anti-muscarinic effects ascribed to the NOS inhibitors with alkyl ester substitutions at the carboxy terminal, and it inhibits both constitutively expressed and i-NOS.

Inhibition of NOS within the systemic circulation was demonstrated by measuring the effect of Ach on MAP. NO is released by the endothelium in response to Ach, and stimulates soluble guanylate cyclase in smooth muscle resulting in a rise in cGMP and relaxation (Southam E and Garthwaite J 1993). Systemic vasodilation induces a transient fall in MAP and attenuation of the hypotensive effect of Ach has been used to confirm chronic NOS inhibition in fetal sheep. Accordingly, the treatment group received the dose of L-NNA employed by Fineman et al and attenuation of the response to Ach was demonstrated throughout the study period (Fineman JR et al 1994). The dose required to achieve this effect (approximately 120

$mg.kg^{-1}.day^{-1}$) was greater that used in previous studies investigating the neuroprotective role of NO in perinatal animals (ranging from 1-100 $mg.kg^{-1}$) (Hamada Y et al 1994; Trifiletti RR 1992). However in previous studies the vascular effects of L-NNA were not assessed and may not have been achieved. In the present study, L-NNA was continuously infused as it readily crosses the placenta and is eliminated through the maternal circulation.

Changes in cerebrovascular tone were measured using NIRS to assess changes in [tHb] from which changes in CBV were calculated using the arterial Hb concentration. The changes in CBV do not differentiate between vascular compartments and give an estimate of the average vascular tone, although can be interpreted without considering the arterial blood pressure.

The effect of NOS inhibition on cerebral oxygenation was assessed by measuring changes in $[HbO_2]$ relative to [tHb]; and changes in $[CytO_2]$. As described in Chapter 4, $\Delta[HbO_2]$ is a measure of overall oxygenation of the cerebral blood whilst the optical signal thought to be derived from oxidised cytochrome oxidase may reflect the redox state of the mitochondria. The decline in [tHb] following the second peak was mainly ascribed to a fall in cerebral [Hb] and therefore there was an overall increase in mean cerebral saturation in both groups by the end of the study period. [tHb] fell below baseline in the L-NNA treated group, implying the presence of vasoconstriction, the relation between [tHb] and $[HbO_2]$ was similar in the 2 groups.

NOS inhibition did not appear to alter the optical signal for $[CytO_2]$ and the relations between maximum fall in $[CytO_2]$ although the measures of outcome described in the preceding chapter were not maintained.

Although maximum fall in $[CytO_2]$ did relate to residual CI immediately following the insult, it did not relate to final ECoG or neuronal score. Among the explanation for this finding is that (1) changes in $[CytO_2]$ as measured by NIRS is a reflection of changes in optical properties of the tissue rather than alteration in mitochondrial oxygenation *per se*; or (2) increased cerebral injury was not the result of altered mitochondrial oxygenation in the treated group. The difficulties in interpreting $[CytO_2]$ in this study is discussed in more detail in chapter 2.

Delayed administration of L-NNA was not associated with a decrease in the extent of cerebral injury assessed 3 days post-ischaemia. The possible mechanisms include reduced cerebral perfusion; increased number of seizure-like episodes; or that L-NNA is neurotoxic through a mechanism independent of NOS inhibition.

5.5 Summary

Delayed NOS inhibition following severe transient cerebral ischaemia in fetal sheep reduced the extent of delayed vasodilation but did not reduce the extent of cerebral injury. This may imply that delayed NO production has a protective role during the period of delayed cerebral injury.

Chapter 6

Discussion

6.1 Conclusions

The first study addressed the hypothesis that transient cerebral ischaemia in the perinatal brain induces changes in cerebral perfusion and oxygenation and that these changes are temporally related to the delayed phase of cerebral injury. The results showed that there were two distinct periods of increased [tHb] following cerebral ischaemia. The first period commenced shortly following reperfusion and persisted for 1-2 hours. The second period occurred several hours later, and preceded the onset of the delayed increase in CI suggesting that the vascular changes occurred before cellular dysfunction lead to a disruption of ionic homeostasis.

Cerebral mean oxygen saturation was estimated by observing the changes in [Hb] and [HbO_2] measured by NIRS. The results showed an increase in mean cerebral saturation by 3-4 days post-ischaemia. However, there was a fall in the NIRS measurement of [$CytO_2$] which commenced approximately 20 hours post-ischaemia. Quantification of the changes in [$CytO_2$] when measured by NIRS is subject to error, and whether it is an accurate representation of mitochondrial oxygenation is questionable.

The second hypothesis that the degree of the changes in cerebral perfusion and oxygenation related to the extent of cerebral injury was addressed by relating changes to histological outcome. The longer duration of the first increase in [tHb] related to worse outcome. Furthermore the duration of the second increase in [tHb] and final [tHb] at 4 days post-ischaemia were related to histological outcome: worse injury was associated with a shorter second period of increased [tHb] and a lower final [tHb]. Maximum fall in [$CytO_2$] by the end

of the study period was related to histological outcome and electrophysiological measures of cerebral injury.

Addressing the third hypothesis, that NOS expression is evident in the perinatal brain following ischaemia, immunohistochemical staining techniques were used to identify the presence of NOS. The n-NOS and e-NOS isoforms were clearly identified in the ischaemic fetal sheep brain, although i-NOS detection was limited. The fourth hypothesis that late changes in cerebrovascular tone are mediated through an increased production of NO and could be altered by NOS inhibition, was addressed by inducing NOS inhibition, two hours post-ischaemia with N^G-nitro-L-arginine (L-NNA). In the treatment group, delayed cerebral vasodilation was attenuated and cerebral vasoconstriction was evident towards the end of the three day study period. Again the duration of the second increase in CBV, and the final CBV at 3 days were related to outcome whether or not the fetus was treated with L-NNA. There was an increase in mean cerebral saturation in both the control and the treatment group. The fall in [$CytO_2$] from 24-36 hours post-ischaemia was of similar magnitude in both groups. Final [$CytO_2$] was related to outcome measured by residual CI immediately following the insult.

The final hypothesis, that NOS inhibition alters the extent of perinatal cerebral injury following ischaemia, was addressed by assessing the effect of NOS inhibition on histological outcome three days post-ischaemia. Although early measurements of CI immediately following resuscitation indicated no difference in severity of the initial insult, histological evidence of injury was increased in all regions of the brain in the treatment compared to control groups.

6.2 Accuracy of NIRS

The accuracy of NIRS for detecting alterations in [tHb], [HbO_2] and [$CytO_2$] requires precise absorption spectra, the validity of the Beer Lambert relationship and a constant optical pathlength throughout the experimental period (Reynolds EOR et al 1988; Wyatt JS et al 1986).

6.2.1 Chromophores and absorption spectra

Characterisation of the near infrared absorption spectra of cytochrome oxidase and haemoglobin have been obtained both *in vitro* and *in vivo* (Ferrari M et al 1990; Wray S et al 1988; Piantadosi CA and Jobsis VanderVliet FF 1984). Cytochrome oxidase spectra were obtained from the brains of rats after replacing the blood with a fluorocarbon substitute, and haemoglobin spectra were obtained at various oxygenation levels from cuvettes studies of lysed human red blood cells. The absorption spectra of haemoglobin and cytochrome oxidase are shown in chapter 2.

Other naturally occurring forms of haemoglobin are found in the blood stream that may also absorb light in the NIR spectrum: carboxyhaemoglobin (Hb-CO), methaemoglobin (Hi) and sulfhaemoglobin. The NIR optical effect of Hb-CO is negligible because of its low specific extinction coefficient. Hi is usually maintained at low proportion but is produced in the presence of excess NO. However, Hi has the same absorption spectra as Hb and the amounts produced are unlikely to incur more than a small error (Waterman MR 1978; Zijlstra WG et al 1991). Normal blood does not contain any SHb. Furthermore, spectra obtained from both adult and fetal haemoglobin indicate no perceptible differences in the NIR spectra between 650-1000 nm (Zijlstra WG et al 1991). Other absorbing compounds with significant NIR extinction coefficients include melanin, within skin, and myoglobin, within muscle. These were not a cause of concern in the present study as they were assumed not to change in each individual throughout the study period. Furthermore, the skull at this stage of gestation is less than 0.2 mm thick and is unlikely to have significantly reduced light intensity (Firbank M et al 1993).

6.2.2 Accuracy of Beer-Lambert Relationship

Light entering the brain is multiply scattered and it is therefore difficult to absolutely quantify the concentration of the chromophores. However, the change in concentration of the chromophores can be calculated by fitting the attenuation changes to the known chromophore spectra using a modification of the Beer Lambert law. The validity of the Beer Lambert law has been confirmed by theoretical modelling and experimental measurement of light in scattering media (Hiraoka M et al 1993; Delpy DT et al 1989). In the modified Beer Lambert equation, *B* or the differential pathlength (DP), can be derived by measuring the mean time delay of a picosecond light pulse passed through a tissue (Delpy DT et al 1988). In this way, DP was determined in the late gestation fetal sheep head at postmortem and was found to approximate that measured in term newborn infants. Surgical fixation of the optodes to the fetal skull, which at this gestational age has fused sutures, eliminated any alteration in optical pathlength due to movement.

The concentrations of Hb, HbO_2 and $CytO_2$ were derived using an algorithm that employed non-linear conversion, to take account of wavelength dependent scattering, and multilinear regression. The mean optical pathlength varies with wavelength because (a) scattering increases at shorter wavelengths (increasing pathlength); and (b) the absorbance of light by chromophores at a given wavelength reduces the probability of light of long pathlengths reaching the detector (decreasing pathlength) (Essenpreis M et al 1993). When more than 3 wavelengths are used, multilinear regression "fits" the component spectra and the accuracy of the fit is checked during the conversion using analysis of variance in the following way (Cope M et al 1991). Multiple regression calculates an *estimate set* (C) of the concentration changes of the chromophores in the tissue based on a *data set* (U) of the absorption coefficient changes. The estimate relies on an error free *design set* (α) whose elements are the specific absorption coefficients of the oxygen sensitive chromophores at the same wavelengths used to generate the data set. The estimate set is never exact as a noise component is superimposed upon its mean value. The problem then to be solved is the *error set* (E) containing elements which are the residual errors at each wavelength, which in matrix form is:

$$U=\alpha C + E$$

Examination of the residuals generated by multilinear regression analysis are significantly improved with the non-linear conversion employed in these studies.

6.2.3 Assumption of constant optical pathlength

The Beer Lambert relationship depends on a constant optical pathlength throughout the study period. The main concern in interpreting the results of these studies relate to the unknown changes that may occur in the optical properties of immature brain tissue following cerebral ischaemia. These are particularly critical to interpretation of the changes in [$CytO_2$], as the concentration of cytochrome oxidase is likely to be very low in the fetal brain. The scattering properties of brain tissue are derived from red blood cells, mitochondria, and lipoprotein membranes plus myelin sheath which constitute 50% solid contents of the immature brain (Cope M, 1991). Changes in the cytoplasmic membranes may follow cerebral ischaemia in the fetal sheep model, as delayed cytotoxic oedema is a prominent feature. At present, there is no evidence to suggest that large scale changes in scattering occur *in vivo* although maybe expected as cellular ionic pumps fail and cells swell due to effects of osmotic pressure.

In summary, the application of NIRS as employed in these studies reliably measured changes in cerebral perfusion and oxygenation during and following cerebral ischaemia. However, the possibility of changes in the optical characteristics of the fetal brain as a consequence of ischaemia can not be excluded. This needs particular consideration when interpreting the changes in [$CytO_2$], only present in low concentrations and susceptible to systematic error.

6.3 Relevance of the fetal sheep preparation

Animal preparations have greatly improved our understanding of the pathogenesis and mechanisms of hypoxic-ischaemic brain injury in the perinatal period. The fetal sheep preparation is particularly instructive as it allows for the study of an isolated cerebral ischaemic insult in an otherwise stable animal. Furthermore the size of the fetal sheep enables complicated monitoring techniques to be implemented for continuous measurements of changes in electrophysiology and haemodynamics over a period of days. Experimental procedures were

instigated at least 2 days post-surgery, and measurement of blood indices and electrophysiology at this time indicated that the fetus had fully recovered from the surgical procedure and had regained normal EEG sleep patterning. Temperature control and the maintenance of arterial blood gases are further advantages of the fetal preparation.

The major advantage of the preparation is that continuous changes in CI can be measured and these reflect the immediate and delayed phases of cerebral injury (Williams CE et al 1991). By simultaneously measuring other parameters, the cascade of processes that culminate in hypoxic-ischaemic brain injury can be elucidated. Delayed cerebral injury is an important feature of perinatal asphyxia in term infants, and has been repeatedly measured with ^{31}P MRS (Azzopardi D and Edwards AD, 1995). The similarities of clinical and pathological consequences of transient cerebral ischaemia in the late gestation sheep and those of certain asphyxiated infants imply that the findings of these studies may have important clinical implications (Williams CE et al 1992). Clinically, delayed seizures are frequently observed in asphyxiated infants and occur earlier if the insult is severe (Wical BS, 1994; Legido A et al 1991). Furthermore early MRI studies following asphyxia have revealed the presence of cerebral oedema at a time during which there was EEG evidence of seizure activity (Rollins NK et al 1994). Although studies on the histopathological features of birth asphyxia are sparse, MRI studies have indicated injury is prominent in the basal ganglia, striatum, hippocampus and parasagittal cortex (Barkovich AJ et al 1995; Kuenzle C et al 1994; Menkes JH and Curran J, 1994; Pasternak JF et al 1991).

The model employed was one of pure cerebral ischaemia and therefore different from the commonly employed perinatal rat model. In the latter the carotid artery is ligated unilaterally followed by exposure to hypoxia of varying degrees. This produces a unilateral infarct of the ipsilateral cerebral hemisphere leaving the contralateral side relatively intact (Mujsce DJ et al 1990; Yager JY et al 1991; Mujsce DJ et al 1990; Vannucci RC 1993). In the fetal sheep model, thirty minutes transient cerebral ischaemia produces bilateral distribution of cerebral injury, with infarction mainly localised to the parasagittal and lateral cortex, and the other regions demonstrating selective neuronal necrosis (Williams CE et al 1992).

The preparation therefore has several advantages over the perinatal rat model, although there are caveats in extrapolating from an isolated cerebral ischaemic injury in an otherwise well fetal sheep to the complex clinical situation of a sick, asphyxiated infant with multiple organ failure (Gluckman PD and Williams CE 1992). Studies in asphyxiated fetal sheep have confirmed that hypotension, accompanying global asphyxia, has a critical influence on the subsequent histological outcome (Gunn AJ et al 1992). Furthermore, the asphyxiated infant is often subjected to repeated brief insults and an acute insult may occur on a background of prolonged fetal distress and hypoxaemia (Mallard CE et al 1993).

6.4 Histological assessment

6.4.1 Neuronal Scoring

The histological staining techniques employed in this study enabled neuronal scoring to be performed and the effect of the changes in cerebral perfusion and oxygenation, and modes of treatment on outcome to be assessed. A reliable neuronal scoring system depends on the accurate identification of irreversibly injured neuronal cells.

Acid-fuchsin stain and thionine counterstain were used to identify neurons that had incurred irreversible damage as a consequence of cerebral ischaemia. Acid-fuchsin, a biological stain, has been used extensively in studies of hypoglycaemic, traumatic and excitotoxic neuronal death in immature and adult brain tissue (Auer RN et al 1984 (a); Auer RN et al 1984 (b)). In time course studies, using serial sections, it has been established that the dye delineates 'moribund neurons' which have suffered irreversible injury and disappear within a week (Auer RN et al 1985). The method can therefore indicate cumulative neuronal death up to the time of sacrifice.

Necrotic cells stain brilliant red with acid-fuchsin, although the target of acid-fuchsin, a tri-sulfonated triphenylmethane, remains obscure. The technique probably depends on the development of eosinophilia, acidophilia or agentophilia within the cytoplasm of dying cells; and intense neuronal acidiophilia can be identified with acid-fuchsin within 5-6 hours of an

intracerebral injection of the potent neurotoxic agent, kainic acid (Lees GJ 1989). Decreased cellular pH, as expected with metabolic failure, certainly enhances the stain but acid-fuchsin only fully decolorizes in a highly basic environment (pH 12-14). The affinity of acid-fuchsin for irreversibly injured neurons probably also results from enhanced cell penetration due to increased membrane permeability, coupled with irreversible binding to denatured proteins (Smith ML et al 1984).

A potential artifact for acid-fuchsin staining is "naturally" acidophillic cells that can lead to false identification of dead cells. In addition, the development of acidophilia in the early stages following trauma or injection of toxins does not necessarily indicate cell death, as a proportion of these cells recover. At later stages this is probably not a problem, since Auer et al found that following severe insulin-induced hypoglycaemia all cells that stained with acid-fuchsin were subsequently phagocytosed by 1 week of recovery (Auer RN et al 1984).

Due to phagocytosis, positive staining methods for detecting dead cells underestimate the extent of neuronal loss. Phagocytosis commences within one to two days of traumatic brain injury and the number of activated astroglia peaks at 5 days of injury (Giulian D et al 1989). Phagocytosed cells lose their ability to stain with Nissl dyes, such as thionine, and therefore counterstaining with thionine only detects viable cells and fails to identify irretrievably lost cells that have been phagocytosed. In the present studies, thionine acid-fuchsin identified dead neurons as those with a cytoplasm stained brilliant red and a contracted nuclei, whilst all other cells stained blue were considered viable.

Neuronal scoring was implemented by estimating the number of dead cells to the total number of cells within each section. In the second study, investigating the effect of NOS inhibition on the extent of cerebral injury, neuronal scoring was performed by an independent assessor so that there was no possibility of introducing bias. The independent assessor is a neuropathologist experienced in the fetal sheep preparation.

6.4.2 Immunohistochemical staining for NOS

The avidin-biotinylated-peroxidase complex method has been extensively used in diagnostic histopathology, and more recently, to demonstrate different isoforms of NOS in both animal and human tissue (Buttery LS et al 1994; Pollock JS et al 1993; Springall D et al 1992). The main problem with the avidin-biotin complex method relates to interference from endogenous immunoglobulins, as the secondary reagent in the process, is directed at primary antibody species- and class-specific determinants (Hsu S et al 1981). This can lead to an unacceptable degree of background staining particularly in the primary antibody-donating species. In the present study, background staining was limited and restricted to the myelin-rich fibres.

The unlabelled primary antibody for the constitutive isoform of NOS, e-NOS and n-NOS, were respectively monoclonal antibodies to an extractable form of NOS from cultured and natural bovine aortic endothelial cells, and a polyclonal antibody raised against an extractable form of rat brain constitutive n-NOS (Pollock JS et al 1993; Buttery LS et al 1994; Springall D et al 1992). Specificity of the antisera has been confirmed in previous studies by their ability to remove enzyme activity from the rat brain, by affinity purification and by Western blots. The positive staining demonstrated that the antisera recognised a similar protein in the fetal sheep brain.

The polyclonal antibody raised against a deduced peptide sequence of macrophage i-NOS failed to significantly stain i-NOS in the ischaemic fetal sheep brain (Buttery LS et al 1994). The limited staining in the present study could be interpreted as either a deficiency of the enzyme or a high specificity of the employed antibody such that it failed to identify i-NOS expression in the brain of fetal sheep. i-NOS antisera has been successfully used to identify the enzyme predominantly in rodents although has been demonstrated in piglets and human tissue, under pathological conditions. i-NOS has not yet been identified within fetal sheep organs including the brain. Furthermore, in a preliminary study to test the specificity of i-NOS antisera, an attempt was made to induce i-NOS expression in macrophages. The buffy coat, containing white blood cells, was isolated from fetal sheep blood following centrifugation and incubated with sheep specific cytokines. Despite the presence of

activated macrophages, it was still not possible to stain i-NOS. It is unlikely that i-NOS expression should be unique in the fetal sheep and therefore the likelihood of specificity problems is increased.

6.5 Implication of these studies

6.5.1 Cerebral vascular changes following ischaemia

The two discrete periods of increased [tHb] that occurred following cerebral ischaemia were not contingent upon alterations in arterial hemoglobin concentration, MAP, arterial blood gases or electrophysiologial changes, and were too large and rapid to be ascribed solely to alterations in cerebral:peripheral haematocrit ratio. Therefore the changes most likely represent periods of cerebral vasodilation.

The first phase followed the termination of the ischaemic insult and may reflect the increase in CBF observed by other investigators. Cerebral hyperaemia is a recognised phenomena following ischaemia and has been observed in perinatal animals following asphyxia, hypoxia-ischaemia and haemorrhagic hypotension (Mujsce DJ et al 1990; Rosenberg AA 1988). Increased CBF is most likely the result of cerebral vasodilation due to the accumulation of vasoactive metabolic products such as CO_2, hydrogen and potassium ions, adenosine, histamine and lactate during ischaemia. The substances released during ischaemia-reperfusion may indirectly stimulate perivascular sensory nerves to release neuropeptides, such as substance P, neurokinin A and calcitonin gene related peptide (CGRP) that act indirectly, through the release of endothelium derived relaxing factors or directly, on the vessel wall to cause vasodilation (Macfarlane R et al 1991). It has also been suggested that increased CBV following resuscitation may reflect capillary recruitment incurred during ischaemia/reperfusion (Tomita M 1988).

Cerebral vasodilation following ischaemia creates a favorable environment for the excess production of free radical overwhelming endogenous scavenger processes and causing membrane injury and cell death (Kirsch JR et al 1992; Traystman RJ et al 1991; Kjellmer I et al

1989). The extent of accumulation of end products during the initial insult may explain the observed relationship between duration of the early hyperemia and outcome.

The second phase of increase cerebral [tHb] suggests that the delayed increase in CI in the fetal sheep was associated with cerebral vasodilation rather than vasoconstriction. Vasoparalysis, cerebral hyperaemia and increased CBV have all been observed in the post-asphyxial newborn infant using the techniques of NIRS and ^{133}Xenon clearance to measure absolute CBF, CBV and CBVR, and Doppler ultrasonography to measure CBFV (see section 1.5.1.1). The magnitude of the delayed cerebrovascular changes observed in infants also correlated with the degree of brain injury.

The mechanism for delayed cerebral vasodilation is not clear although the role of NO investigated in this thesis is further discussed in section 6.5.3. In addition, the vasoactive mediators involved in the early increase in [tHb] may be involved. The response may represent a protective mechanism; or reflect the release of a vasodilatory agent that contributes to the development of delayed cerebral injury. There was no accompanying cerebral hypoxia, or systemic hypercarbia and acidosis, suggesting that these potent mediators of cerebral vasodilation were not involved, although they were not measured within the brain during the present studies. Other possible mediators include adenosine, prostaglandins and lactate (Ruth VJ et al 1993; Laudignon N et al 1990; Powell CL et al 1985; Golanov EV and Reis DJ 1994). Delayed cerebral lactate production has been observed by proton spectroscopy in neonatal piglets and asphyxiated infants, and local lactic acidosis may well have an influence on cerebrovascular tone (Azzopardi D and Edwards AD 1995). The presence of seizures may also have contributed to the increased cerebral [tHb] observed. Studies in adults have confirmed that increased CBF occurs during seizure activity (Johnson DW et al 1993). This is thought to reflect coupling between CBF and metabolism as a result of vasodilation during seizure activity. Furthermore, NO appears to contribute to dilatation of cerebral arterioles observed during seizures (Faraci M et al 1993).

6.5.2 Cerebral oxygenation following ischaemia

Changes in cerebral oxygenation following cerebral ischaemia were measured with NIRS by observing changes in [HbO_2],and [Hb] relative to [tHb], and [$CytO_2$]. It is best to consider changes in [HbO_2] as changes in cerebral blood oxygen saturation and an indicator of brain hypoxia, whilst changes in [$CytO_2$] reflect a wide variety of factors that alter the rate of cellular respiration.

[tHb] declined after reaching its second peak, and most of the fall was accounted for by a decrease in cerebral [Hb] implying that relatively more haemoglobin remaining in the brain was oxygenated, and there was an overall increase in mean cerebral oxygen saturation. This result may suggest a reduction in oxygen consumption in the post-ischaemic brain during this period. A decrease in oxygen consumption has been demonstrated immediately following ischaemia or asphyxia, and is thought to be a consequence of mitochondrial injury. Sims et al demonstrated a decrease in the rate of oxygen uptake by adult rat brain homogenates 24 and 48 hours post-ischaemia, and this early change preceded the histological evidence of ischaemic cell death (Sims NR and Pulsinelli WA 1987). In newborn lambs, Rosenberg et al showed altered oxygen metabolism immediately following asphyxia (Rosenberg AA 1986). Measurements of CBF, and arterial and cerebral venous oxygen contents, performed immediately after resuscitation suggested an increase in cerebral oxygen delivery was associated with significantly decreased cerebral oxygen consumption. Furthermore, cerebral fractional oxygen extraction, the relationship between oxygen uptake and delivery, also fell. In severely asphyxiated infants, persistent increased cerebral lactate concentration measured by ^1H MRS may reflect a disruption of oxidative phosphorylation to be predicted in the face of mitochondrial dysfunction (Azzopardi D and Edwards AD 1995).

The results of these studies therefore parallel those observed by others and suggest that the delayed increase in mean cerebral oxygenation may reflect mitochondrial dysfunction. Mitochondrial dysfunction has been proposed to cause a progressive decline in the production of high energy phosphates following cerebral ischaemia and may also result in a progressive fall

in [$CytO_2$] despite increased [HbO_2] (Sun D and Gilboe DD 1994; Wagner KR et al 1989). Disruption of cytochrome oxidase activity is one of the earliest indicators of neuronal injury in a perinatal stroke model (Nelson C and Silverstein FS 1994). Mitochondrial injury may limit the reaction between O_2 and the oxygen binding site of the cytochrome oxidase complex, Cu_B-haem a_3, so that Cu_A becomes progressively more reduced.

The progressive fall in [$CytO_2$] observed in these studies may reflect a progressive reduction of the Cu_A complex of cytochrome oxidase commencing several hours after the initial insult. Δ[$CytO_2$], as measured *in vivo* by NIRS, is obtained from the changes in the redox state of Cu_A as described in chapter 2, and does not necessarily reflect changes in mitochondrial oxygenation. Indeed, although the copper atom forms an integral part of the cytochrome oxidase complex, which accepts four electrons from cytochrome *c* and reduces one molecule of O_2 to H_2O in the generation of ATP, the Cu_A centre itself is not involved in this reaction.

Electrons are transferred along the 4 redox-active metal centres of the cytochrome oxidase complex in the following way:

$$\text{Cytochrome } c \rightarrow \mathbf{Cu_A} \rightarrow a \rightarrow Cu_B \rightarrow a_3$$

and ferrous a_3 finally reacts with O_2. Cu_A is a simple one-electron acceptor. Changes in its redox state can be achieved either by changing the rate of electron entry to cytochrome oxidase complex from cytochrome *c*, or by changing the rate of electron transfer from Cu_A to haem a_3 (Wrigglesworth JM et al 1993). In the presence of inhibitors binding to haem a_3 (eg cyanide) or the absence of O_2, which both prevent electron transfer to the haem a_3/ Cu_B site, haem *a* and Cu_A become fully reduced. Increasing the rate of electron entry to Cu_A from cytochrome *c* will also increase the reduction of Cu_A (Cooper CE et al 1994). The flow of electrons into Cu_A is increased by reducing the membrane potential across the inner mitochondrial membrane and this occurs when ADP concentration is increased (Brown GC 1992). Progressive reduction of Cu_A therefore reflects either (i) an increase in electron transfer from cytochrome *c* or (ii) a decrease in the rate of electron transfer from Cu_A to haem a_3.

The results may comply with other studies measuring the concentration of high energy phosphates during and following hypoxia-ischaemia in the immature brain. In asphyxiated infants and perinatal animals, [ATP] partially recovers following resuscitation only to commence a progressive fall some 10-20 hours later (Yager JY et al 1992; Palmer C et al 1990; Wyatt JS et al 1989). Increased flow of electrons from cytochrome *c* to Cu_A, would be expected in the face of falling [ATP] and increased [ADP] as the inhibition normally exerted on the electron respiratory chain by the proton motive force would be diminished in an "effort" to generate more ATP.

However, the interpretation of the changes in cytochrome oxidase observed in these studies is not straightforward. The problems, that have been discussed in detail in the previous sections, depend in part on the scatter changes induced by cerebral ischaemia, and the relatively low concentration of cytochrome oxidase in the fetal brain. Nevertheless, although the measurements of [$CytO_2$] may be misleading, the large late fall in [$CytO_2$] was closely related to two independent measures of severity of brain injury: the number of dead cells and the final depression of the ECoG; and it is therefore likely to be a biological marker of injury.

6.5.3 Role of nitric oxide

n-NOS and e-NOS expression was demonstrated in the ischaemic perinatal brain four days after transient cerebral ischaemia. e-NOS upregulation has been demonstrated in the adult brain commencing within a few hours of cerebral ischaemia. Nagafuji T et al, investigating the temporal profile of e-NOS activity in rats brain microvessels, demonstrated marked increases in e-NOS activity at 4 and 24 hours post-ischaemia that had normalised by 48 hours (Nagafuji T et al 1994). Sections obtained from brain tissue 4 days post-ischaemia may have missed the period of maximum expression.

Increased i-NOS expression was however not clearly demonstrated in the ischaemic fetal sheep brains following cerebral ischaemia. This may reflect the technical problems in the immunohistochemical staining techniques employed in these studies discussed in section 6.4.2. Increased i-NOS expression has been previously demonstrated in adult animals using

immunohistochemical techniques (Iadecola 1995 (a)). The peak presence of i-NOS induction in the ischaemic adult rat brain following middle cerebral artery occlusion occurred at 2 days and had disappeared by 7 days. i-NOS is capable of generating high concentrations of NO over prolonged periods and is thought to be important in the generation of ischaemic brain injury. However, unlike in adult animals, a role for the increased production of NO by i-NOS in the development of perinatal hypoxic-ischaemic brain injury has not been convincingly demonstrated (Iadecola C et al 1995 (b)). The importance of n-NOS after hypoxia-ischaemia has been recently described by Ferriero et al in a study on perinatal rats in which the extent of damage following hypoxia-ischaemia was reduced by selective destruction of NOS neurons with quisqualate (Ferriero DM et al 1995).

In the perinatal brain, a delayed increase in NO production has been suggested by the *in vivo* demonstration of a delayed increase in cerebral citrulline concentrations in the fetal sheep brain following transient cerebral ischaemia (Tan KMW et al 1995). The vasodilatory and neurotoxic potential of NO prompted the second study in which the role of NO in the generation of the delayed increase in cerebral perfusion and histological outcome was investigated using an inhibitor of NOS. The results of this study suggest that delayed NOS inhibition reduced the extent of delayed cerebral vasodilation and increased the degree of cerebral injury.

The effect of NOS inhibitors on the delayed changes in cerebral perfusion following hypoxia-ischaemia have not been previously investigated in either the adult or perinatal brain. However, during the early recovery period in adult animals, NO is thought to have an important role in maintaining CBF immediately following cerebral ischaemia. NO donors and L-arginine given during, or immediately following, the insult improve cerebral perfusion and long term histological outcome (Zhang F and Iadecola C 1993; Morikawa E et al 1994). NOS inhibitors given over the same time course reduce early recovery of cerebral perfusion and have a detrimental effect on outcome (Prado R et al 1993; Wei HM et al 1994). The role of early NO production in the immature brain following cerebral ischaemia have not been studied.

The results of the studies described in chapter 5 implicate NO in the generation of delayed cerebral vasodilation and this finding may have important implications for the use of NOS inhibitors in the treatment of perinatal hypoxia-ischaemia.

Recognition of the potential therapeutic value of NOS inhibitors follows the results of studies performed in adult animals in which NOS inhibitors significantly reduced the extent of cerebral injury when administered in the hours following focal or global cerebral ischaemia (Nishikawa T et al 1993; Nowicki JP et al 1991; Nagafuji T et al 1992). However, these findings have not been verified in perinatal animals although pretreatment has been found to be remarkably effective in 7 day old rats. Even if pretreatment was of clinical relevance, the late changes in cerebral haemodynamics observed in perinatal rats are very different from those seen in asphyxiated infants (Mujse DJ et al 1990). The importance and mechanism of the delayed cerebrovascular changes remains to be elucidated but it would certainly appear in fetal sheep that delayed NOS inhibition is detrimental and this effect may be mediated through altered cerebral haemodynamcis.

The contradictory results of NOS inhibition on outcome may reflect a dose related effect on the different NOS isoforms. Dose-dependent neuroprotective effects have been demonstrated in the perinatal rat and whilst low dose was effective, high dose did not improve outcome (Palmer C 1995). This might be related to inhibition of various isoforms of NOS and low dose may be protective through the effect on i-NOS or n-NOS whilst high dose alters cerebrovascular tone and may induce cerebral ischaemia in the already compromised brain. The differential effects of blocking different isoforms of NOS have been demonstrated in adults. Aminoguanidine, a selective inhibitor of i-NOS, administered 24 hours post-ischaemia, significantly reduced infarct volume without affecting resting CBF or the cerebrovasodilation elicited by hypercarbia (Iadecola C et al 1995). In addition, knock-out mice deficient in n-NOS have reduced ischaemic damage after middle cerebral artery occlusion but damage is increased when L-NNA is commenced and the vascular production of NOS is inhibited (Huang Z et al 1994).

Delayed NOS inhibition may have failed to induce neuroprotection through mechanism other than vascular. NO can induce neuroprotection through *S*-nitrosylation of the NMDA receptor such that Ca^{2+} influx is prevented (Stamler JS 1994). Microdialysis studies suggest that marked increases in glutamate concentration occur during the delayed phase and maybe involved in the development of delayed cortical seizures (Tan KMW et al 1995). NMDA inhibition with MK-801 abolishes seizures and is associated with moderate neuroprotection (Tan WK et al 1992). Although NOS inhibition is generally associated with decreased NMDA-induced neurotoxicity, it is possible that inhibiting the generation of nitrosium ions (NO^+) with L-NNA increased cerebral injury.

The delayed increase in [HbO_2] was attenuated in the L-NNA treatment group in the presence of a similarly attenuated delayed increase in [tHb], and this finding did not reflect a reduction in mean cerebral oxygen saturation. Of particular interest was the similarity in the delayed fall in [$CytO_2$] in the two groups despite a significantly greater cerebral injury in the treatment group.

The findings of the second study might therefore seem to conflict with those of the first study where it was suggested that a greater delayed fall in [$CytO_2$] was associated with a more extensive cerebral injury. However, the later finding might be explained by the effect of excess NO production on mitochondrial function. *In vitro* studies have demonstrated that NO is particularly toxic to mitochondrial enzymes including mitochondrial complexes I and II and mitochondrial aconitase (Drapier JC and Hibbs JJB 1986; Wharton M et al 1988). The inhibitory effect exerted by NO on mitochondrial respiration may well contribute to the cytotoxic effects of NO, and NOS inhibition may reduce the degree of cellular injury that occurs as a result of mitochondrial disruption.

However this does not explain the increased histological injury observed in the treatment group unless NOS inhibition decreased cellular injury due to mitochondrial dysfunction but increased cell death due to other mechanisms possibly involving signal transduction, macrophage activation, DNA damage and apoptosis. The effect of NOS inhibition on the scattering properties of the brain also needs to be considered.

6.6 Postulated pathogenesis of perinatal hypoxia-ischaemia

The results of these studies improve our understanding of the pathogenesis of cerebral hypoxic-ischaemic injury in the immature brain. Following transient cerebral ischaemia there was a delayed phase of increased cerebral perfusion that coincided with a delayed phase of cerebral injury. This phase was attenuated by NOS inhibition although this was not associated with cerebral protection.

The delayed increase in [tHb] might reflect a protective mechanism. Certainly the duration of this period was related to outcome and was more prolonged when the injury was less severe. Furthermore final [tHb] assessed 3-4 days post-ischaemia was greater in association with less severe cerebral injury. In addition, attenuation of the delayed cerebral vasodilation following treatment with L-NNA, an NOS inhibitor, increased the degree of cerebral injury.

The delayed increase in [tHb] preceded and accompanied the delayed increase in CI, indicating the possibility of a shared pathological mechanism. Although cortical infarction results in the release of numerous vasoactive substances, the temporal relationship implies a different mechanism for the onset of the cerebral vasodilation. It suggests that vascular changes occurred before cellular function was sufficiently deranged to impair ion transport.

The results of the changes in cerebral oxygenation suggest that, despite an increase in mean cerebral oxygen saturation, there was a progressive decline in [$CytO_2$] following cerebral ischaemia. This might reflect decreased oxygen consumption in the face of mitochondrial dysfunction and the results therefore correlate well with the current concepts of the changes in cerebral energetics and mitochondrial function following perinatal hypoxia ischaemia. Studies measuring concentrations of high energy phosphates suggest that a delayed disruption in cerebral energetics commences several hours following resuscitation and progresses over a period of several hours to days. Furthermore mitochondrial injury is an early feature of ischaemic brain injury causing a disruption of oxidative phosphorylation.

Interpretation of changes in [$CytO_2$] measured by NIRS is however subject to error, not least because of the unknown changes in the scattering properties of the immature brain following transient ischaemia. However, the extent of fall in [$CytO_2$] was related to electrophysiological and histological measures of outcome and therefore appears to be a biological measure that warrants further investigation.

The clinical and histological similarities between the fetal sheep preparation of cerebral ischaemia and some asphyxiated infants might make these findings of clinical relevance. Certainly, this is the first experimental model in which the delayed increases in CBV and cerebral oxygenation during the recovery period were correlated with delayed cerebral injury and histological outcome.

6.7 Future directions

The present study has demonstrated the use of NIRS in the investigation of cerebral ischaemia in a fetal sheep preparation over a period several days. In order to improve reliability of NIRS, particularly in the estimation of $\Delta[CytO_2]$, changes in optical pathlength need to be continuously measured throughout the study period and incorporated into the algorithm. This can be performed using phase resolved optical spectroscopy which measures the phase shift across tissue experienced by intensity modulated near-infrared light.

NIRS can also be used to quantitate cerebral haemodynamics and could be used to determine if the delayed cerebral vasodilation was a reflection of increased CBF. The technique for measuring CBF with NIRS was initially developed in infants and depends on the Fick principle. By making small alterations in the inspired O_2 content of oxygen-dependent infants, CBF can be calculated from the changes in arterial oxygen saturation and $\Delta[HbO_2]$ in the brain. As it is not always possible to change the inspired oxygen content in sick infants, a newer technique utilises indocyanine green, a strong absorber of NIR light, to measure CBF. This technique could be readily implemented in the fetal sheep to quantify delayed changes in cerebral haemodynamics. By measuring CBF with NIRS, together with cerebral venous and arterial oxygen saturation using a sagittal sinus catheter, much more information could be obtained about the temporal relation of changes in cerebral oxygen consumption, mitochondrial dysfunction and delayed cerebral injury.

The influence of other mediators of cerebral vasodilation in the delayed processes needs to be addressed with particular emphasis on prostaglandins, adenosine and lactate. It may be possible to incorporate microdialysis techniques such that the concentration of vasoactive substances could be measured simultaneously in the brain. Furthermore, the importance of the delayed increase in cerebral perfusion in relation to outcome maybe investigated using a vasodilator during this phase in an attempt to improve outcome.

Much more information could be obtained about the role of delayed NO production in the development of ischaemic brain injury by using different doses and more selective inhibitors of

NOS. Inhibition of n-NOS has been shown to be protective in adult rats even when administered late in the cascade. Furthermore, [citrulline] could be measured simultaneously with microdialysis to determine the extent of NOS inhibition outside the cerebral vasculature.

Bibliography

American Academy of Pediatrics; Editors Poland RL and Freeman RK. Guidelines for Perinatal Care 3rd ed. Elk Grove Village, Illinois: American Academy of Pediatrics, 1992; Relationship between perinatal factors and neurological outcome 221-4

Andre M, Matisse N, Vert P and Debruille C 1988 Neonatal seizures--recent aspects. Neuropediatrics 19, 201-207

Armstead WM, Mirro R, Busija DW, Leffler CW 1988 Postischemic generation of superoxide by newborn pig brain. Am J Physiol 225, H401-H403

Asano K, Chee CB, Gaston B, Lilly C.M, Gerard C, Drazen J.M, Stamler JS 1994 Constitutive and inducible nitric oxide synthase gene expression, regulation, and activity in human lung epithelial cells. Proc Natl Acad Sci USA. 91, 10089-10093

Auer RN, Kalimo H, Olsson Y, Siesjo BK 1985 The temporal evolution of hypoglycemic brain damage. I. Light and electron microscopic findings in the rat cerebral cortex. Acta Neuropathol. (Berl) 67, 13-24

Auer RN, Olsson Y, Siesjo BK 1984 (a) Hypoglycemic brain injury in the rat. Correlation of density of brain damage with the EEG isoelectric time: a quantitative study. Diabetes 33, 1090-1098

Auer RN, Wieloch T, Olsson Y, Siesjo BK 1984 (b) The distribution of hypoglycaemic brain damage. Acta Neuropathol. (Berl) 64, 177-191

Azzopardi D, Edwards AD 1995 Magnetic resonance spectroscopy in neonates. Curr Opin Neurol 8, 145-149

Azzopardi D, Wyatt JS, Cady EB, Delpy DT, Baudin J, Stewart AL, Hope PL, Hamilton PA and Reynolds EOR 1989 Prognosis of newborn infants with hypoxic-ischemic brain injury assessed by phosphorus magnetic resonance spectroscopy. Pediatr Res 25, 445-451

Bagenholm R, Nilsson UA, Gotborg CW and Kjellmer I 1994 Free radicals are formed during reperfusion after ischemia in the brain of fetal sheep. Proc 14th Eur Cong Perinatal Med

Baldwin B, F Bell 1963 The anatomy of the cerebral circulation in the sheep and ox. The dynamic distribution of the blood supply by the carotid and vertebral arteries to cranial regions. J Anat 97, 203-215

Barkovich AJ 1992.MR and CT evaluation of profound neonatal and infantile asphyxia. Am J Neuroradiol 13, 959-972

Barkovich AJ, Westmark K, Partridge C, Sola A, Ferriero DM 1995 Perinatal asphyxia: MR findings in the first 10 days. Am J Neuroradiol 16, 427-438

Becerra JE, Fry YW, Rowley DL 1991 Morbidity estimates of conditions originating in the perinatal period: United States, 1986 through 1987. Pediatrics 88, 553-559

Beckman JS, Beckman TW, Chen J, Marshall PA, Freeman BA 1990 Apparent hydroxyl radical production by peroxynitrite: implications for endothelial injury from nitric oxide and superoxide. Proc Natl Acad Sci USA. 87, 1620-1624

Beilharz EJ, Williams CE, Dragunow M, Sirimanne E, Gluckman PD 1995 .Mechanisms of delayed cell death following hypoxic-ischemic injury in the immature rat: evidence for apoptosis during selective neuronal loss. Mol Brain Res 29, 1-14

Beinert H, Shaw RW, Hansen RE, Hartzell CR 1980 Studies on the origin of the near-infrared (800-900 nm) absorption of cytochrome c oxidase. Biochim Biophys Acta 591, 458-470

Benveniste H, Jorgensen MB, Diemer NH, Hansen A 1988 Calcium accumulation by glutamate receptor activation is involved in hippocampal cell damage after ischemia. Acta Neurol Scand 78, 529-536

Blumberg RM, Cady EB, Wigglesworth JS, Edwards AD 1994 Delayed impairment of cerebral energy metabolism following transient focal hypoxia-ischemia in the 14 day old rat. Pediatr Res 37, 376A

Brown AW, Brierley JB 1973 The earliest alterations in rat neurones and astrocytes after anoxia-ischaemia. Acta Neuropathol Berl 23, 9-22

Brown AW, JB Brierley 1966 Evidence for early anoxic-ischaemic cell damage in the rat brain. Experientia 22, 546-547

Brown GC 1992 Control of respiration and ATP synthesis in mammalian mitochondria and cells. Biochem J 284, 1-13

Brown GC, Crompton M, Wray S 1991 Cytochrome oxidase content of rat brain during development. Biochim Biophys Acta 1057, 273-275

Buttery LD, Evans TJ, Springall D, Carpenter A, Cohen J, Polak JM 1994 Immunochemical localisation of inducible nitric oxide synthase in endotoxin-treated rats. Lab Investig 71, 755-764

Carter BS, Haverkamp AD, Merenstein GB 1993 The definition of acute perinatal asphyxia. Clin Perinatol 20, 287-304

Chan SI, Li PM 1990 Cytochrome c oxidase: Understanding natures design of a proton pump. Biochemistry 29, 1-12

Clancy R, Legido A, Newell R, Bruce D, Baumgart S, Fox W 1988 Continuous intracranial pressure monitoring and serial electroencephalographic recordings in severely asphyxiated neonates. Am J Dis Child 142, 740-747

Clifford DB, Olney JW, Benz AM, Fuller TA, Zorumski CF 1990 Ketamine, phencyclidine, and MK-801 protect against kainic acid-induced seizure-related brain damage. Epilepsia 31, 382-390

Cooper CE, Matcher SJ, Wyatt JS, Cope M, Brown GC, Nemoto EM, Delpy DT 1994 Near-infrared spectroscopy of the brain: relevance to cytochrome oxidase bioenergetics. Biochem Soc Trans 22, 974-980

Cope M 1991 The development of a near infrared spectroscopy system and its application for non-invasive monitoring of cerebral blood and tissue oxygenation in the newborn infant. PhD thesis (London, England)

Cope M, Delpy DT, Reynolds EOR, Wray S, Wyatt J, van der Zee P 1988 Methods of quantitating cerebral near infrared spectroscopy data. Adv Exp Med Biol 222, 183-189

Cope M, van der Zee P, Essenpreis M, Arridge SR, Delpy DT 1991 Data analysis methods for near infrared spectroscopy of tissue: problems in determining the relative cytochrome aa_3 concentration. Proc. SPIE-Int Soc Opt Eng 1431, 251-262

Cowan FM, Pennock JM, Hanrahan JD, Manji KP, Edwards AD 1994 Early detection of cerebral infarction and hypoxic ischemic encephalopathy in neonates using diffusion-weighted magnetic resonance imaging. Neuropediatrics 25, 172-175

Dalkara T, Moskowitz MA 1994 The complex role of nitric oxide in the pathophysiology of focal cerebral ischemia. Brain Pathol 4, 49-57

Dawes GS, Fox HE, Leduc BM, Liggins GC, Richard RT 1972 Respiratory movements and rapid eye movement sleep in the fetal lamb. J Physiol Lond 220, 119-143

Dawson TM, Dawson VL, Snyder SH 1993: Nitric oxide as a mediator of neurotoxicity. NIDA. Res Monogr 136, 258-271

Dawson VL, Dawson TM, London ED, Bredt DS, Snyder SH 1991 Nitric oxide mediates glutamate neurotoxicity in primary cortical cultures. Proc Natl Acad Sci USA. 88, 6368-6371

de Boer J, Klein HC, Postema F, Go KG, Korf J 1989 Rat striatal cation shifts reflecting hypoxic-ischemic damage can be predicted by on-line impedance measurements. Stroke 20, 1377-1382

Delpy DT, Arridge SR, Cope M, Edwards AD, Reynolds EOR, Richardson CE, Wray S, Wyatt JS, van der Zee P 1989 Quantitation of pathlength in optical spectroscopy. Adv Exp Med Biol 248, 41-46

Delpy DT, Cope M, van der Zee P, Arridge S, Wray S, Wyatt J 1988 Estimation of optical pathlength through tissue from direct time of flight measurement. Phys Med Biol 33, 1433-1442

Dimlich R, Showers MJ, Shipley MT 1990 Densitometric analysis of cytochrome oxidase in ischemic rat brain. Brain Res 516, 181-191

Drapier JC, JB Hibbs Jnr 1986 Murine cytotoxic activated macrophages inhibit aconitase in tumour cells. Inhibition involves the iron-sulfur prosthetic group and is reversible J Clin Invest 78, 790-797

D'Souza SW, Black P, Cadman J, Richards B 1983 Umbilical venous blood pH: a useful aid in the diagnosis of asphyxia at birth. Arch Dis Child 58, 15-19

Edwards AD, Brown GC, Cope M, Wyatt JS, McCormick DC, Roth SC, Delpy DT, Reynolds EOR 1991 Quantification of concentration changes in neonatal human cerebral oxidized cytochrome oxidase. J Appl Physiol 71, 1907-1913

Ellenberg JH, Nelson KB 1988 Cluster of perinatal events identifying infants at high risk of death or disability. J Pediatr 113, 546-552

Erganger U, Eriksson M, Zetterstrom R 1983 Severe neonatal asphyxia. Acta Paediatr Scand 72, 321-325

Essenpreis M, Cope M, Elwell CE, Arridge SR, van der Zee P, Delpy DT 1993 Wavelength dependence of the differential pathlength factor and the log slope in time-resolved tissue spectroscopy. Adv Exp Med Biol 333, 9-20

Faraci FM, Brian JEJ 1994 Nitric oxide and the cerebral circulation. Stroke 25, 692-703

Faraci FM, KR Breese, DD Heistad 1993 Nitric oxide contributes to dilatation of cerebral arterioles during seizures. Am J Physiol 265, H2209-H2212

Ferrari M, Hanley DF, Wilson DA, Traystman RJ 1990 Cerebral cytochrome-C-oxidase copper band quantification in perfluorocarbon exchange transfused cats. Adv Exp Med Biol 277, 85-93

Ferriero DM, Sheldon A, Black SM, Chuai J 1995 Selective destruction of nitric oxide synthase neurons with quisqualate reduces damage after hypoxia-ischaemia in the neonatal rat. Pediatr Res 38, 912-918

Fineman JR, Wong J, Morin FC, Wild LM, Soifer SJ 1994 Chronic nitric oxide inhibition in utero produces persistent pulmonary hypertension in newborn lambs. J Clin Invest 93, 2675-2683

Finer NN, Robertson CM, Richards RT, Pinnell LE, Peters KL 1981 Hypoxic-ischaemic encephalopathy in term infants: Perinatal factors and outcome. J Pediatr 98, 112-117

Firbank M, Hiraoka M, Essenpreis M, Delpy DT 1993 Measurement of the optical properties of the skull in the wavelength range 650-950 nm. Phys Med Biol 38, 503-510

Ford LM, Sanberg PR, Norman AB, Fogelson MH 1989 MK-801 prevents hippocampal neurodegeneration in neonatal hypoxic-ischemic rats. Arch Neurol 46, 1090-1096

Freeman JM, Nelson KB 1988 Intrapartum asphyxia and cerebral palsy. Pediatrics 82, 240-249

Gaffney G, Sellers S, Flavell V, Squier M, Johnson A 1994 Case-control study of intrapartum care, cerebral palsy, and perinatal death BMJ 308, 743-750

Gasser T, Bacher P, Mocks J 1982 Transformations towards the normal distribution of broad band spectral parameters of the EEG. Electroencepalogr Clin Neurophysiol 53, 119-124

Gilstrap LC, Leveno KJ, Burris J, Williams ML, Little BB 1989 Diagnosis of birth asphyxia on the basis of fetal pH, Apgar score, and newborn cerebral dysfunction. Am J Obstet Gynecol 161, 825-830

Giulian D, Chen J, Ingeman JE, George JK, Noponen M 1989 The role of mononuclear phagocytes in wound healing after traumatic injury to adult mammalian brain. J Neurosci 9, 4416-4429

Gluckman PD, Parsons Y 1983 Stereotaxic method and atlas for the ovine fetal forebrain. J Dev Physiol 5, 101-128

Gluckman PD, Williams CE 1992 Is the cure worse than the disease? Caveats in the move from laboratory to clinic. Dev Med Child Neurol 34, 1015-1018

Golanov EV, Reis DJ 1994 Nitric oxide and prostanoids participate in cerebral vasodilation elicited by electrical stimulation of the rostral ventrolateral medulla. J Cereb Blood Flow Metab 14, 492-502

Goodwin TM, Belai I, Hernandez P, Durand M, Paul RH 1992 Asphyxial complications in the term newborn with severe umbilical acidemia. Am J Obstet Gynecol 167, 1506-1512

Goplerud JM, Delivoria Papadopoulos M 1993 Nuclear magnetic resonance imaging and spectroscopy following asphyxia. Clin Perinatol 20, 345-367

Grant A, O'Brien N, Joy MT, Hennessy E, MacDonald D 1989 Cerebral palsy among children born during the Dublin randomised trial of intrapartum monitoring. Lancet 2:1233-1236

Grigg Damberger MM, Coker SB, Halsey CL, Anderson CL 1989 Neonatal burst suppression: its developmental significance. Pediatr Neurol 5, 84-92

Groenendaal F, Veenhoven RH, van der Grond J, Jansen GH, Witkamp TD, De Vries LS 1994 Cerebral lactate and N-acetyl-aspartate / choline ratios in asphyxiated full-term neonates demonstrated in-vivo using proton magnetic resonance spectroscopy. Pediatr Res 35, 148-151

Guan J, Williams CE, Gunning MI, Mallard EC, Gluckman PD 1993 The effect of IGF-1 treatment after hypoxic-ischaemic brain injury in adult rats. J Cereb Blood Flow Metab 13, 609-616

Gunn AJ, CE Williams, EC Mallard, KMW Tan, PD Gluckman 1994 Flunarizine, a calcium channel antagonist, is partially prophylactically neuroprotective in hypoxic-ischemic encephalopathy in the fetal sheep. Pediatr Res 35, 657-663

Gunn AJ, Mydlar T, Bennet L, Faull R, Gorter S, Cook CJ, Johnston BM, Gluckman PD 1989 The neuroprotective actions of a calcium channel antagonist, flunarizine, in the infant rat. Pediatr Res 25, 573-576

Gunn AJ, Parer JT, Mallard EC, Williams CE, Gluckman PD 1992 Cerebral histologic and electrocorticographic changes after asphyxia in fetal sheep. Pediatr Res 31, 486-491

Hagberg H, Andersson P, Kjellmer I, Thiringer K, Thordstein M 1987 Extracellular overflow of glutamate, aspartate, GABA and taurine in the cortex and basal ganglia of fetal lambs during hypoxia-ischemia. Neurosci Lett 78, 311-317

Hamada Y, Hayakawa T, Hattori H, Mikawa H 1994 Inhibitor of nitric oxide synthesis reduces hypoxic-ischemic brain damage in the neonatal rat. Pediatr Res 35, 10-14

Hashimoto K, Kikuchi H, Ishikawa M, Kobayashi S 1992 Changes in cerebral energy metabolism and calcium levels in relation to delayed neuronal death after ischemia. Neurosci Lett 137, 165-168

Hellstrom Westas L, Rosen I, Svenningsen NW 1995 Predictive value of early continuous amplitude integrated EEG recordings on outcome after severe birth asphyxia in full term infants. Arch Dis Child Fetal Neonatal Ed 72, F34-F38

Heroux P, Bourdages M 1994 Monitoring living tissues by electrical impedance spectroscopy. Ann Biomed Eng 22, 328-337

Hiraoka M, Firbank M, Essenpreis M, Cope M, Arridge SR, van der Zee P, Delpy DT 1993 A Monte Carlo investigation of optical pathlength in inhomogenous tissue and its application to near-infrared spectroscopy. Phys Med Biol 38, 1859-1876

Holden KR, Mellits ED, Freeman JM 1982 Neonatal seizures. I. Correlation of prenatal and perinatal events with outcomes. Pediatrics 70, 165-176

Holst K, Andersen E, Philip J, Henningsen I 1989 Antenatal and perinatal conditions correlated to handicap among 4-year-old children. Am J Perinatol 6, 258-267

Horvath I, Sandor NT, Ruttner Z, McLaughlin AC 1994 Role of nitric oxide in regulating cerebrocortical oxygen consumption and blood flow during hypercapnia. J Cereb Blood Flow Metab 14, 503-509

Hossmann KA 1971 Cortical steady potential, impedance and excitability changes during and after total ischemia of cat brain. Exp Neurol 32, 163-175

Hossmann KA 1993 Ischemia-mediated neuronal injury. Resuscitation 26, 225-235

Hsu S, Raine L, Fanger H 1981 Use of an avidin-biotin-peroxidase complex (ABC) in immunoperoxide technique: a comparison between ABC and unlabelled antibody (PAP) procedures. J Histochem Cytochem 29, 577-580

Huang Z, Huang PL, Panahian N, T Dalkara, MC Fishman, MA Moskowitz 1994 Effects of cerebral ischemia in mice deficient in neuronal nitric oxide synthase. Science 265, 1883-1885

Huie RE, Padmaja S 1993 The reaction rate of nitric oxide with superoxide. Free Rad Res Commun 18, 195-199

Iadecola C, Pelligrino DA, Moskovitz MA, Lassen NA 1994 State of the art review: Nitric oxide synthase inhibition and cerebrovascular regulation. J Cereb Blood Flow Metab 14, 175-192

Iadecola C, Xu X, Zhang F, el Fakahany EE, Ross ME 1995 (a) Marked induction of calcium-independent nitric oxide synthase activity after focal cerebral ischemia. J Cereb Blood Flow Metab 15, 52-59

Iadecola C, Zhang F, Xu X 1995 (b) Inhibition of inducible nitric oxide synthase ameliorates cerebral ischemic damage. Am J Physiol 268, R286-R292

Ichord RN, Helfaer MA, Kirsch JR, Wilson D, Traystman RJ 1994 Nitric oxide synthase inhibition attenuates hypoglycemic cerebral hyperemia in piglets. Am J Physiol 266, H1062-H1068

Iwata S, Ostermeier C, Ludwig B, Michel H 1995 Structure at 2.8 A resolution of cytochrome c oxidase from *Paracoccus denitrificans*. Nature 376, 660-669

Jobsis FF, Keizer JH, LaManna JC, Rosenthal M 1977 Reflectance spectrophotometry of cytochrome aa_3 in vivo. J Appl Physiol 43, 858-872

Johnson DW, Hogg JP, Dasheiff R, Yonas H, Pentheny S, Jumao A 1993 Xenon/CT cerebral blood flow studies during continuous depth electrode monitoring in epilepsy patients Am J Neuroradiol 14, 245-252

Johnston BM, Mallard EC, Williams CE, Gluckman PD 1995 Neuronal rescue with insulin-like growth factor-1 treatment after cerebral hypoxic-ischemic injury in fetal sheep J Matern Fetal Invest 5, 188

Kagstrom E, Smith ML, Siesjo BK 1983 Local cerebral blood flow in the recovery period following complete cerebral ischemia in the rat. J Cereb Blood Flow Metab 3, 170-182

Katsura K, Rodriguez de Turco EB, Folbergrova J, Bazan NG, Siesjo BK 1993 Coupling among energy failure, loss of ion homeostasis, and phospholipase A2 and C activation during ischemia. J Neurochem 61, 1677-1684

Katz VL, Bower WA Jnr 1992 Meconium aspiration syndrome: Reflections on a murky subject. Am J Obstet Gynecol 166; 171-175

Kirino T, Robinson HP, Miwa A, Tamura A, Kawai N 1992 Disturbance of membrane function preceding ischemic delayed neuronal death in the gerbil hippocampus. J. Cereb. Blood Flow Metab 12, 408-417

Kirsch JR, Helfaer MA, Haun SE, Koehler RC, Traystman RJ 1993 Polyethylene glycol-conjugated superoxide dismutase improves recovery of postischemic hypercapnic cerebral blood flow in piglets. Pediatr Res 34, 530-537

Kirsch JR, Helfaer MA, Lange DG, Traystman RJ 1992 Evidence for free radical mechanisms of brain injury resulting from ischemia/reperfusion-induced events. J Neurotrauma 9 Suppl 1, S157-S163

Kjellmer I, Andine P, Hagberg H, Thiringer K 1989 Extracellular increase of hypoxanthine and xanthine in the cortex and basal ganglia of fetal lambs during hypoxia-ischemia. Brain Res 478, 241-247

Kontos HA, EP Wei 1986 Superoxide production in experimental brain injury. J Neurosurg 64, 803-807

Kozma M, Mehmet H, Edwards AD 1995 Protection of apototic cell death by hypothermia in tissue culture. Pediatr Res (in press)

Kuenzle C, Baenziger O, Martin E, Thun Hohenstein L, Steinlin M, Good M, Fanconi S, Boltshauser E, Largo RH 1994 Prognostic value of early MR imaging in term infants with severe perinatal asphyxia. Neuropediatrics 25, 191-200

Kuenzle C, Baenziger O, Martin E, Thun Hohenstein L, Steinlin M, Good M, Fanconi S, Boltshauser E, Largo RH 1994 Prognostic value of early MR imaging in term infants with severe perinatal asphyxia. Neuropediatrics 25, 191-200

Lafon Cazal M, Pietri S, Culcasi M, Bockaert J 1993 NMDA-dependent superoxide production and neurotoxicity. Nature 364, 535-537

Langendoerfer S, Havercamp AD, Murphy J 1980 Pediatric follow-up of a randomised controlled trial of intrapartum fetal monitoring techniques. J Pediatr 97; 103-107

Laudignon N, Farri E, Beharry K, Rex J, Aranda JV 1990 Influence of adenosine on cerebral blood flow during hypoxic hypoxia in the newborn piglet. J Appl Physiol 68, 1534-1541

Lees GJ 1989 In vivo and in vitro staining of acidophilic neurons as indicative of cell death following kainic acid-induced lesions in rat brain. Acta Neuropathol Berl 77, 519-524

Legido A, Clancy RR, Berman PH 1991 Neurologic outcome after electroencephalographically proven neonatal seizures. Pediatrics 88, 583-596

Levene MI, Fenton AC, Evans DH, Archer LN, Shortland DB, Gibson NA 1989 Severe birth asphyxia and abnormal cerebral blood-flow velocity. Dev Med Child Neurol 31, 427-434

Levene MI, Gibson NA, Fenton AC, Papathoma E, Barnett D 1990 The use of a calcium channel blocker, nicardipine, for severely asphyxiated newborn infants. Dev Med Child Neurol 32, 567-574

Lipton SA, Choi YB, Pan ZH, Lei SZ, Chen HS, Sucher NJ, Loscalzo J, Singel DJ, Stamler JS 1993 A redox-based mechanism for the neuroprotective and neurodestructive effects of nitric oxide and related nitroso-compounds. Nature 364, 626-632

Lorek A, Takei Y, Cady EB, Wyatt JS, Penrice J, Edwards AD, Peebles DM, Wylezinska M, Owen-Rees H, Kirkbridge V, Cooper C, Aldridge RF, Roth SC, Brown GC, Delpy DT, Reynolds EOR 1994 Delayed ('secondary') cerebral energy failure following acute hypoxia-ischemia in the newborn piglet: continuous 48-hour studies by ^{31}P magnetic resonance spectroscopy. Pediatr Res 36, 699-706

Lupton BA, Hill A, Roland EH, Whitfield MF, Flodmark O 1988 Brain swelling in the asphyxiated term newborn: pathogenesis and outcome. Pediatrics 82, 139-146

Macfarlane R, Tasdemiroglu E, Moskowitz MA, Uemura Y, Wei EP, Kontos HA 1991 Chronic trigeminal ganglionectomy or topical capsaicin application to pial vessels attenuates postocclusive cortical hyperemia but does not influence postischemic hypoperfusion. J Cereb Blood Flow Metab 11, 261-271

Malinski T, Bailey F, Zhang ZG, Chopp M 1993 Nitric oxide measured by a porphyrinic microsensor in rat brain after transient middle cerebral artery occlusion. J Cereb Blood Flow Metab 13, 355-358

Mallard EC, Waldvogel HJ, Williams CE, Faull RL, Gluckman PD 1995 Repeated asphyxia causes loss of striatal projection neurons in the fetal sheep brain. Neuroscience 65, 827-836

Mallard EC, Williams CE, Gunn AJ, Gunning MI, Gluckman PD 1993 Frequent episodes of brief ischemia sensitize the fetal sheep brain to neuronal loss and induce striatal injury. Pediatr Res 33, 61-65

Malmstrom BG 1990 Cytochrome oxidase: some unsolved problems and controversial issues. Arch Biochem Biophys 280, 233-241

Matcher SJ, Elwell CE, Cooper CE, Cope M, Delpy DT 1995 Performance comparison of several published tissue near-infrared spectroscopy algotithms. Anal Biochem 227, 54-68

Mayhan WG, Amundsen SM, Faraci FM, Heistad DD 1988 Responses of cerebral arteries after ischemia and reperfusion in cats. Am J Physiol 255, H879-H884

McCormick DC, Edwards AD, Brown GC, Wyatt JS, Potter A, Cope M, Delpy DT, Reynolds EOR 1993 Effect of indomethacin on cerebral oxidized cytochrome oxidase in preterm infants. Pediatr Res 33, 603-608

McDonald JW, Silverstein FS, Cardona D, Hudson C, Chen R, Johnston MV 1990 Systemic administration of MK-801 protects against N-methyl-D-aspartate and quisqualate-mediated neurotoxocity in perinatal rats. Neuroscience 36, 589-599

McGee Russell SM, Brown AW, Brierley JB 1970 A combined light and electron microscope study of early anoxic-ischaemic cell change in rat brain. Brain Res 20, 193-200

McNeill H, Williams CE, Guan J, Sirimanne E, Gluckman PD 1994 Neuronal rescue with transforming growth factor-beta (1) after hypoxic-ischaemic brain injury. Neuroreport 5, 901-904

Mehmet H, Yue X, Squier MV, Lorek A, Cady EB, Penrice J, Sarraf C, Wylezinska M, Kirkbride V, Cooper CE, Brown GC, Wyatt JS, Reynolds EOR, Edwards AD 1994 Increased apoptosis in the cingulate sulcus of newborn piglets following transient hypoxia-ischaemia is related to the degree of high energy phosphate depletion during the insult. Neurosci Lett 181, 121-125

Meis PJ, Hobel CJ, Ureda JR 1982 Late meconium passage in labor - a sign of fetal distress? Obstet Gynecol 59, 332-335

Mellits ED, Holden KR, Freeman JM 1982 Neonatal seizures. II. A multivariate analysis of factors associated with outcome. Pediatrics 70, 177-185

Menkes JH, Curran J 1994 Clinical and MR correlates in children with extrapyramidal cerebral palsy. AJNR 15, 451-457

Miller FC, DA Sacks, SY Yeh, RH Paul, BS Schifrin, CB Martin, EH Hon 1975 Significance of meconium during labor. Am J Obstet Gynecol 122, 573-580

Minchom P, Niswander K, Chalmers I, Dauncey M, Newcombe R, Elbourne D, Mutch L, Andrews J, Williams G 1987 Antecedents and outcome of very early neonatal seizures in infants born at or after term. Br J Obstet Gynaecol 94, 431-439

Moncada S 1992 Nitric oxide gas: mediator, modulator, and pathophysiologic entity. J Lab Clin Med 120, 187-191

Moncada S 1992 The 1991 Ulf von Euler Lecture. The L-arginine:nitric oxide pathway. Acta Physiol Scand 145, 201-227

Morikawa E, Moskowitz MA, Huang Z, Yoshida T, Irikura K, Dalkara T 1994 L-arginine infusion promotes nitric oxide-dependent vasodilation, increases regional cerebral blood flow, and reduces infarction volume in the rat. Stroke 25, 429-435

Mujsce DJ, Christensen MA, Vannucci RC 1990 Cerebral blood flow and edema in perinatal hypoxic-ischemic brain damage. Pediatr Res 27, 450-453

Mulligan JC, Painter MJ, O'Donoghue PA, MacDonald HM, Allen AC, Taylor P 1980 Neonatal asphyxia II. Neonatal mortality and long-term sequelae. J Pediatr 96, 903-907

Naeye RL, Peters EC, Bartholomew M, Landis JR 1989 Origins of cerebral palsy. Am J Dis Child; 1154-1161

Nagafuji T, Matsui T, Koide T, Asano T 1992 Blockade of nitric oxide formation by N omega-nitro-L-arginine mitigates ischemic brain edema and subsequent cerebral infarction in rats. Neurosci Lett 147, 159-162

Nagafuji T, Sugiyama M, Matsui T 1994 Temporal profiles of Ca^{2+}/calmodulin-dependent and -independent nitric oxide synthase activity in the rat brain microvessels following cerebral ischemia. Acta Neurochir Suppl Wien 60, 285-288

Nakamura K, Hatakeyama T, Furuta S, Sakaki S 1993 The role of early Ca2+ influx in the pathogenesis of delayed neuronal death after brief forebrain ischemia in gerbils. Brain Res 613, 181-192

Nelson C, Silverstein FS 1994 Acute disruption of cytochrome oxidase activity in brain in a perinatal rat stroke model. Pediatr Res 36, 12-19

Nelson CW, Wei EP, Povlishock JT, Kontos HA, Moskowitz MA 1992 Oxygen radicals in cerebral ischemia. Am J Physiol 263, H1356-H1362

Nelson KB 1988 What proportion of cerebral palsy is related to birth asphyxia. J Pediatr 112, 572-575

Nelson KB, Ellenberg JH 1986 Antecedents of cerebral palsy: Multivariate analysis of risk N Eng J Med 315; 81-86

Nelson KB, Ellenberg JH 1987 The asymptomatic newborn and risk of cerebral palsy. Am J Dis Child 141, 1333-1335

Nelson KB, Emery ES 1993 Birth asphyxia and the neonatal brain: what do we know and when do we know it? Clin Perinatol 20, 327-344

Nishikawa T, Kirsch JR, Koehler RC, Bredt DS, Snyder SH, Traystman RJ 1993 Effect of nitric oxide synthase inhibition on cerebral blood flow and injury volume during focal ischemia in cats. Stroke 24, 1717-1724

Niwa K, Lindauer U, Villringer A, Dirnagl U 1993 Blockade of nitric oxide synthesis in rats strongly attenuates the CBF response to extracellular acidosis. J Cereb Blood Flow Metab 13, 535-539

Northington FJ, Matherne GP, Berne RM 1992 Competitive inhibition of nitric oxide synthase prevents the cortical hyperemia associated with peripheral nerve stimulation. Proc Natl Acad Sci USA 89, 6649-6652

Nowicki JP, Duval D, Poignet H, Scatton B 1991 Nitric oxide mediates neuronal death after focal cerebral ischemia in the mouse. Eur J Pharmacol 204, 339-340

Nozaki K, Beal MF 1992 Neuroprotective effects of L-kynurenine on hypoxia-ischaemia and NMDA lesions in neonatal rats. J Cereb Blood Flow Metab 12, 400-407

Palmer C 1995 Hypoxic-ischemic encephalopathy: Therpaeutic approaches against microvascular injury, and role of neutrophils, PAF, and free radicals. Clin Perinatol 22, 481-517

Palmer C, Brucklacher RM, Christensen MA, Vannucci RC 1990 Carbohydrate and energy metabolism during the evolution of hypoxic-ischemic brain damage in the immature rat. J Cereb Blood Flow Metab 10, 227-235

Palmer C, Vannucci RC 1993 Potential new therapies for perinatal cerebral hypoxia-ischemia. Clin Perinatol 20, 411-432

Paneth N, Stark RI 1983 Cerebral palsy and mental retardation in relation to indicators of perinatal asphyxia. An epidemiologic overview. Am J Obstet Gynecol 147, 960-966

Pasternak JF, Predey TA, Mikhael MA 1991 Neonatal asphyxia: vulnerability of basal ganglia, thalamus, and brainstem. Pediatr Neurol 7, 147-149

Pasternak JF, Predey TA, Mikhael MA 1991Neonatal asphyxia: vulnerability of basal ganglia, thalamus, and brainstem. Pediatr Neurol 7, 147-149

Perlman JM 1989 Systemic abnormalities in term infants following perinatal asphyxia: relevance to long-term neurologic outcome. Clin Perinatol 16, 475-484

Perlman JM, Risser R 1993 Severe fetal acidemia: neonatal neurologic features and short-term outcome. Pediatr Neurol 9, 277-282

Perlman JM, Tack ED, Martin T, Shackelford G, Amon E 1989 Acute systemic organ injury in term infants after asphyxia. Am J Dis Child 143, 617-620

Perlman JM, Volpe JJ 1983 Seizures in the preterm infant: effects on cerebral blood flow velocity, intracranial pressure, and arterial blood pressure. J Pediatr 102, 288-293

Phelan JP, Ahn MO 1994 Perinatal observations in forty-eight neurologically impaired term infants. Am J Obstet Gynecol 171, 424-431

Phibbs RH Editors: Avery GB. Neonatology: Pathophysiology and management of the newborn. Philadelphia: JB Lippincott, 1981; Delivery room management of the newborn; 183-196

Piantadosi CA, Jobsis Vander Vliet FF 1984 Spectrophotometry of cerebral cytochrome aa_3 in bloodless rats. Brain Res 305, 89-94

Pollock JS, Nakane M, Buttery LD, Martinez A, Springall D, Polak JM, Forstermann U, Murad F 1993 Characterization and localization of endothelial nitric oxide synthase using specific monoclonal antibodies. Am. J Physiol 265, C1379-C1387

Powell CL, Hernandez MJ, Vannucci RC 1985 The effect of lactacidemia on regional cerebral blood flow in the newborn dog. Brain Res 349, 314-316

Prado R, Watson BD, Wester P 1993 Effects of nitric oxide synthase inhibition on cerebral blood flow following bilateral carotid artery occlusion and recirculation in the rat. J Cereb Blood Flow Metab 13, 720-723

Pryds O, Greisen G, Lou H, Friis Hansen B 1990 Vasoparalysis associated with brain damage in asphyxiated term infants. J Pediatr 117, 119-125

Pryds O, Greisen G, Skov LL, Friis Hansen B 1990 Carbon dioxide-related changes in cerebral blood volume and cerebral blood flow in mechanically ventilated preterm neonates: comparison of near infrared spectrophotometry and ^{133}Xenon clearance. Pediatr Res 27, 445-449

Radi R, Beckman JS, Bush KM, Freeman BA 1991 Peroxynitrite-induced membrane peroxidation. The cytotoxic potential of superoxide and nitric oxide. Arch Biochem Biophys 288, 481-487

Raff MC, Barres BA, Burne JF, Coles HS, Ishizaki Y, Jacobson MD 1993 Programmed cell death and the control of cell survival - lessons from the nervous system. Science 262, 695-700

Rees DD, Palmer RM, Schulz R, Hodson HF, Moncada S 1990 Characterisation of three inhibitors of endothelial nitric oxide synthase in vitro and in vivo. Br J Pharmacol 101, 746-752

Reynolds EOR, JS Wyatt, D Azzopardi, DT Delpy, EB Cady, M Cope, S Wray 1988 New non-invasive methods for assessing brain oxygenation and haemodynamics. Br Med Bull 44, 1052-1075

Robillard P, Poussart D 1979 Spatial resolution of four electrode array. IEEE Trans Biomed Eng 26, 465-470

Rollins NK, Morriss MC, Evans D, Perlman JM 1994 The role of early MR in the evaluation of the term infant with seizures. AJNR 15, 239-248

Rosenberg A 1988 Regulation of cerebral blood flow after asphyxia in neonatal lambs. Stroke 19, 239-244

Rosenberg A, Murdaugh E, White BC 1989 The role of oxygen free radicals in postasphyxia cerebral hypoperfusion in newborn lambs. Pediatr Res 26, 215-219

Rosenberg AA 1986 Cerebral blood flow and O_2 metabolism after asphyxia in neonatal lambs. Pediatr Res 20, 778-782

Roth SC, Edwards AD, Cady EB, Delpy DT, Wyatt JS, Azzopardi D, Baudin J, Townsend J, Stewart AL, Reynolds EOR 1992 Relation between cerebral oxidative metabolism following birth asphyxia, and neurodevelopmental outcome and brain growth at one year Dev Med Child Neurol 34, 285-295

Ruth VJ, Park TS, Gonzales ER, Gidday JM 1993 Adenosine and cerebrovascular hyperemia during insulin-induced hypoglycemia in newborn piglet. Am J Physiol 265, H1762-8

Ruth VJ, Raivio KO 1988 Perinatal brain damage: predictive value of metabolic acidosis and the Apgar score. Br Med J 297, 24-37

Sarnat HB, Sarnat MS 1976 Neonatal encephalopathy following fetal distress. A clinical and electroencephalographic study study. Arch Neurol 33, 696-705

Schlichtig R, Klions HA, Kramer DJ, Nemoto EM 1992 Hepatic dysoxia commences during O_2 supply dependence. J Appl Physiol 72, 1499-1505

Shu S, Ju G, Fan L 1988 The glucose oxidase-DAB-nickel method in peroxidase histochemistry of the nervous system. Neurosci Lett 85, 169-171

Shy KK, Luthy DA, Bennett FC 1990 Effects of electronic fetal monitoring on the neurological development of premature infants. N Eng J Med 322; 588-592

Siesjo BK 1988 Acidosis and ischemic brain damage. Neurochem Pathol 9, 31-88

Siesjo BK 1988 Historical overview. Calcium, ischemia, and death of brain cells. Ann N Y Acad Sci 522, 638-661

Siesjo BK, Bengtsson A 1989 Calcium fluxes, calcium antagonists, and calcium-related pathology in brain ischemia, hypoglycemia, and spreading depression: a unifying hypothesis. J Cereb Blood Flow Metab 9, 127-140

Siesjo BK, Bengtsson F, Grampp W, Theander S 1989 Calcium, excitotoxins, and neuronal death in the brain. Ann N Y Acad Sci 568, 234-251

Silverstein FS, Buchanan K, Hudson C, Johnston MV 1986 Flunarizine limits hypoxia-ischemia induced morphologic injury in immature rat brain. Stroke 17, 477-482

Sims NR, Pulsinelli WA 1987 Altered mitochondrial respiration in selectively vulnerable brain subregions following transient forebrain ischemia in the rat. J Neurochem 49, 1367-1374

Smith ML, Auer RN, Siesjo BK 1984 The density and distribution of ischemic brain injury in the rat following 2-10 min of forebrain ischemia. Acta Neuropathol Berl 64, 319-332

Southam E, Garthwaite J 1993 The nitric oxide-cyclic GMP signalling pathway in rat brain. Neuropharmacology 32, 1267-1277

Springall D, Riveros-Moreno V, Buttery LD, Suburo A, Bishop AE, Merret M, Moncada S, Polak JM 1992 Immunological detection of nitric oxide synthase(s) in human tissues using heterologous antibodies suggesting different isoforms. Histochem 98, 259-266

Stamler JS 1994 Redox signaling: Nitrosylation and related target interactions of nitric oxide. Cell 78, 931-936

Stein DT, Vannucci RC 1988 Calcium accumulation during the evolution of hypoxic-ischemic brain damage in the immature rat. J Cereb Blood Flow Metab 8, 834-842

Sun D, Gilboe DD 1994 Ischemia-induced changes in cerebral mitochondrial free fatty acids, phospholipids, and respiration in the rat. J Neurochem 62, 1921-1928

Sykes G, Molloy P, Johnson P, Gu W, Ashworth F, Stirrat G, Turnbull A 1982 Do Apgar scores indicate asphyxia? Lancet 1; 494-496

Szatkowski M, Attwell D 1994 Triggering and execution of neuronal death in brain ischaemia: two phases of glutamate release by different mechanisms. TINS 17, 359-365

Takashima S, Kuruta H, Mito T 1990 Immunohistochemistry of superoxide dismutase-1 in developing brain. Brain Dev 12, 211-213

Tamura M 1992 Protective effects of a PG12 analogue OP-2507 on hemorrhagic shock in rats - with an evaluation of the metabolic recovery using near-infrared optical monitoring. Jpn Circ J 56, 366-375

Tan KMW, Williams CE, Mallard C, Bossano D, Gluckman PD 1995 Changes in ECF concentrations of excitatory amino acids, lactate and glucose in the parasagittal cortex of fetal sheep subjected to global hypoxia-ischaemia, using intracerebral microdialysis. Pediatr Res (In Press)

Tan WK, Williams CE, Gunn AJ, Mallard CE, Gluckman PD 1992 Suppression of postischemic epileptiform activity with MK-801 improves neural outcome in fetal sheep. Ann Neurol 32, 677-682

Tan WK, Williams CE, Gunn AJ, Mallard EC, Gluckman PD 1993 Pretreatment with monosialoganglioside GM1 protects the brain of fetal sheep against hypoxic-ischemic injury without causing systemic compromise. Pediatr Res 34, 18-22

Thoresen M, Penrice J, Lorek A, Cady EB, Wylezinska M, Kirkbride V, Cooper CE, Brown GC, Edwards AD, Wyatt JS 1995 Mild hypothermia after severe transient hypoxia-ischemia ameliorates delayed cerebral energy failure in the newborn piglet. Pediatr Res 37, 667-670

Tominaga T, Sato S, Ohnishi T, Ohnishi ST 1993 Potentiation of nitric oxide formation following bilateral carotid occlusion and focal cerebral ischemia in the rat: in vivo

detection of the nitric oxide radical by electron paramagnetic resonance spin trapping. Brain Res 614, 342-346

Tomita M. 1988 Significance of cerebral blood volume. In: Cerebral Hyperemia and Ischemia: From the standpoint of Cerebral Blood Volume, eds. M. Tomita, T. Sawada, H. Naritomi and W. Heiss (Elsevier Science Publishers, New York) pp. 3-31

Traystman RJ, Kirsch JR, Koehler RC 1991 Oxygen radical mechanisms of brain injury following ischemia and reperfusion. J Appl Physiol 71, 1185-1195

Traystman RJ, Kirsch JR, Koehler RC 1991 Oxygen radical mechanisms of brain injury following ischemia and reperfusion. J Appl Physiol 71, 1185-1195

Trifiletti RR 1992 Neuroprotective effects of N^G-nitro-L-arginine in focal stroke in the 7-day old rat. Eur. J Pharmacol 218, 197-198

Uematsu D, Greenberg J, Reivich M, Karp A 1988 In vivo measurement of cytosolic free calcium during cerebral ischaemia and reperfusion. Ann Neurol 24, 420-428

Umemura A, Mabe H, Nagai H 1992 A phospholipase C inhibitor ameliorates postischemic neuronal damage in rats. Stroke 23, 1163-1166

van der Zee P, Arridge SR, Cope M, Delpy DT 1990 The effect of optode positioning on optical pathlength in near infrared spectroscopy of brain. Adv Exp Med Biol 277, 79-84

Vannucci RC 1993 Experimental models of perinatal hypoxic-ischemic brain damage. APMIS Suppl 40, 89-95

Vannucci RC, Christensen MA, Yager JY 1993: Nature, time-course, and extent of cerebral edema in perinatal hypoxic-ischemic brain damage. Pediatr Neurol 9, 29-34

Vige X, Carreau A, Scatton B, Nowicki JP 1993 Antagonism by NG-nitro-L-arginine of L-glutamate-induced neurotoxicity in cultured neonatal rat cortical neurons. Prolonged application enhances neuroprotective efficacy. Neuroscience 55, 893-901

Vlessis AA, Widener LL, Bartos D 1990 Effect of peroxide, sodium, and calcium on brain mitochondrial respiration in vitro: potential role in cerebral ischemia and reperfusion. J Neurochem 54, 1412-1418

Volpe JJ Hypoxic-ischemic Encephalopathy 1995 Clinical aspects. In: Neurology of the Newborn, WB Saunders, Philadelphia pp. 236-250

Wagner KR, Kleinholz M, Myers RE 1989 Delayed neurologic deterioration following anoxia: brain mitochondrial and metabolic correlates. J Neurochem 52, 1407-1417

Wagner KR, Kleinholz M, Myers RE 1990 Delayed onset of neurologic deterioration following anoxia/ischemia coincides with appearnace of impaired brain mitochondrial respiration and decreased cytochrome oxidase activity. J Cereb Blood Flow Metab 10, 417-423

Wasterlain CG, Fujikawa DG, Penix L, Sankar R 1993 Pathophysiological mechanisms of brain damage from status epilepticus. Epilepsia 34 Suppl 1, S37-S53

Waterman MR 1978 Spectral characterization of human hemoglobin and its derivatives. Methods Enzymol 52, 456-463

Wei HM, Chi OZ, Liu X, Sinha AK, Weiss HR 1994 Nitric oxide synthase inhibition alters cerebral blood flow and oxygen balance in focal cerebral ischemia in rats. Stroke 25, 445-449

Wertheim D, Mercuri E, Faundez JC, Rutherford MA, Acolet D, Dubowitz LM 1994 Prognostic value of continuous electroencephalographic recording in full term infants with hypoxic-ischaemic encephalopathy. Arch Dis Child 71, F97-102

Westgate J, Harris M, Curnow JS, Greene KR 1992 Randomised trial of cardiotocography alone or with ST waveform analysis for intrapartum monitoring Lancet 340, 194-198

Wharton M, Granger DL, Durack DT 1988 Mitochondrial iron loss from leukemia cells injured by macrophages. A possible mechanism for electron transport chain defects. J Immunol 1311-1317

Wical BS 1994 Neonatal seizures and electrographic analysis: evaluation and outcomes. Pediatr Neurol 10, 271-275

Williams CE 1991 Pathogenesis of Perinatal Hypoxic Ischaemic Brain Injury. PhD thesis (London, England)

Williams CE, Gluckman PD 1990 Real-time spectral intensity analysis of the EEG on a common microcomputer. J Neurosci Methods 32, 9-13

Williams CE, Gunn AJ, Gluckman PD 1991 Time course of intracellular edema and epileptiform activity following prenatal cerebral ischemia in sheep. Stroke 22, 516-521

Williams CE, Gunn AJ, Mallard C, Gluckman PD 1992 Outcome after ischemia in the developing sheep brain: an electroencephalographic and histological study. Ann Neurol 31, 14-21

Williams CE, Gunn AJ, Synek B, Gluckman PD 1990 Delayed seizures occurring with hypoxic-ischemic encephalopathy in the fetal sheep. Pediatr Res 27, 561-565

Williams CE, Mallard C, Tan WK, Gluckman PD 1993 Pathophysiology of perinatal asphyxia. Clin Perinatol 20, 305-325

Winkler CL, Hauth JC, Tucker JM, Owen J, Brumfield CG 1991 Neonatal complications at term as related to the degree of umbilical artery acidemia. Am J Obstet Gynecol 164, 637-641

Wray S, Cope M, Delpy DT, Wyatt JS, Reynolds EOR 1988 Characterization of the near infrared absorption spectra of cytochrome aa3 and haemoglobin for the non-invasive monitoring of cerebral oxygenation. Biochim Biophys Acta 933, 184-192

Wrigglesworth JM, Sharpe MA, Cooper CE 1993 Regulation of electron flux through cytochrome c oxidase: pH, delta pH and fatty acids. Biochem Soc Trans 21, 781-784

Wyatt JS 1993 Near-infrared spectroscopy in asphyxial brain injury. Clin Perinatol 20, 369-378

Wyatt JS, Cope M, Delpy DT, van der Zee P, Arridge S, Edwards AD, Reynolds EOR 1990 Measurement of optical path length for cerebral near-infrared spectroscopy in newborn infants. Dev Neurosci 12, 140-144

Wyatt JS, Cope M, Delpy DT, Wray S, Reynolds EOR 1986 Quantification of cerebral oxygenation and haemodynamics in sick newborn infants by near infrared spectrophotometry. Lancet 2, 1063-1066

Wyatt JS, Edwards AD, Azzopardi D, Reynolds EOR 1989 Magnetic resonance and near infrared spectroscopy for the investigation of perinatal hypoxic ischaemic brain injury. Arch Dis Child 64, 953-963

Wyatt JS, Edwards AD, Cope M, Delpy DT, McCormick DC, Potter A, Reynolds EOR 1991 Response of cerebral blood volume to changes in arterial carbon dioxide tension in preterm and term infants. Pediatr Res 29, 553-557

Wyllie AH 1981 Cell death: a new classification separating apoptosis from necrosis. In: Cell death in biology and pathology, Editors: Chapman & Hall, New York pp. 9-34

Wyllie AH, Morris RG, Smith AL, Dunlop D 1984 Chromatin cleavage in apoptosis: association with condensed chromatin morphology and dependence on macromolecular synthesis. J Pathol 142, 67-78

Yager J, Towfighi J, Vannucci RC 1993 Influence of mild hypothermia on hypoxic-ischemic brain damage in the immature rat. Pediatr Res 34, 525-529

Yager JY, Brucklacher RM, Vannucci RC 1991 Cerebral oxidative metabolism and redox state during hypoxia-ischemia and early recovery in immature rats. Am J Physiol 261, H1102-H1108

Yager JY, Brucklacher RM, Vannucci RC 1992 Cerebral energy metabolism during hypoxia-ischemia and early recovery in immature rats. Am J Physiol 262, H672-H677

Yudkin PL, Johnson A, Clover LM, Murphy KW 1995 Assessing the contribution of birth asphyxia to cerebral palsy in term singletons. Paediatr Perinat Epidemiol 9, 156-170

Zhang F, Iadecola C 1993 Nitroprusside improves blood flow and reduces brain damage after focal ischemia. Neuroreport 4, 559-562

Zhang J, Dawson VL, Dawson TM, Snyder SH 1994 Nitric oxide activation of poly(ADP-ribose) synthetase in neurotoxicity. Science 263, 687-689

Zijlstra WG, Buursma A, Meeuwsen van der Roest WP 1991 Absorption spectra of human fetal and adult oxyhemoglobin, de-oxyhemoglobin, carboxyhemoglobin, and methemoglobin. Clin Chem 37, 1633-1638

Publications and Abstracts

KA Marks, C Mallard, I Roberts, E Sirimanne, C Williams, P Gluckman, AD Edwards 1994 Relation between cerebral haemodynamics, cortical impedance and neuronal loss following brain ischaemia in fetal sheep. Pediatr Res; 36:27A.

KA Marks, C Mallard, I Roberts, E Sirimanne, C Williams P Gluckman, AD Edwards 1994 Changes in the cerebral concentration of oxidized cytochrome aa_3 following ischaemia in fetal sheep, as measured by near infrared spectroscopy. Pediatr Res 36:27A.

KA Marks, AD Edwards 1994 Cerebral protection after hypoxia-ischaemia in newborn infants. Current Medical Literature (Paediatrics), The Royal Society of Medicine 7(4):95-102.

KA Marks, EC Mallard, I Roberts, CE Williams PD Gluckman, AD Edwards 1995 N^G-Nitro-L-arginine, a nitric oxide synthase inhibitor, alters the delayed changes in cerebal haemodynamics that follow transient cerebral ischaemia in fetal sheep. Early Human Development (In press).

KA Marks, C Mallard, I Roberts, E Sirimanne, C Williams P Gluckman, AD Edwards 1995 Delayed vasodilation and altered oxygenation after cerebral ischemia in fetal sheep. Pediatr Res (In press)

KA Marks, EC Mallard, I Roberts, CE Williams, PD Gluckman, AD Edwards 1996 Nitric oxide synthase inhibition attenuates delayed cerebral vasodilation and increases injury following cerebral ischemia in fetal sheep. Pediatr Res (In press)